京都大学理学博士学位申請論文

Observational studies on the atmospheric general circulation using global meteorological data

（全球気象データを用いた大気大循環の観測的研究）

１９８７年　１月

塩谷　雅人

主論文

Observational Studies on the Atmospheric General Circulation Using Global Meteorological Data

by

Masato Shiotani

Geophysical Institute
Kyoto University

A dissertation submitted in partial fulfillment
of the requirements for the degree of
Doctor of Science

January 1987

ACKNOWLEDGMENTS

The main body of this work was carried out under the supervision of Prof I. Hirota at the Geophysical Institute of Kyoto University during 1982 to 1987 I wish to thank Prof I. Hirota for his continuing guidance and valuable discussions throughout this work. Part of this work was carried out while I was a student visitor at the National Center for Atmospheric Research (NCAR) during September 1985 to October 1986. I am also grateful to Dr J. C. Gille for his giving me a chance to visit the NCAR and work with his group. Thanks are also due to all the members of our laboratory and of Dr J. Gille's group. The computation were performed on the FACOM M382/380 and VP100 computer at the Data Processing Center of Kyoto University and on the Cray-1 computer at the NCAR.

ABSTRACT

By the use of global meteorological data, observational studies are made for better understanding of the general circulation in the troposphere and stratosphere. The main data set used in this study is made up of the global tropospheric data for levels from 1000 to 100 mb and the global stratospheric data for levels from 70 to 0.4 mb from the National Meteorological Center (NMC) Eliassen-Palm (E-P) flux diagnostics is used as a powerful and useful tool to investigate the wave-mean flow interaction.

In PART 1, dynamical interaction between planetary waves and mean zonal winds in the stratosphere is investigated, by paying special attention to the difference between the northern hemisphere (NH) and the southern hemisphere (SH) It is found that from winter to summer the seasonal march of wave activity and mean zonal winds is different between the two hemispheres, resulting from differences of planetary wave activity in the two hemispheres.

As an extention of PART 1, the propagation and temporal variation of planetary waves in the troposphere and stratosphere are investigated in PART 2. It is found that there are two typical cases of correspondence during the NH winter from December 1981 to March 1982: In December and early January, the time variation of wave activity in the troposphere and stratosphere is out of phase; In February and March, after the stratospheric sudden warming, the tropospheric wave activity seems to propagate into the stratosphere. The different configuration of mean zonal winds in the two periods could explain the two different types of the correspondence of planetary wave activity

In PART 3, relation between ozone distribution and dynamical factors is investigated to have further insight of the stratospheric circulation. Special attention is paid to the Antarctic lower stratosphere where a remarkable decrease of total ozone has been observed during springtime of the last decade. The year-to-year variation of the ozone mixing ratio at high latitudes is related to that of the wave activity during the winter and spring; when the wave activity is vigorous, we see weaker westerlies, higher temperatures and higher ozone mixing ratios at high latitudes.

TABLE OF CONTENTS

ACKNOWLEDGMENTS i

ABSTRACT ii

TABLE OF CONTENTS iii

GENERAL INTRODUCTION 1

DATA AND METHOD OF ANALYSIS 3

PART 1 5

Planetary Wave-Mean Flow Interaction in the Stratosphere: a Comparison between Northern and Southern Hemispheres

PART 2 34

Planetary Wave Activity in the Troposphere and Stratosphere during the Northern Hemisphere Winter

PART 3 56

Dynamical Factors Affecting Ozone Mixing Ratios in the Antarctic Lower Stratosphere

SUMMARY 85

REFERENCES 87

GENERAL INTRODUCTION

Since the FGGE (First GARP Global Experiment) year (1979) a network of ground based observations has been extended, particularly in the SH. Around the same time the advent of observational techniques such as satellite measurements of infrared radiation enables us to investigate the stratosphere with better data coverage in both time and space (Fritz and Soules, 1970; Labitzke and Barnett, 1973; Barnett, 1974; Hirota, 1976; Hirota and Barnett, 1977) Thus, we can now get global meteorological data set routinely, both in the troposphere and stratosphere, and both in the NH and the SH.

One of the best ways to make good use of global meteorological data set is a comparison of dynamical features between the NH and the SH. This approach provides a valuable insight into the nature of general circulation; in other words, two hemispheres provide a kind of controlled experiment. To give a guide to understanding the result of this study (in particular, PART 1 and PART 3), we summarize briefly the notable features of the thermal field, mean zonal winds, and planetary waves in the two hemispheres.

For the thermal field:

(1) Upper stratospheric temperatures in polar regions are higher in the SH than in the NH (Barnett, 1974)

(2) The latitudinal gradient of the zonal-mean temperature at high latitudes in the SH upper stratosphere is reversed in late winter (Labitzke and Barnett, 1973; Barnett, 1974; Hirota *et al.*, 1983).

For the mean zonal wind field:

(1) The winter stratospheric westerlies are stronger in the SH than in the NH (Hartmann, 1976; Hirota *et al.*, 1983)

(2) The stratospheric westerly jet in the SH shifts poleward and downward in late winter (Harwood, 1975; Hartmann, 1976) The shifting of the westerly jet is associated with the reversal of the zonal-mean temperature through the thermal wind relation.

For the planetary wave:

(1) Both of wave 1 and wave 2 in the NH are quasi-stationary, while in the SH eastward traveling wave 2 is dominant (Harwood, 1975; Hartmann, 1976) although wave 1 is quasi-stationary

Another interesting use of the data set is to make an analysis of the general circulation, treating the troposphere and stratosphere as a whole system. Although we have a benefit of investigating the troposphere and

stratosphere as a whole, most of observational studies have treated the tropospheric and stratospheric circulations as systems separate from each other

An important stage of recent progress in theoretical studies on the wave-mean flow interaction is the "generalized Lagrangian-mean" (GLM) theory by Andrews and McIntyre (1976, 1978) Motivated by their GLM theory, they re-formulated the traditional wave equations into "transformed Eulerian-mean" equations, which have most of the advantages of the Lagrangian-mean approach but are framed primarily in terms of observable Eulerian quantities. In this formalism a vector quantity the so-called "Eliassen-Palm (E-P) flux" is most important. Details about the transformed Eulerian-mean formalism and the motivation for the use of the E-P flux are seen, for instance,in Edmon *et al.* (1980), Dunkerton *et al.* (1981) and Kanzawa (1982)

With this view, I made observational studies for better understanding of the general circulation in the troposphere and stratosphere, by using the global meteorological data set and the E-P flux diagnostics. In PART 1, a comparison of dynamical interaction between the NH and the SH is made. In PART 2, the correspondence of wave activity between the troposphere and stratosphere is investigated. In PART 3, relation between ozone distribution and dynamical factors are investigated. Each of the three parts is based on a separate paper by Shiotani and Hirota (1985), Shiotani (1986), and Shiotani and Gille (1987), respectively. Detailed motivation for each study will be found in Introduction section of each part. Figures are collected at the end of each part.

DATA AND METHOD OF ANALYSIS

The temperature and geopotential height data used in this study are made up of the global tropospheric data for levels from 1000 to 100 mb from the National Meteorological Center (NMC) of the U. S. National Oceanic and Atmospheric Administration (NOAA) and global stratospheric data for levels from 70 to 0.4 mb from the NOAA Climate Analysis Center (Hereafter, we simply refer to this data set as the NMC data set.) The NMC data were interpolated to 5° latitude circles, then Fourier transformed to provide a zonal mean and coefficients for 6 longitudinal waves. The NMC data are available on the following 18 pressure levels: 1000, 850, 700, 500, 400, 300, 250, 200, 150, 100, 70, 50, 30, 10, 5, 2, 1 and 0.4 mb. (For details about the NMC data set, see Geller *et al.*, 1983)

Following Kanzawa (1982) (notations are based on Holton, 1975 and Dunkerton *et al.* 1981), we define the E-P flux F for the quasi-geostrophic motions in spherical coordinates (λ, θ, $z = -H\ln(p/p_s)$) as

$$\mathbf{F} = (F(\theta), F(z)), \tag{1}$$

where

$$F(\theta) = -\rho_0(z)\, a \cos\theta\, \overline{u'v'}, \tag{2}$$

$$F(z) = +\rho_0(z)\, a \cos\theta \left(\frac{f}{N^2}\right) \overline{v'\Phi_z'}, \tag{3}$$

$$\rho_0(z) = \rho_0 = \rho_s \exp(-z/H) \tag{4}$$

We also define "residual meridional circulation" ($\overline{v}^*$, $\overline{w}^*$) as

$$\overline{v}^* = \overline{v} - \frac{1}{\rho_0}\frac{\partial}{\partial z}\left(\rho_0 \frac{\overline{v'\Phi_z'}}{N^2}\right), \tag{5}$$

$$\overline{w}^* = \overline{w} + \frac{1}{a\cos\theta}\frac{\partial}{\partial \theta}\left(\cos\theta \frac{\overline{v'\Phi_z'}}{N^2}\right). \tag{6}$$

Then we can transform traditional equations into following ones:

$$\frac{\partial \overline{u}}{\partial t} - f\overline{v}^* = \frac{1}{\rho_0 a\cos\theta}\nabla \cdot \mathbf{F}. \tag{7}$$

$$\frac{\partial \overline{\Phi}_z}{\partial t} + N^2\overline{w}^* = Q, \tag{8}$$

$$\frac{1}{a\cos\theta}\frac{\partial}{\partial \theta}(\overline{v}^*\cos\theta) + \frac{1}{\rho_0}\frac{\partial}{\partial z}(\rho_0\overline{w}^*) = 0, \tag{9}$$

where

$$\nabla \cdot \mathbf{F} = \frac{1}{a\cos\theta}\frac{\partial}{\partial\theta}(F(\theta)\cos\theta) + \frac{\partial}{\partial z}F(z). \tag{10}$$

The vector quantity **F** and its divergence $\nabla \cdot \mathbf{F}$ play a central role in this formalism. From the theoretical consideration as in Kanzawa (1982) we can interpret **F** as westward angular wave momentum flux propagating through westerly flow and ∇ **F** as wave induced torque per unit volume acting on the mean flow. In the transformed formalism the non-acceleration theorem is simply represented as $\nabla \cdot \mathbf{F}=0$. To calculate the E-P flux we assume H to be constant ($H=7\times10^3$ m).

In addition, to see the effect of waves on the time change of the mean zonal wind, we define D_F as

$$D_F = \frac{1}{\rho_0 a\cos\theta}\nabla \mathbf{F}, \tag{11}$$

then we can rewrite eq.(7) as

$$\frac{\partial \bar{u}}{\partial t} - f\bar{v}^* = D_F \tag{12}$$

This shows that D_F can be regarded as a zonal force per unit mass acting on the mean state. Hereafter, we refer to $F(\theta)$ and $(a\cos\theta)^{-1}\partial(F(\theta)\cos\theta)/\partial\theta$ as $F(y)$ and $\partial F(y)/\partial y$, respectively

PART 1

Planetary Wave-Mean Flow Interaction in the Stratosphere: a Comparison between Northern and Southern Hemispheres

1.1 Introduction

It has been widely recognized that vertically propagating planetary waves excited in the troposphere are dynamically important in the stratosphere because they provide a large part of eddy momentum and heat fluxes. The propagation of planetary waves is controlled by the mean zonal wind profile, and the background flow may, in turn, be changed through the deposition of zonal momentum by planetary waves. Thus, it is important to study the properties of vertically propagating waves and the nature of their interaction with the mean zonal wind for an understanding of the general circulation of the stratosphere.

The history of wave-mean flow interaction studies began with the derivation of a "non-acceleration theorem" by Eliassen and Palm (1960) for gravity waves and by Charney and Drazin (1961) for planetary waves. This theorem states that the mean zonal wind can be forced to accelerate or decelerate only when the vertically propagating waves have the effects of transience and damping. Dickinson (1969a, b) made theoretical studies on the wave-mean flow interaction problem taking account of the effects of the existence of a critical line and the presence of a Newtonian cooling process. He concluded that at least one of these effects is necessary for the forcing of zonal atmospheric motions on the planetary scale as implied by the non-acceleration theorem.

On the other hand, as a counterpart of these theoretical studies, Hirota and Sato (1969) made an analysis of day-to-day variations of planetary waves and the mean zonal wind in the NH winter stratosphere. They found that wave amplitude at 30 mb varies intermittently with a period of about two weeks and that time variations of the mean zonal wind are negatively correlated with those of the wave amplitude. Their results suggest that the transience of vertically propagating planetary waves excited in the troposphere has the effect of varying the mean zonal wind states; this wave transience is one of the conditions for violating the non-acceleration theorem.

Observational studies based on the new diagnostic tool, E-P flux diagnostics, have been carried out by many authors. Among them, Palmer (1981a, b), Kanzawa (1982) and O'Neill and Youngblut (1982) obtained significant results for stratospheric sudden warmings. As regards the climatological general circulations in the stratosphere, Smith (1983) and Geller *et al.* (1983) applied the E-P flux diagnostics to the monthly mean field in the NH winter Hartmann *et al.* (1984) also investigated observational features of the wave-mean flow interaction in the SH using the E-P flux diagnostics.

However, these studies were carried out for limited periods (such as sudden warmings) or for a limited region (one of the two hemispheres) Making a good use of satellite measurements we should grasp *global* pictures of the stratospheric circulation and the *seasonal evolutions* of wave activity and the mean zonal wind. In this sense, it is stressed that comparisons of dynamical features between the NH and the SH provide a valuable insight into the nature of stratospheric circulations. Moreover, the seasonal march of wave activity and the mean zonal wind must be one of the most interesting problems in the dynamics of the stratosphere. For example, a sudden warming in the NH, in a sense that the westerly jet is broken to the easterlies, has never been reported in early winter (in November and December); we should understand the sudden warming event as it is realized in the seasonal march of wave activity and the mean zonal wind.

With this in view, Hirota *et al.* (1983) recently studied the difference of upper stratospheric circulations in the NH and the SH. In addition, they found that the seasonal evolutions of wave activity in the two hemispheres are different: from winter to spring the wave activity is more vigorous in the NH than in the SH; whereas from spring to summer, more vigorous in the SH than in the NH. In this part, we will present some observational evidence of wave-mean flow interaction in the stratosphere by expanding their work.

1.2 Seasonal March

First we describe the seasonal march of the mean zonal wind and that of the E-P flux. For the purpose of studying the wave-mean flow interaction we make an analysis for the period of vigorous wave activity; in practice we select six months - December 1981 to May 1982 for the NH and June 1981 to November 1981 for the SH.

One of the most important results of Hirota *et al.* (1983) is that the seasonal march of zonal mean temperatures and wave amplitudes is different between the NH and the SH in the upper stratosphere. They showed this by simple statistics of standard deviations with respect to time for two seasons: "winter to spring and spring to summer" In correspondence with their result the period of the first three months (for the NH, December to February and for the SH, June to August) is called "winter to spring and the period of the second three months (for the NH, March to July and for the SH, September to November) is called "spring to summer"

a. Mean zonal wind

Fig. 1 1 shows latitude-time sections of the mean zonal wind at the 1 mb level, estimated geostrophically We selected this level to see the poleward shifting of the maximum westerlies clearly From Fig. 1.1 we can see the following features:

For the NH (Fig. 1 1(a)),

(1) from December to early January the maximum westerlies, with a speed of about 100 m s^{-1} , are slowly shifting poleward.

(2) Around 8 January a minor warming occurs and after that the maximum westerlies are established at high latitudes, about 60°N (16 January).

(3) Then a major warming occurs and the westerlies are reversed to the easterlies at high latitudes (around 26 January)

(4) In February the westerlies are re-established but the jet profile is not so clearly formed as seen in December Summer easterlies appear at this level in April to the north of 60°N and in May to the south of 60°N.

For the SH (Fig. 1.1(b)),

(1) from June to July the maximum westerlies, with a speed of about 130 m s^{-1} , stronger than in the NH, are sharply located at around 40°S and their time variations are small.

(2) In mid-August the maximum westerlies shift poleward about 20 degrees in about a week.

(3) From the shifting (around August 15) to October the maximum westerlies are located at around 60°S and their time variations in this period are larger than those in the pre-shifting period.

(4) In early November summer circulations are established for all lati-

tudes simultaneously.

b. E-P flux

Next we describe the seasonal march of the E-P flux for the two hemispheres. Cross-section analysis will be shown later In this section we regard the E-P flux as a measure of the net propagation of wave activity To calculate the E-P flux we assume N to be constant $N=2\times10^{-2}$ s^{-1} Fig. 1.2 shows latitude-time sections of the E-P flux at the 5 mb level for total wavenumber (1- 6) contributions. We selected this level to see the switching of the E-P vectors clearly From Fig. 1.2 we can see the following features:

For the NH (Fig. 1.2(a)):

(1) From December to March the wave activity varies intermittently with a rhythm of about two weeks; such a quasi-periodic change has been reported earlier by Hirota and Sato (1969) and Madden (1975) from the analysis of wave amplitude variations.

(2) For most of the period in vigorous wave activity the E-P vectors point equatorward and upward, with their main sources around 60°N. These features agree well with previous results for the normal winter stratosphere using E-P flux diagnostics (e.g. Smith, 1983: Geller *et al.*, 1983).

(3) However, when the major warming occurs in late January, the E-P vectors point strongly upward with weak poleward components. Notice that there is little difference in the magnitude of the wave activity from one event to another Thus, it is not true that the most vigorous wave activity brings about a major warming; more important is the direction of the E-P flux.

For the SH (Fig. 1.2(b)):

(1) From June to July the wave activity is relatively weak, corresponding to the strong and sharp westerly jet at the same period. As regards the wave-mean flow interaction it is interesting to note the relation between the weak wave activity and the small time variations of the maximum westerlies.

(2) In August the wave activity increases, and varies intermittently with a rhythm of about 10 days. From September to October wave activity goes on continually. not intermittently as in the NH. The magnitude of the wave activity is rather less in the SH than in the NH.

(3) For most of the period in vigorous wave activity the E-P vectors

point equatorward and upward as in the NH. Also in the SH, there are occasions when the E-P vectors point strongly upward with weak poleward components (around 17 September) However, unlike the NH, a major warming event in which westerlies are replaced by easterlies does not occur

To see the role of each wavenumber, we present a picture similar to Fig. 1.2 but for wavenumbers 1 and 2 separately, for a selected period of three months, for the NH December to February (Fig. 1.3(a)), and for the SH August to October (Fig. 1.3(b)) Referring to Fig. 1.2 we see from Fig. 1.3 that almost all the contribution is from wavenumbers 1 and 2 components; and that the periods of vigorous wave activity for waves 1 and 2 does not overlap in general.

In the NH (Fig. 1.3(a)) if we consider the E-P flux separately for each wavenumber contribution, the rhythm of the wave-1 activity is interrupted in late January; however, at around the same time the wave-2 activity rises and compensates for the falling wave-1 activity. Thus in the total wavenumber contribution we can see the rhythm of the wave activity with a timescale of about 2 weeks. It seems that the wave-1 and wave-2 activities in the NH appear with no obvious pattern in time.

On the other hand, in the SH, the times of the wave activity for waves 1 and 2 are different (Fig. 1.3(b)); the wave-2 activity lies mainly in August, whereas the wave-1 activity lies from late August (just after the shifting of the westerly jet) to mid-October As was shown in earlier studies, planetary wave properties for both hemispheres are different; in the NH waves 1 and 2 are quasi-stationary, while in the SH eastward traveling wave 2 is prominent though wave 1 is quasi-stationary. Regarding the different wave properties of waves 1 and 2 in the SH, it is interesting to see that the wave-1 activity begins in association with the poleward shifting of the westerly jet.

1.3 Vertical Cross-Section Analysis

In section 1.2 we observed how the mean zonal wind and the E-P flux vary in the seasonal march at one level. Next we make a vertical cross-section analysis to see the behavior of the mean zonal wind and the E-P flux in the whole stratosphere. Our main interest is in comparison of the two hemispheres. Figs. 1 4 to 1.8 show sequences of latitude-height cross-sections of the total

E-P flux and its divergence expressed as the zonal force per unit mass (D_F) (left), and the mean zonal wind (right) Fig. 1 4 is presented every five days and Figs. 1.5 to 1.8 are presented every three days. For representing the E-P flux in vertical cross-sections, we followed the graphical conventions as described by Edmon *et al.* (1980)

a. The rhythm of minor warmings in the NH

Fig. 1.4 shows an example of a sequence for a minor warming in the NH. On 28 November wave activity is weak while the mean zonal winds are strong in high latitudes, especially in the lower stratosphere. Then wave activity is enhanced and the mean zonal winds in high latitudes are weakened, resulting in the appearance of the easterlies there (3 December); however, the speed of the stratospheric westerly jet is little changed but contour lines in the poleward flank of the westerly jet are packed. In terms of zonal mean potential vorticity ($\bar{q}$) (e.g. recent studies by McIntyre (1982) and Matsuno (1984)), we can interpret these features in the mean zonal wind change as a decrease of $\bar{q}$ in high latitudes and an increase in middle latitudes; that is, propagating planetary waves bring a change in the distribution of $\bar{q}$.

Around 3 December, the E-P vectors point strongly upward in the lower stratosphere, bend equatorward in the middle stratosphere and point nearly equatorward in the upper stratosphere. Values of D_F, representing the effect of waves on the mean flow, are negative in almost the whole stratosphere. The pattern of the E-P vectors agrees well with all previous results for the normal winter in the NH stratosphere (e.g. Smith, 1983: Geller *et al.*, 1983).

From around 8 December the wave activity is gradually weakened, then the westerlies in high latitudes are strengthened again; contour lines in the poleward flank of the westerly jet are gradually spread. On 13 December when there are no strong upward E-P vectors in the lower stratosphere the E-P vectors in the middle stratosphere point nearly equatorward. In addition, the distribution of D_F shows a dipole pattern, i.e., positive at high latitudes and negative at middle or lower latitudes. Again, in terms of $\bar{q}$, we can interpret this returning back process of the mean zonal wind as a redistribution of $\bar{q}$, i.e. an increase of $\bar{q}$ in high latitudes and a decrease in middle latitudes. Because $\nabla \cdot \mathbf{F}$ is related to the meridional flux of potential vorticity as shown in Edmon *et al.* (1980) and Kanzawa (1982), this dipole pattern is consistent with time changes of $\bar{q}$.

As an interpretation of the near-equatorward E-P flux and dipole pattern

of D_F, Hartmann *et al.* (1984) suggested that, on the basis of their observations in the SH, these configurations are due to an *in situ* source of wave activity, such as large scale shear instability. whereas Palmer and Hsu (1983) stated that the nonlinear interaction between waves 1 and 2 could give rise to such a dipole pattern, in a flow that was internally stable.

Positive D_F works to strengthen the mean zonal wind in the high latitude stratosphere (13 December), then the wave activity becomes large. In this way a minor warming in the NH repeats itself

b. *Shifting of the westerly jet*

As seen in Fig. 1.1 the maximum westerlies in both hemispheres tend to shift poleward in their seasonal evolutions. The shifting of the stratospheric westerly jet is important for understanding the stratospheric circulations in the two hemispheres. Hence we describe the behavior of the mean zonal wind and the feature of the E-P flux around the period of the shifting in the two hemispheres.

In the NH (Fig. 1.5), the stratospheric westerly jet in the mid-latitude upper stratosphere is weakened due to a minor warming (after January 3) We see large D_F regions in the mid-latitude stratosphere on 3 January and in the high latitude stratosphere on 6 January. On 9 January, although the upward E-P flux exists in the lower stratosphere, the E-P flux in the middle stratosphere point nearly equatorward and the distribution of D_F shows a dipole pattern as seen in Fig. 1.4 (on 13 December). This means that the westerlies are accelerated at high latitudes and decelerated at mid-latitudes. Then, on 12 January the stratospheric westerlies are established at high latitudes. We can interpret these features as a redistributing process of potential vorticity

In the SH the poleward and downward shifting of the stratospheric westerly jet in late winter has been reported by many authors, e.g., Leovy and Webster (1976), Hartmann (1976) and Hartmann *et al.* (1984) for the 1971 winter, the 1973 winter and the 1979 winter, respectively However, they paid little attention to day-to-day variations of the mean zonal wind and wave activity.

From Fig. 1.6 we can see the poleward and downward shifting of the westerly jet; it takes about 10 days. Relating to the wave activity we can conclude that a minor warming (12 to 15 August) which leads the negative D_F at mid-latitudes and the positive D_F at high latitudes contributes to the shifting of the westerly jet. The scale of the wave activity and values of D_F which

leads to the shifting of the westerly jet are less in the SH than in the NH. Time variations of the maximum westerlies are also smaller in the SH than in the NH. Again, we are interested in the distributions of the E-P flux and D_F on 15 August, a so-called dipole pattern, also seen in the NH.

A complementary (but compatible) idea of the physical cause of the shifting of the westerly jet is presented by McIntyre (1982) and McIntyre and Palmer (1983, 1984), in terms of erosion of the potential vorticity distribution in the polar vortex.

c. Episodes after the shifting of the westerly jet

With regard to the shifting of the westerly jet the seasonal march of the mean zonal wind in the two hemispheres is similar; however, episodes after the shifting are quite different.

In the NH (Fig. 1 7) the stratospheric westerly jet situated in the high latitude upper stratosphere (18 January) leads to the focusing of the E-P flux (18 January- 24 January). Before the shifting of the westerly jet the E-P vectors point upward and equatorward, but after the shifting they point strongly upward and, at high latitudes, poleward. Negative D_F regions are observed for almost whole stratosphere and maximum values are 9×10^{-4} m s^{-2} in the high latitude stratosphere on 24 January Then the westerlies are dramatically broken to the easterlies; this is a so-called major warming.

In the SH, on the other hand, after the shifting the stratospheric westerly jet continues to be stably situated in the high latitude middle stratosphere for about two months. The E-P flux occasionally focuses into high latitudes, but the westerlies are not broken to the easterlies. Fig. 1.8 is just one example in 1981 to show the focusing of the E-P flux into high latitudes (17 September) The maximum values of D_F are about 6×10^{-4} m s^{-2} in the high latitude stratosphere, weaker than 9×10^{-4} m s^{-2} in the NH on 24 January However, no major warming occurs and no change of its position.

1.4 Wave-mean flow interaction

In this section, we will discuss the relationship between the E-P flux, its divergence expressed as the zonal force per unit mass, D_F, and the time changes of the mean zonal wind. Fig. 1.9 shows an example of the latitude-time sections of the E-P flux, D_F, and $\partial\bar{u}/\partial t$ at the 5 mb level for three selected

months in the NH. To see the gross features of D_F and $\partial\bar{u}/\partial t$, we applied a 5-day running mean to their time series.

First, we notice the relation between D_F and $\partial\bar{u}/\partial t$ The zonal force per unit mass (D_F) implies the effect of the waves on the mean flow; moreover, from the theoretical prediction by Matsuno and Nakamura (1979) and Dunkerton *et al.* (1981), poleward residual flow $\bar{v}^*$ arises when the mean flow is decelerated. Therefore the sense of variation in D_F and $\partial\bar{u}/\partial t$ is expected to be the same near a maximum of D_F Indeed, Figs. 1.9(b) and (c) show that this is the case in middle and high latitudes. To confirm this relation we calculate the correlation coefficients between the time series of D_F and $\partial\bar{u}/\partial t$ ($COR(D_F, \partial\bar{u}/\partial t)$) at each latitude and pressure level.

Fig. 1 10 shows latitude-height sections of the coefficient $COR(D_F, \partial\bar{u}/\partial t)$ for six months from winter to summer in the two hemispheres. In the NH (Fig. 1.10(a)) the coefficient is positive and significantly large at high latitudes, with the maximum value in excess of 0.8 in the upper stratosphere, and it decreases toward the equator In the SH (Fig. 1.10(b)) the coefficient is also large at around 60°S and 40°S in the upper stratosphere with maximum values in excess of 0.5, though it is smaller than in the NH. The larger value of the coefficient in the NH is perhaps due to the larger time change of the mean zonal wind in the NH than in the SH. The two maxima in the SH reflect the position of the westerly jet before and after the shifting. The result for the SH is in good agreement with similar statistics by Hartmann *et al.* (1984)

Next we examine the relationship between the two terms $|\mathbf{F}|$ and D_F (Figs. 1.9(a) and (b)) As a measure of the wave activity we define $|F|$, from the theoretical consideration as in Palmer (1982), in such a way as

$$|\mathbf{F}| = [(F(y))^2 + \{(\frac{N}{f})F(z)\}^2]^{1/2} \qquad (13)$$

A deformation factor N/f appears because we should treat the two components of the E-P flux isotropically The deformation factor is evaluated as 158 for θ=60°; this is nearly equal to the scaling factor c(=125) Therefore we can regard the E-P flux represented in this study as having been treated approximately isotropically.

It is clear that at the 5 mb level the term D_F has a large negative value when the wave activity is vigorous. That is, the two terms $|\mathbf{F}|$ and D_F are in good negative correlation. On the observational basis Hirota and Sato (1969) showed that the wave amplitudes and mean zonal wind are in good negative

correlation. Their results are commonly accepted as a good representation of the effect of wave transience; however, based on their results $|\mathbf{F}|$ (regarded as a measure of wave amplitude) should be in negative correlation with the mean zonal wind $\bar{u}$, namely from Fig. 1 10, $-\partial D_F/\partial t$

To clarify the relation between the wave activity and the mean zonal wind we calculate the correlation coefficients between the time series of $|\mathbf{F}|$ and $\bar{u}$ ($COR(|\mathbf{F}|, \bar{u})$) and those between the time series of $|\mathbf{F}|$ and $\partial\bar{u}/\partial t$ ($COR(|\mathbf{F}|, \partial\bar{u}/\partial t)$) at each latitude and pressure level for six months from winter to summer Fig. 1.11 shows latitude-height sections of the coefficient $COR(|\mathbf{F}|, \partial\bar{u}/\partial t)$ and Fig. 1.12 shows those of the coefficient $COR(|\mathbf{F}|, \bar{u})$ To calculate the coefficient $COR(|\mathbf{F}|, \bar{u})$ we remove long-term variations of the mean zonal wind $\bar{u}$ by a high pass filter The numerical filter was designed to have a half power period of 39 days.

Fig. 1.11 shows that the most negative values, less than -0.4 are observed in the middle latitude upper stratosphere for both hemispheres; this is a confirmation of the relationship between the two terms $|\mathbf{F}|$ and D_F (Figs. 1.9(a) and (b)) On the other hand, in Fig. 1 12(a) for the NH we can see two minima, less than -0.4 in the high latitude lower stratosphere and less than -0.5 at the middle latitude stratopause level. The negative correlation in the high latitude lower stratosphere supports the result of Hirota and Sato (1969). In Fig. 1.12(b) for the SH we can see the minimum, less than -0.3 in the mid-latitude middle stratosphere.

It seems that the coefficients in Figs. 1.11 and 1 12 are rather small. However, this is because we selected a long period (180 days) from winter to summer for the statistics. If we select a limited period in which the wave-mean flow interaction typically takes place, these coefficients become more confident. For example, in the statistics of $COR(|\mathbf{F}|, \partial\bar{u}/\partial t)$ for 90 days from December to February for the NH and from August to October for the SH, the most negative values become -0.67 and -0.68, respectively

We suppose that the negative correlation between the two terms $|\mathbf{F}|$ and $\bar{u}$ in the high latitude lower stratosphere of the NH is probably due to the transience of vertically propagating planetary waves. Figs. 1.11 and 1.12 suggest, however, that this is not always the case in the whole stratosphere. It is interesting to note that the configulation of $COR(|\mathbf{F}|, \partial\bar{u}/\partial t)$ in the two hemispheres are similar (Fig. 1.11); the most negative values are observed in the middle latitude upper stratosphere. In connection with recent studies of wave-breaking (McIntyre and Palmer, 1983, 1984), the deceleration of the

mean zonal wind in these regions may be associated with the dissipation due to the wave transience of small scales. It is a further problem to study a physical mechanism for the wave-mean flow interaction in the middle latitude upper stratosphere. The negative correlation between $|F|$ and $\bar{u}$ at the mid-latitude stratopause level in the NH is also still open to question.

1.5 Concluding Remarks

a. Schematic pictures

The results presented in sections 1.2 to 1 4 are based on only one year's statistics; however, most of the characteristics of the mean zonal wind and the wave activity for the NH and the SH are generally supported by many observations for other years.

For example, the rhythm of time variations in the mean zonal wind and the wave activity in the NH, with a typical time scale of 2 weeks, has been reported by Hirota and Sato (1969) and Madden (1975) The result in this study gives a modern version of the interpretation of the relation between the mean zonal wind and wave activity using a new diagnostic tool, the E-P flux.

The poleward shifting of the westerly jet in the NH, which is important for preconditioning a sudden warming, has been reported by Quiroz *et al.* (1975), Kanzawa (1980, 1982) and Palmer (1981a, b) For the SH the poleward and downward shifting of the westerly jet, which is one of the most important aspects in the SH, has been reported by Hartmann (1976) and Leovy and Webster (1976). Hirota *et al.* (1983) have shown the shifting in terms of the reversal of the meridional temperature gradient in the upper stratosphere for four years.

An enhancement of the wave 1 activity after the shifting of the westerly jet in the SH has been first pointed out clearly in this work. A similar feature has been reported recently by Hartmann *et al.* (1984) for the 1979 winter It is also interesting to see that the period of weak wave activity in the SH mid-winter is simulated in a simplified general circulation model by Holton and Wehrbein (1980).

Concerning the question of interannual variability. Holton and Tan (1982) and Labitzke (1982) have discussed the relationship between the extratropical circulation in the NH stratosphere and the equatorial zonal wind change, i.e., the quasi-biennial oscillation. In the SH there is no major warming; however,

it is interesting to see the relation between the time of the shifting of the westerly jet and the wind regime of the quasi-biennial oscillation (Table 1.1) We will give an interpretation of this table in the subsection (b)

Apart from the interannual variability in the two hemispheres, our present results for one year, 1981-1982, give some characteristics of the seasonal march of the mean zonal wind and the wave activity, as shown in a schematic picture (Fig. 1 13) The features in Fig. 1 13 are representative of the mid-latitude upper stratosphere.

For the NH (upper):

(1) Wave activity, with contributions from both wave 1 and wave 2, varies erratically from winter to spring, with no systematic pattern but with a characteristic time scale of about two weeks.

(2) The time change of the mean zonal wind $(\partial \bar{u}/\partial t)$ is in negative correlation with the wave activity

(3) In mid-winter the stratospheric westerly jet shifts poleward owing to the occurrence of a minor warming. After the shifting, subsequent wave activity brings about a major warming.

For the SH (lower):

(1) In winter time the wave activity is weak, resulting in the small time changes of the mean zonal wind.

(2) In late winter the stratospheric westerly jet shifts poleward and downward in association with the wave activity

(3) After the shifting, the wave-1 activity is enhanced and continues till late spring. In this period the time change of the mean zonal wind $(\partial \bar{u}/\partial t)$ is, as in the NH, in negative correlation with the wave activity.

Next we describe schematically how the mean zonal wind profile changes in time evolutions. Fig. 1 14 shows sequences of wind profile changes in vertical cross-sections.

For the NH (Fig. 1.14(a)):

(1) The stratospheric westerlies in high latitudes change their speeds with a characteristic time scale of two weeks ($A \rightarrow B$) ; that is, the rhythm of minor warmings.

(2) At some time the westerly jet is established in the high latitude stratosphere after a minor warming ($B \rightarrow C$)

(3) Then the propagating wave through this wind profile breaks down the westerlies to easterlies ($C \rightarrow D$) ; this is a so-called major warming.

After a major warming the wind profile does not necessarily return back to the state *C*.

For the SH (Fig. 1 14(b)):

(1) The strong and sharpened westerly jet exists in mid winter (*A*)

(2) In late winter the westerly jet shifts poleward and downward in association with the wave activity (*A*→*B*)

(3) After the shifting, unlike the NH, the westerly jet does not change its position (in the high latitude middle stratosphere) but oscillates in speed (*B*↔*C*)

b. Interannual variability

Concerning the interannual variability the relation between the quasi-biennial oscillation in the tropical region and the seasonal march of the mean zonal wind in the stratosphere is suggestive in both two hemispheres. In particular, this problem is interesting in relation to the shifting of the westerly jet. The shifting is essential for the two hemispheres in the stratospheric general circulations, although the evolution of the mean zonal wind after the shifting is different between the hemispheres.

Table 1.1 shows the relation between the time of the shifting of the westerly jet in the SH and the wind regime of the quasi-biennial oscillation. From this table it appears that the equatorial wind regime and the time of the shifting in the SH are closely connected. In general, when the equatorial zonal winds at the 50 mb level are easterly the time of the shifting is early (July) and when they are westerly it is late (August or September) On the other hand, Labitzke (1982) noted that mid-winter major warmings in the NH occur readily when the equatorial zonal wind regime is easterly. These features are interpreted as follows: when the regime of the quasi-biennial oscillation is easterly the poleward shifting is earlier for both hemispheres, and particularly in the NH it leads to the mid-winter stratospheric sudden warming.

c. Troposphere-stratosphere coupling

Finally, we discuss possible mechanisms to explain the time variation of wave activity In our results, there are two clues to explain the mechanism: (i) in the NH, in the rhythm of minor warmings wave activity rises when the westerlies in the high latitude lower stratosphere are enhanced; (ii) in the SH, after the shifting of the westerly jet, which provides an enhancement of

the westerlies in the high latitude lower stratosphere, wave activity of wave 1 rises and continues until the westerlies are weakened. In view of these results, we can say that wave momentum flux is strongly connected with the wind profile in the lower stratosphere and perhaps also in the troposphere. Thus we present two hypotheses concerning the mechanism of variations of wave activity:

(1) A direct excitement of wave activity by the enhanced westerlies in the high latitude troposphere; e.g., the excitation of tropospheric wave activity by the orographic effect.

(2) A shutter" mechanism at around tropopause level, which assumes constant wave activity in the troposphere. When the westerlies are enhanced at the high latitude tropopause level the shutter is open and tropospheric waves easily penetrate into the stratosphere. Then, because of wave-mean flow interaction the westerlies are weakened and the shutter is closed to prohibit tropospheric activity entering the stratosphere.

Fig. 1.15 illustrate the two hypotheses, stressing the region of the lower stratosphere and the troposphere. In (a) (the first hypothesis), the stronger the westerlies in the high latitude troposphere are, the more tropospheric wave activity is excited; the wave is free to propagate into the stratosphere.

In (b) (the second hypothesis), even if the wave activity at the bottom of the troposphere is constant the direction of wave propagation is controlled by the wind profile around the tropopause level. When the westerlies around the high latitude tropopause level are weak the E-P vectors point to the tropospheric westerly jet; when the westerlies at high latitudes are enhanced the E-P vectors are guided to the stratospheric maximum westerlies. This mechanism is somewhat similar to that of stratospheric vacillation models (Holton and Mass, 1976; Holton and Dunkerton, 1978; Schoeberl, 1983). Recently, O'Neill and Youngblut (1982) tried to explain the amplification of wave activity which causes sudden warmings using a mechanism similar to the second hypothesis.

For both hypotheses the mechanism for weakening westerlies is considered to be interaction between the mean zonal wind and propagating waves. However, the mechanism to accelerate the westerlies, as observed in the seasonal evolution of the mean zonal wind or in the situation such as the dipole pattern of the E-P flux divergence, is not yet clear In PART 2, we will make

more extensive analyses of the wind field and the planetary waves, including the troposphere.

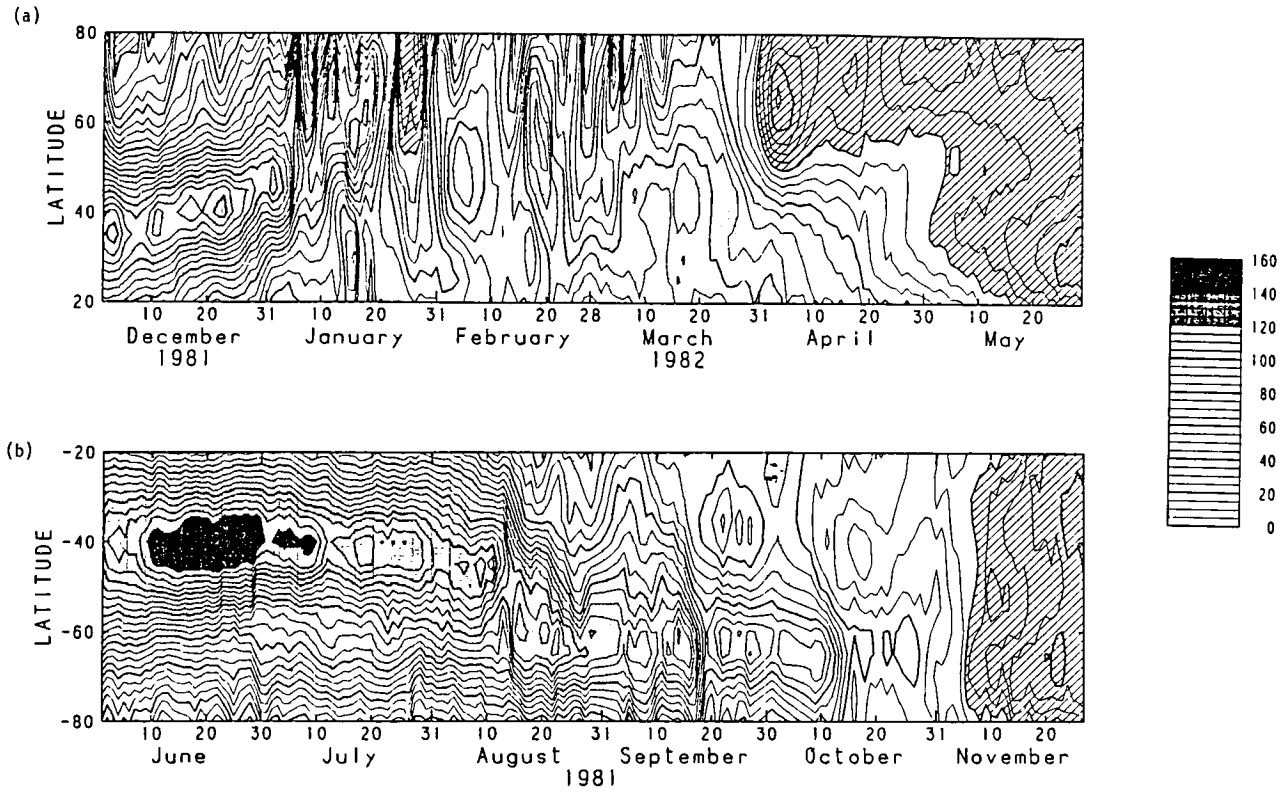

Fig. 1.1 Latitude-time sections of the mean zonal wind at the 1 mb level, estimated geostrophically, from winter to summer (see text) for (a) the NH and (b) the SH. Absolute values of the wind speed are shown by tone patterns (see the tone bar, unit: m s^{-1}) Easterlies are over oblique lines.

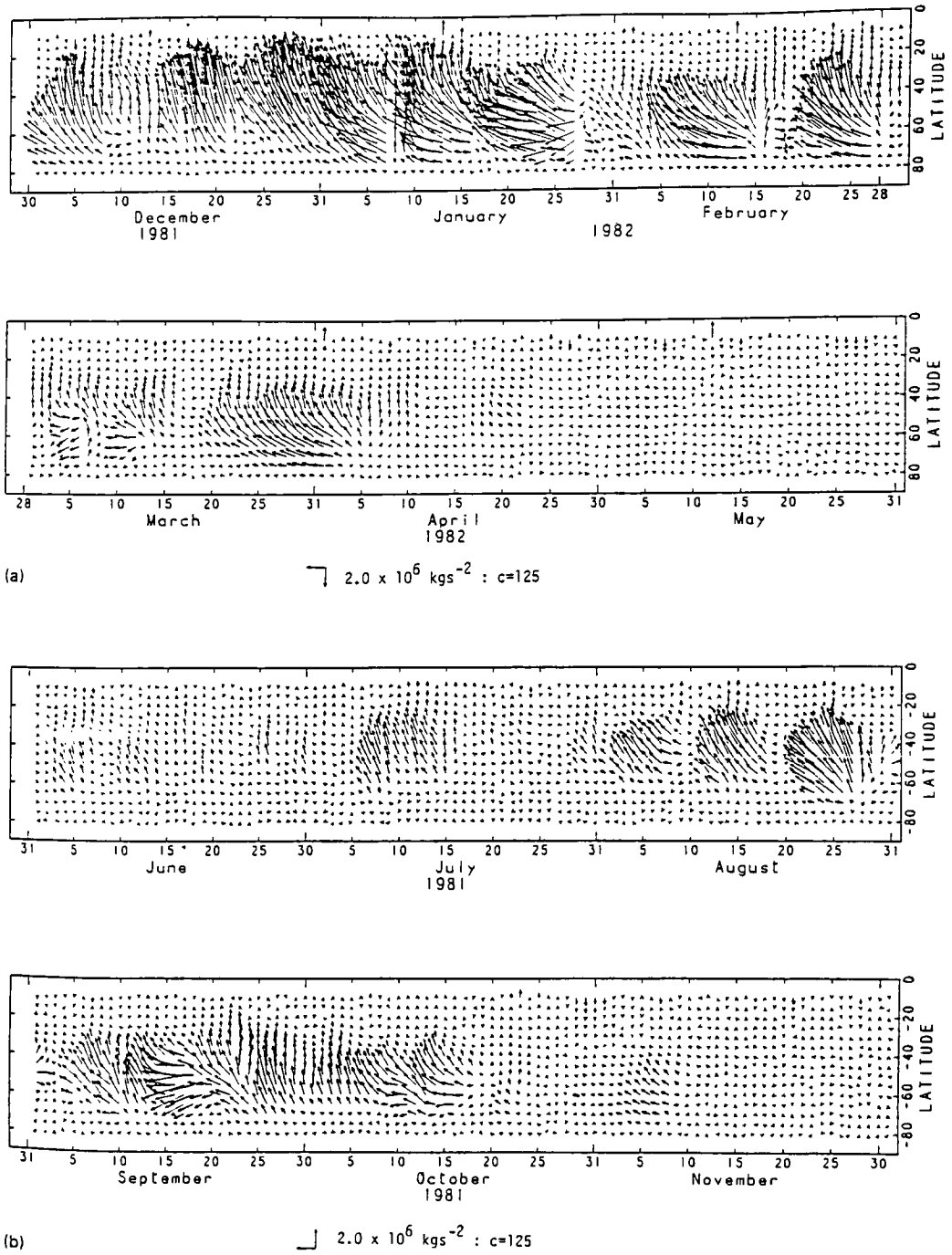

Fig. 1.2 Latitude-time sections of the total E-P flux at the 5 mb level from winter to summer for (a) the NH and (b) the SH. Reference arrow shows 2.0×10^6 kg s^{-2} for horizontal direction and $2.0\times10^6/c$ (c=125) kg s^{-2} for vertical direction.

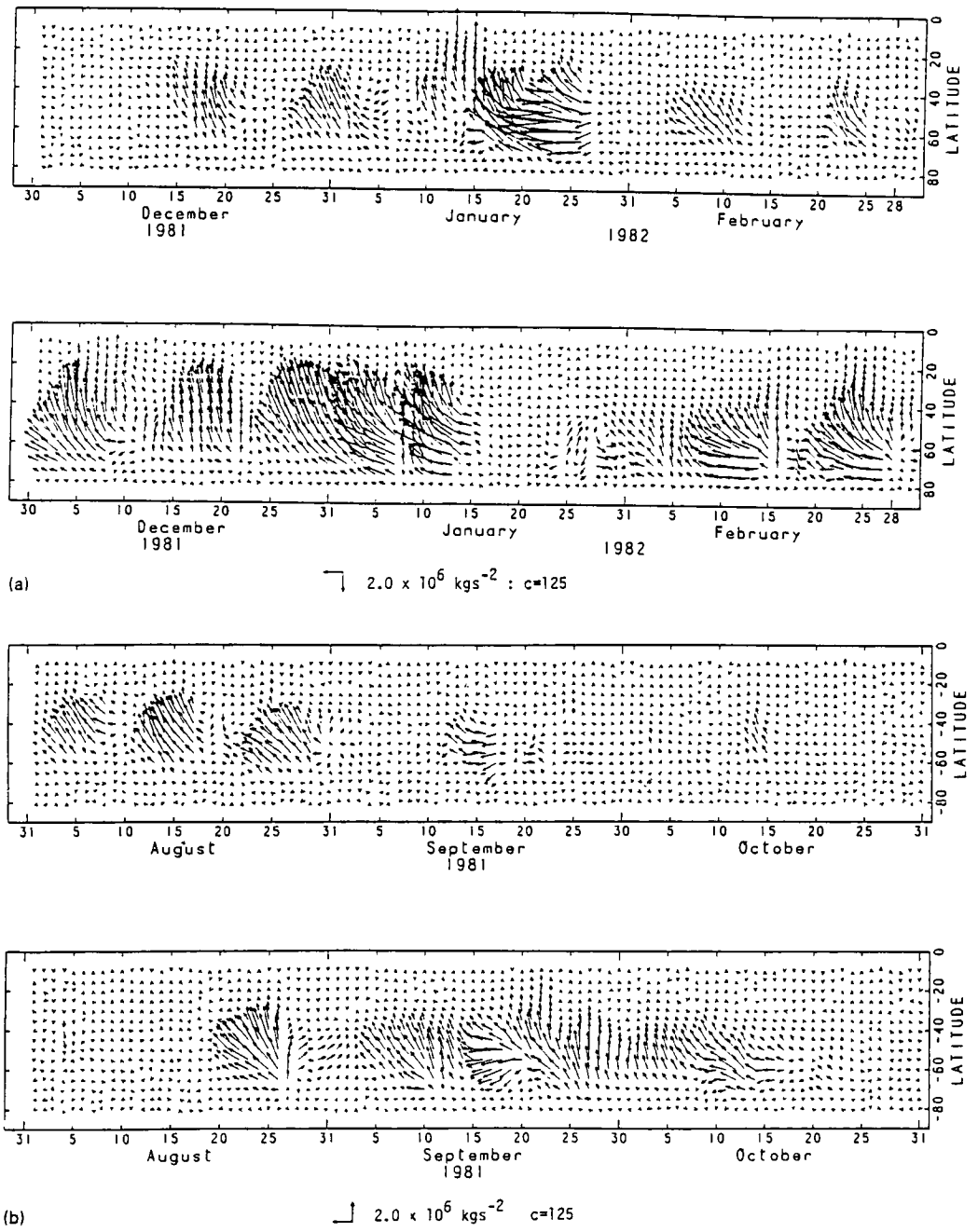

Fig. 1.3 Latitude-time sections of the E-P flux for wavenumbers 1 (lower) and 2 (upper) at the 5 mb level for selected three-months periods: (a) from December 1981 to February 1982 in the NH and (b) from August 1981 to October 1981 in the SH. Reference arrow shows 2.0×10^6 kg s^{-2} for horizontal direction and $2.0\times10^6/c$ (c=125) kg s^{-2} for vertical direction.

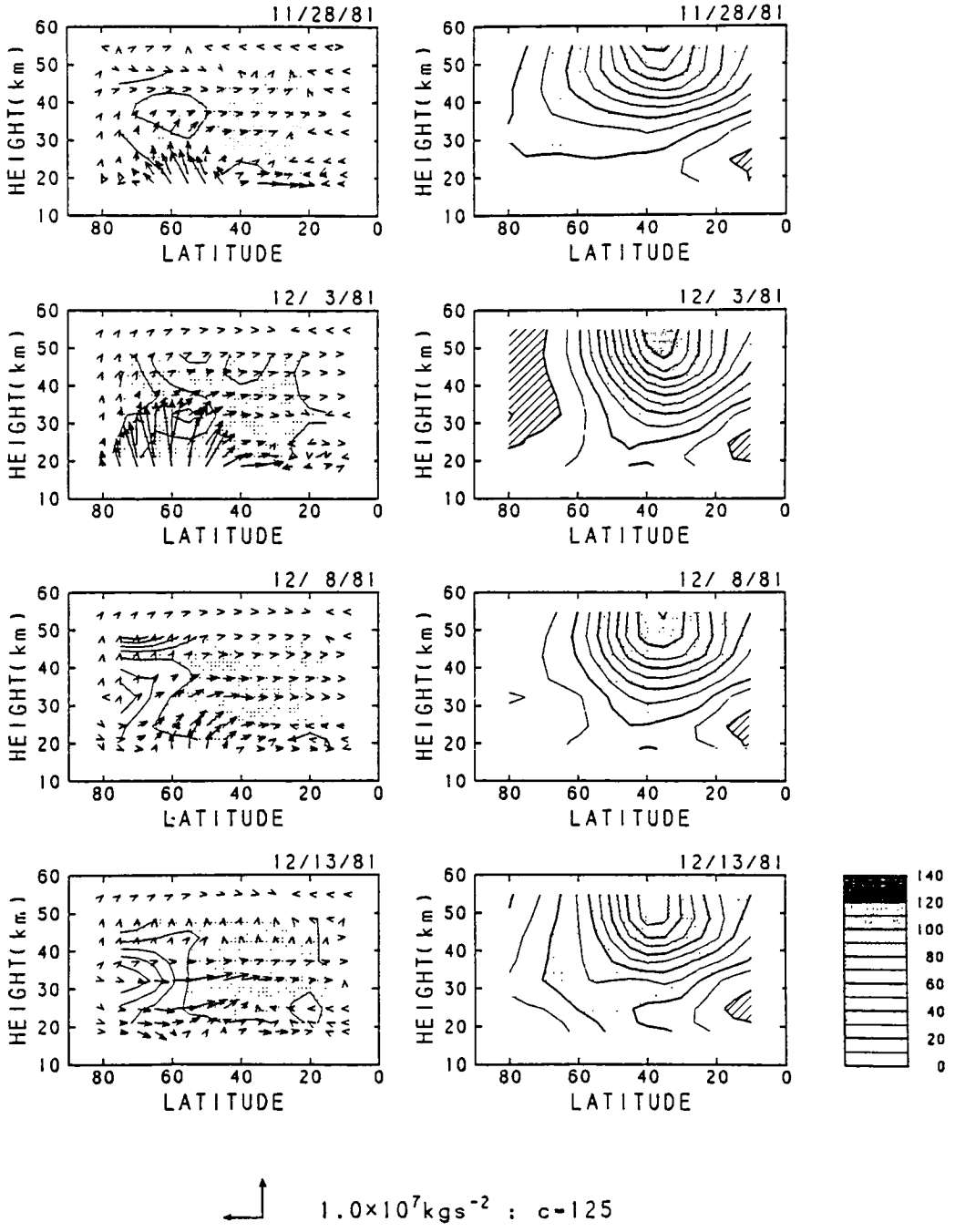

Fig. 1.4 Latitude-height sections of the total E-P flux and its divergence expressed as the zonal force per unit mass, D_F, (left) and the mean zonal wind (right) for the NH from 28 November to 13 December 1981. Reference arrow shows 1.0×10^7 kg s^{-2} for horizontal direction and $1.0\times10^7/c$ (c=125) kg s^{-2} for vertical direction. The contour interval for D_F is 10^{-4} m s^{-2}; negative values are shaded. Absolute values of the wind speed are shown by tone patterns (see the tone bar, unit: m s^{-1}). Easterlies are over oblique lines.

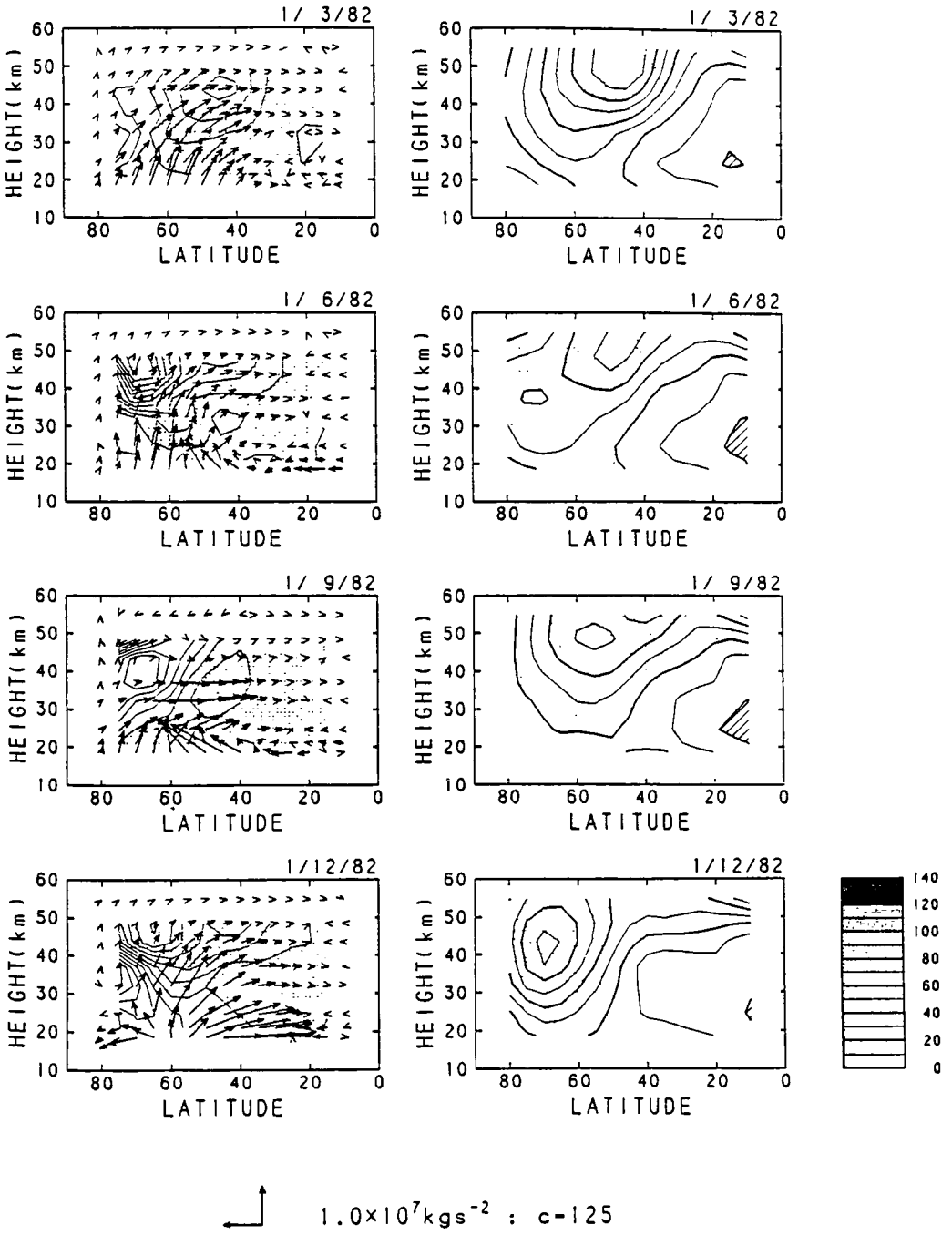

Fig. 1.5 As Fig. 1.4 but for the NH from 3 to 12 January 1982.

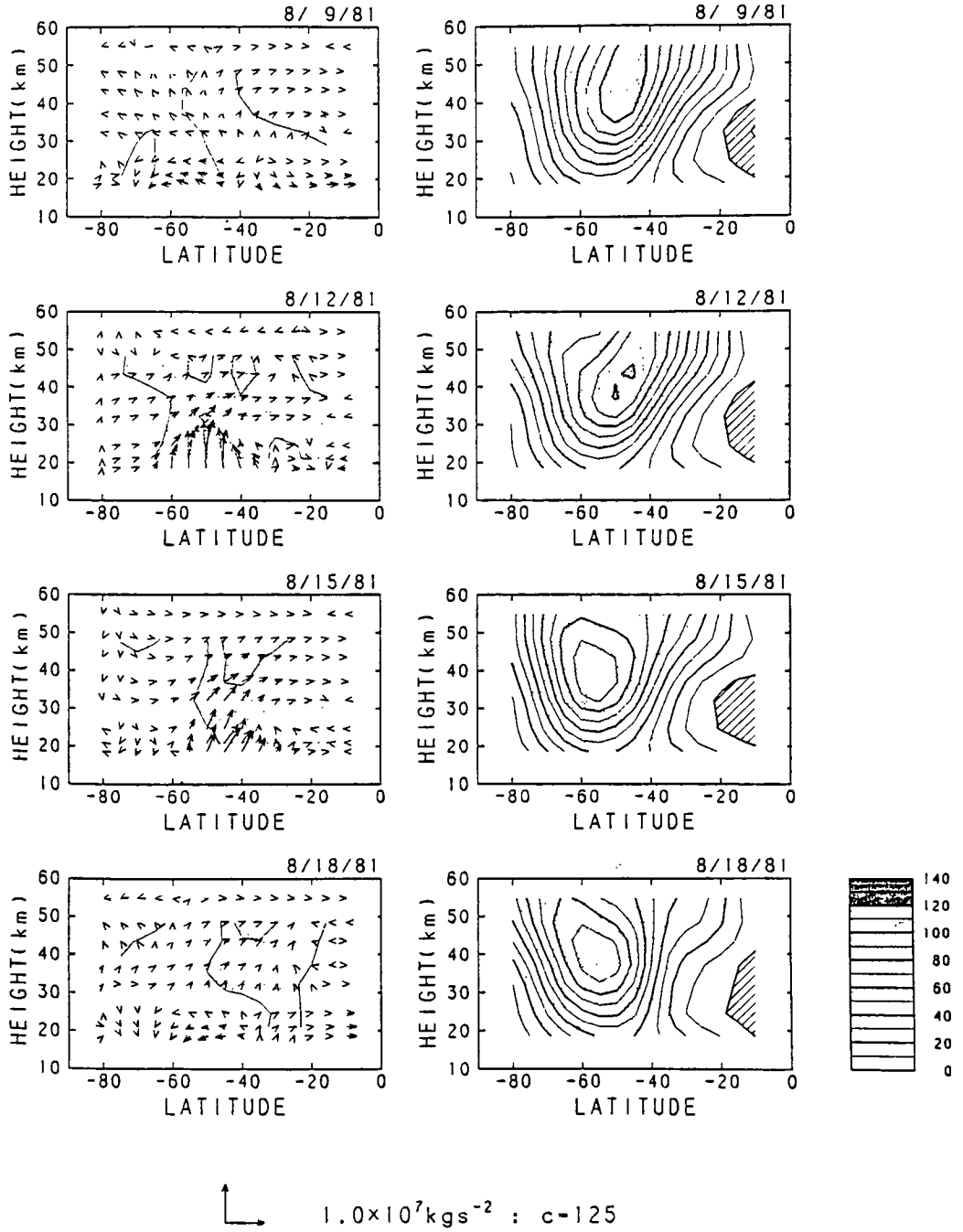

Fig. 1.6 As Fig. 1.4 but for the SH from 9 to 18 August 1981.

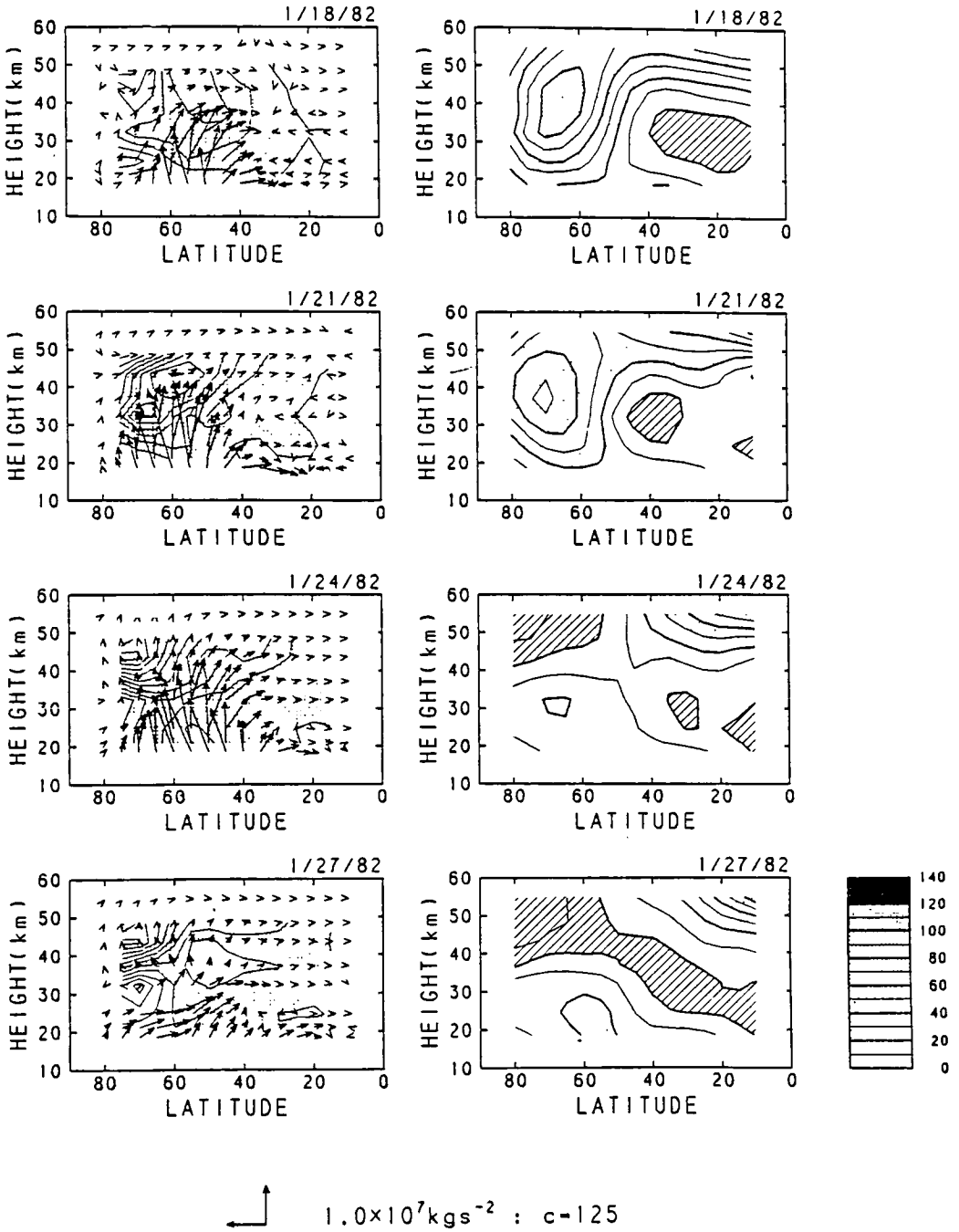

Fig. 1.7 As Fig. 1.4 but for the NH from 18 to 27 January 1982.

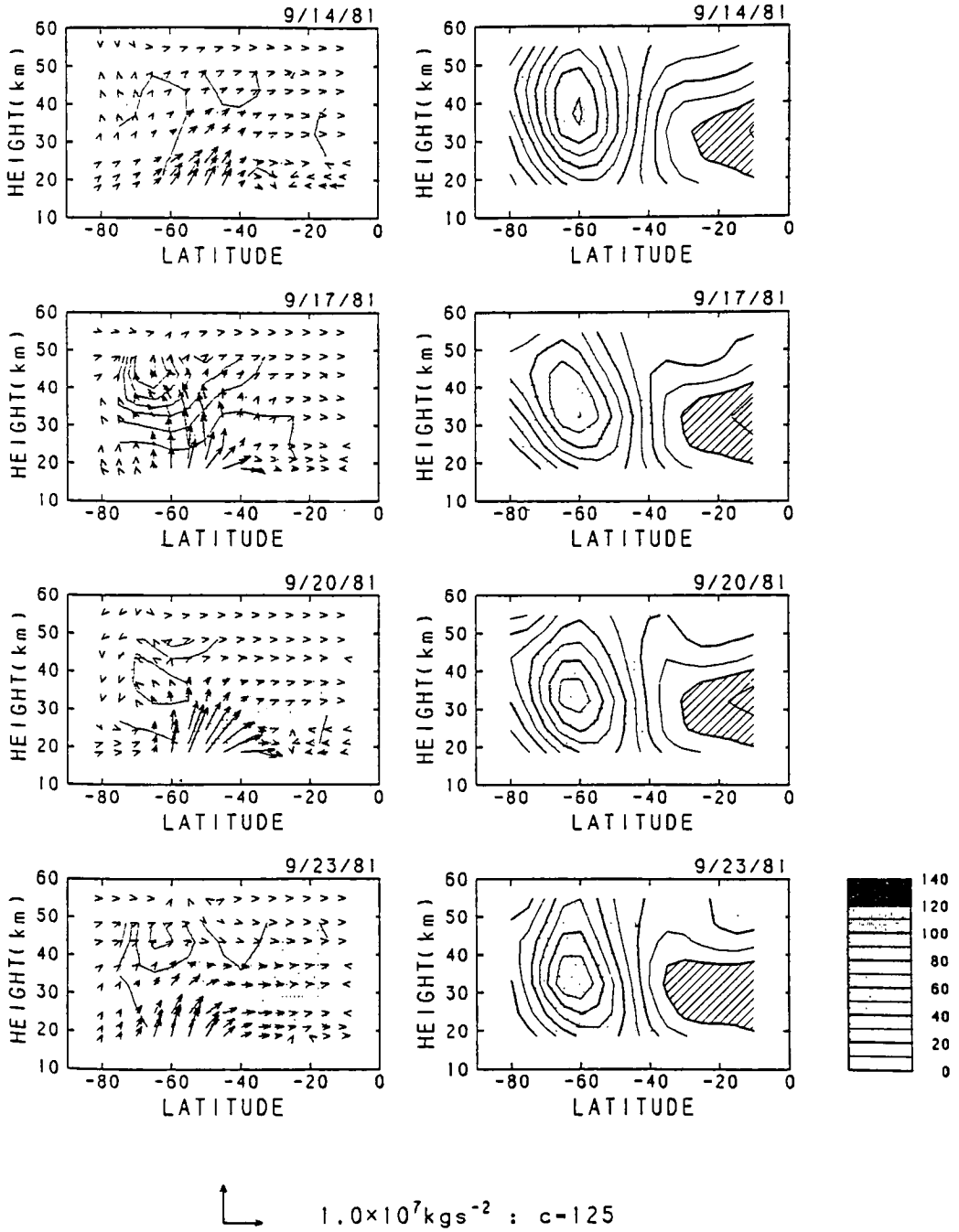

Fig. 1.8 As Fig. 1.4 but for the SH from 14 to 23 September 1981.

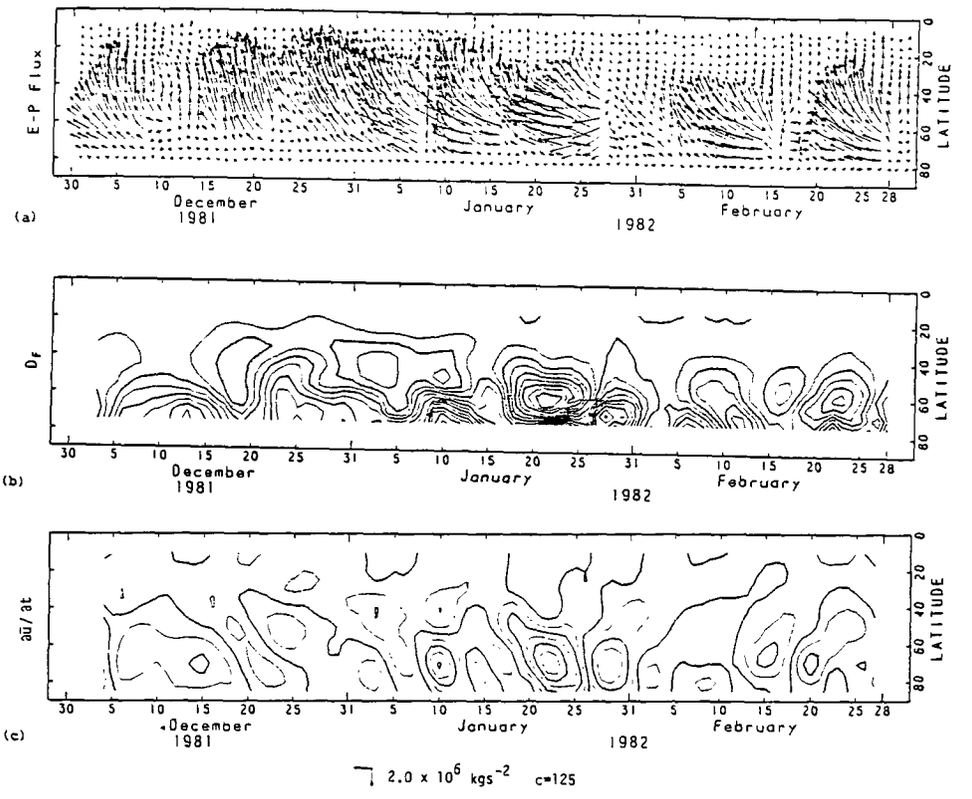

Fig. 1.9 Latitude-time sections of (a) the total E-P flux; (b) its divergence expresses as the zonal force per unit mass (D_F); and (c) the time changes of the mean zonal wind ($\partial\bar{u}/\partial t$) at the 5 mb level from December 1981 to February 1982 in the NH. The contour intervals of (D_F) and ($\partial\bar{u}/\partial t$) are 4.0 m s^{-1} day^{-1} and 2.0 m s^{-1} day^{-1} respectively. Negative values are shaded.

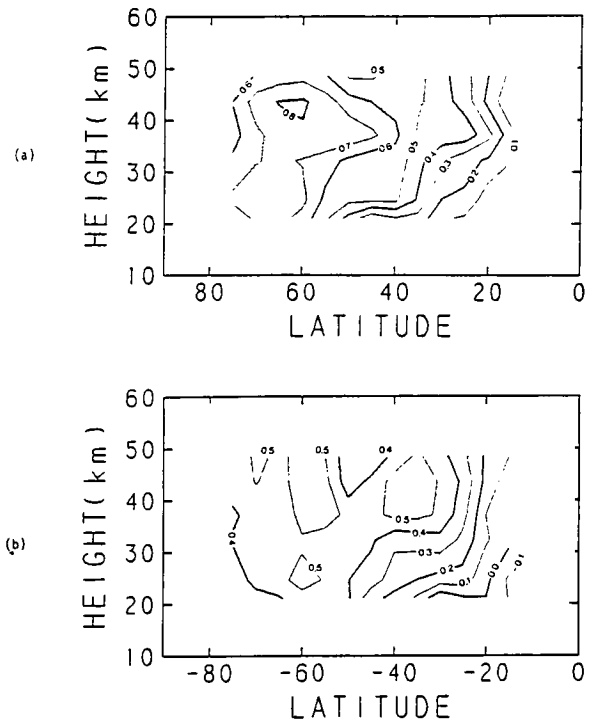

Fig. 1.10 Latitude-height sections of correlation coefficients between D_F and $\partial \bar{u}/\partial t$, $COR(D_F, \partial \bar{u}/\partial t)$, for (a) the NH and (b) the SH.

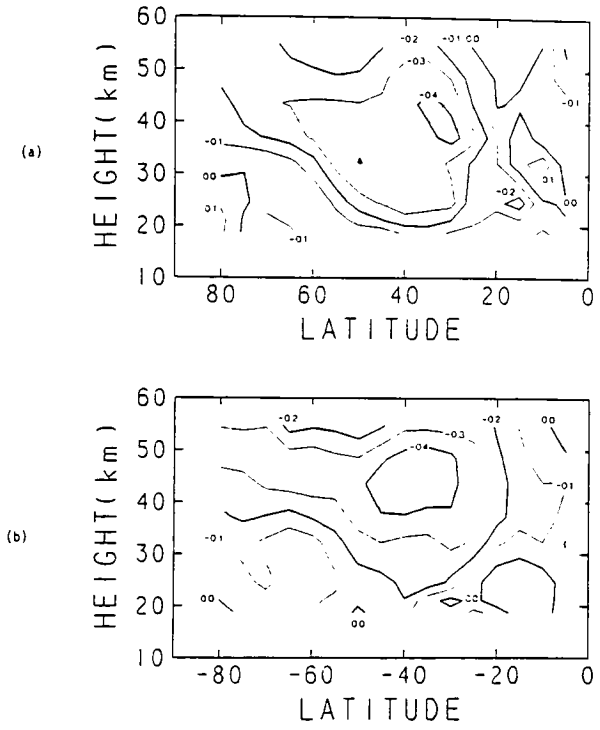

Fig. 1.11 As Fig. 1.10 but for the coefficient $COR(|F|, \partial\bar{u}/\partial t)$ in (a) the NH and (b) the SH.

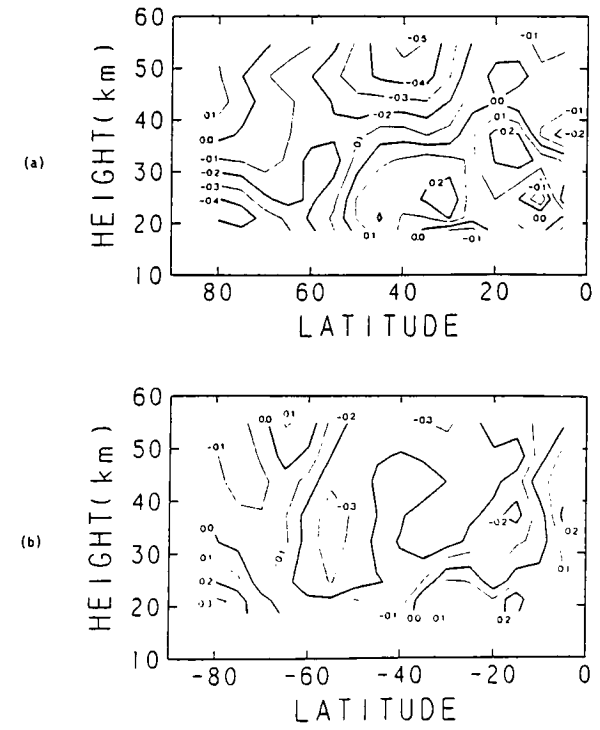

Fig. 1.12 As Fig. 1.10 but for the coefficient $COR(|F|, \bar{u})$ in (a) the NH and (b) the SH.

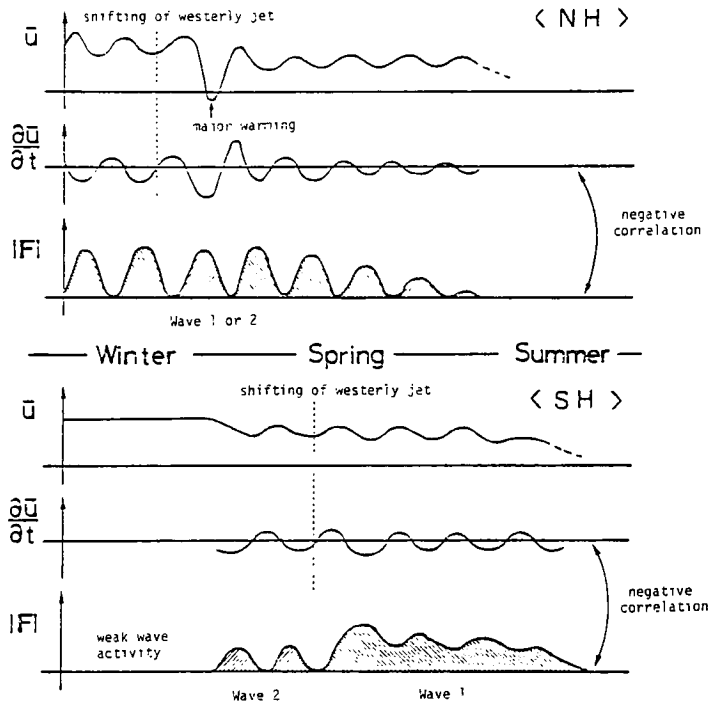

Fig. 1.13 Schematic diagram on the seasonal march of the mean zonal wind, its time changes and the wave activity represented as $|F|$ from winter to summer for (upper) the NH and (lower) the SH.

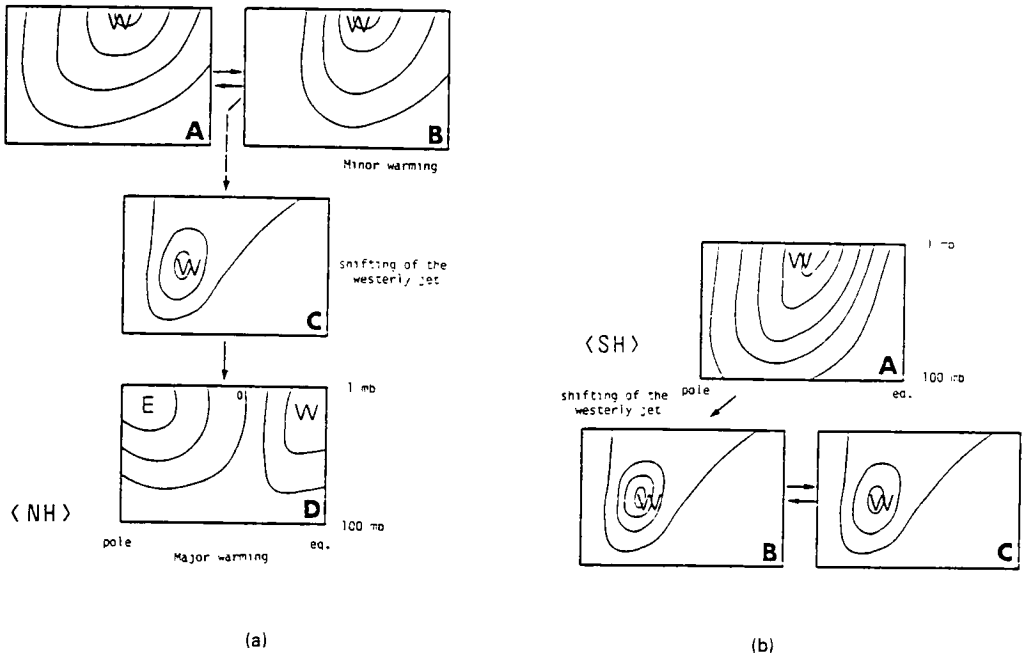

Fig. 1.14 Schematic vertical cross-sections on the time evolution of the mean zonal wind for (a) the NH and (b) the SH.

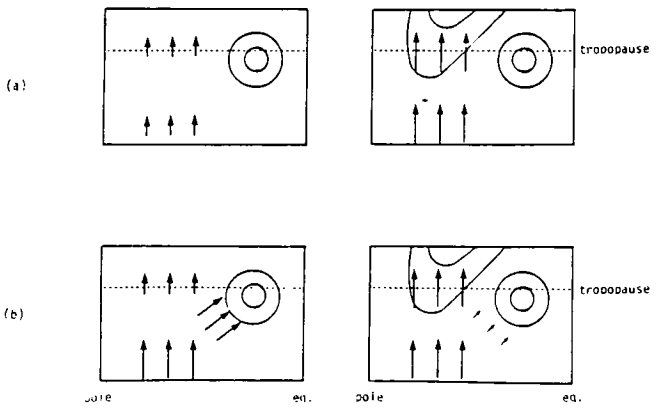

Fig. 1.15 Schematic vertical cross-sections of the mean zonal wind and the wave activity for two hypotheses (see text).

Year	QBO	Jun.	Jul.	Aug.	Sep.	Data source
1968	E					
69	W			*		Nimbus 3 SCR: Fritz and Soules (1970)
70	E					
71	W			*		Nimbus 4 SCR: Labitzke and Barnett (1973)
72	E					
73	W			*		Nimbus 5 SCR
74	(E)		*			Nimbus 5 SCR
75	—					
76	W					
77	E					
78	W					
79	E		*			NMC: Hartmann *et al.* (1984)
80	W				*	SSU
81	W			*		NMC
82	E		*			NMC

Table 1.1 Relation between the time of the shifting of the stratospheric westerly jet in the SH and the wind regime of the quasi-biennial oscillation at the 50 mb level. The wind regime of the QBO (second) is derived from Fig. 3 in Labitzke (1982). Notations are; W: westerly; E: easterly; ( ): weak zonal wind; -: undetermined. The time of the shifting is depicted by the symbol * It is classified as the first, middle and last part of a month. For the first four observations the time of the shifting is deduced from the thermal field in the upper stratosphere. For reference, data source and observers are listed; lack of observer means that the data source belongs to our laboratory (Kyoto).

PART 2

Planetary Wave Activity in the Troposphere and Stratosphere during the Northern Hemisphere Winter

2.1 Introduction

The propagation and temporal variation of planetary waves in the atmosphere are fundamental problems in observational and theoretical studies of dynamical meteorology These problems have been discussed for a long time, and still are fascinating to many meteorologists.

In the winter stratosphere of the NH a spectacular event occurs, a so-called stratospheric sudden warming. Since Matsuno(1971)'s pioneering numerical experiment on the sudden warming, it has been widely recognized that this event comes from the dynamical interaction between the mean flow and the vertically propagating planetary waves originated in the troposphere.

Recently. because of the advantages of using satellite measurements, many observations of the sudden warming have been performed to confirm Matsuno's concept by using a powerful tool, Eliassen-Palm (E-P) flux diagnostics. (e.g. Palmer 1981a, b; O'Neill and Youngblut 1982; Kanzawa 1982; Gille and Lyjak 1984; see also a suggestive review on the theoretical aspect of the sudden warming by McIntyre 1982.) The E-P flux diagnostics are particularly useful for understanding wave-mean flow interaction and planetary wave propagation. For details about the formalism and the motivation for the use of the E-P flux, the reader may refer to Edmon *et al.* (1980) and Dunkerton *et al.* (1981)

With regards to sudden warmings, there has been much discussion of why anomalous amplification of planetary waves takes place in the troposphere, in connection with various observations of low frequency variability in the troposphere. This atmospheric variability should include anomalous amplification related to a so-called blocking phenomenon (Wallace and Blackmon 1983).

However, most of these studies have treated the tropospheric and stratospheric circulations as systems separate from each other They only stressed the dynamical links between the troposphere and stratosphere. For example, in his model study of the stratospheric sudden warming, Matsuno (1971) simply assumed the extreme growth of planetary waves as a lower boundary condition. It is the same with studies of the low frequency variability in the tro-

posphere; few of them have mentioned the relation to the stratospheric circulation.

Tung and Lindzen (1979) made an approach to explaining the amplification of planetary waves by regarding the troposphere and stratosphere as a whole system. Using a general circulation model, Boville (1984) showed the influence of the stratospheric wind structure on the tropospheric circulation, and stressed the importance of treating the troposphere and stratosphere as a whole system. On observational studies, Muench (1965) and Hirota and Sato (1969) showed the vertical propagation of planetary waves from the troposphere to the stratosphere, by presenting time-height cross-sections of wave amplitudes of wavenumbers 1 and 2. Many people observing the tropospheric and stratospheric circulations have noticed that some wave events in the troposphere can be traced into the stratosphere, but sometimes they cannot. At present, however, there is few good presentations about the relation of the wave activity between the troposphere and stratosphere.

This study will present the whole picture of planetary wave activity in the troposphere and stratosphere, by showing that there exist two different types of correspondence of wave activity between the troposphere and stratosphere. Calculation of physical quantities is the same as in PART 1 except that the buoyancy frequency is allowed to be vary with latitude and height. We applied a 5-day running mean to most of the figures such as time-height and time-latitude cross-sections for improving the graphical appearance.

2.2 General Description

As predicted by the theory of E-P flux diagnostics, the vertical component of the E-P flux, $F(z)$, is a measure of the vertical propagation of wave activity. Fig. 2.1 shows a time-height cross-section of $F(z)$ averaged over the latitude band of 40-70°N (not area-weighted). The validity for selecting these latitude band will be confirmed in section 2.3. Major maximum points of the time series for each level are marked by a '+' sign, which was objectively determined from the low-pass ($\geqq$6.7 days) filtered data. (We used this data only to find maxima.) The contour interval is magnified five times above the 200 mb level. PART 1 may be consulted for a detailed description of the dynamical aspect of the 1981/82 winter stratosphere in the NH. We simply note for a reminder that a sudden warming occurred in late January 1982.

At first sight, we can see that the magnitude of $F(z)$ varies with a period of 10-15 days both in the troposphere and stratosphere; however, the correspondence of wave activity in the troposphere and stratosphere is different during the pre- and post-warming period. In December and early January the time variation of wave activity in the troposphere and stratosphere is out-of-phase; when the tropospheric wave activity is vigorous the stratospheric wave activity is quiet, and vice versa. In middle and late January the correspondence of wave activity in the troposphere and stratosphere is not clear The major wave event in the stratosphere around 22 January, which was associated with the sudden warming, cannot be as simply traced back to the troposphere as wave events seen in February After the sudden warming, in February and March, maximum wave activity can be traced from the troposphere to the stratosphere. The vertical propagation of planetary waves is obvious as shown by Muench (1965) and Hirota and Sato (1969) However, the progress of wave activity is not regular but lagged around the tropopause level. This feature is similar to the result of Madden (1983), who showed the effect of the interference of traveling and stationary waves by using composited data to extract the 16-day waves.

As will be partly supported later (Figs. 2.5 and 2.15), the main contribution to the total wave activity comes from wavenumber 1 to 3 in the troposphere during the NH winter Really. we can reproduce almost the same figure as Fig. 2.1 with contributions from wavenumber 1 to 3. Thus, the features seen in Fig. 2.1 are due to the planetary scale wave activity

Regarding the negative correlation of wave activity in the troposphere and stratosphere, Koermer and Kao (1980) briefly reported a similar feature from the analysis of eddy kinetic energy. They compared the major and minor stratospheric warmings in the winter of 1976-77 and 1975-76 respectively and noted that the time variation of the eddy kinetic energy in the troposphere and stratosphere is almost out-of-phase for the minor warming, but in-phase for the major warming.

Fig. 2.2 shows a time-height cross-section of wave driving D_F It is striking that a strong convergence zone exists around the 400 mb level, and that its magnitude varies with a time scale of 10-15 days. In their climatological studies of monthly or seasonal mean statistics using E-P flux diagnostics, the convergence zone in the upper troposphere is described by Edmon *et al.* (1980) and Geller *et al.* (1983,1984) for the NH and by Hartmann *et al.* (1984) and Mechoso *et al.* (1985) for the SH. We also observe the large

temporal variation of D_F in the upper stratosphere; however, we do not discuss it here (in detail, see PART 1)

By comparison with Fig. 2.1, we can see that the time variation of D_F in the upper troposphere is closely related to the vertical component of the E-P flux, $F(z)$; they are in good negative correlation. (Notice $D_F<0$.) We will show later that $(\rho_0(z)a\cos\theta)^{-1}\partial F(z)/\partial z$ is the main contributor to the wave driving D_F in the upper troposphere (see Fig. 2.4).

We will briefly look into the following evidence in the upper troposphere (Figs. 2.3- 2.5) before moving into the next section. Fig. 2.3 shows line plots of wave driving D_F and $\partial\bar{u}/\partial t$ averaged over the 40-70°N latitude band and 250-500 mb pressure level. We regard this region as representative of the upper troposphere. The difference of the mean value of D_F and $\partial\bar{u}/\partial t$ is large; this means strong poleward residual circulation. However, they are in reasonable correlation (correlation coefficient : r=0.51) For investigating the effect of wave driving on the zonal flow in the troposphere, correlation statistics of the relation between D_F and $\partial\bar{u}/\partial t$ were performed by Hartmann *et al.* (1984) for the 1979 winter of the SH and Baldwin *et al.* (1985) for the 1979 winter of the NH. In the former analysis, using each latitude-height grid point, they found a good correlation (r>0.6) around the tropopause level. In the latter study, however, for the upper troposphere averaged over 30-60°N and 200-500 mb, they did not find as strong a relation (r=0.34). Extending our statistics for each latitude-height grid point, we find a maximum r>0.6 in the upper troposphere. The reason for the low correlation coefficient of Baldwin *et al.* (1985) may be due to an inappropriate selection of the representative region.

Figs. 2.1 and 2.2 suggested that the vertical derivative of $F(z)$ is important to the wave driving D_F in the upper troposphere. Fig. 2.4 shows line plots of the contribution of $(\rho_0(z)a\cos\theta)^{-1}\ \partial F(y)/\partial y$ and $(\rho_0(z)a\cos\theta)^{-1}\ \partial F(z)/\partial z$ Around the high latitude upper troposphere, most of the contribution to D_F comes from the vertical derivative of $F(z)$.

Fig. 2.5 shows line plots of the total (wavenumber 1 to 6) $F(z)$ and the contribution from wavenumber i (i = 1 to 3) for the same region as Figs. 2.3 and 2.4; the contribution from wavenumber 4 to 6 is small during this period. Most of the total variation is explained by the wavenumber 2 (and 3) contribution. (Some statistical comparisons with the SH will be shown in section 2.5) The tendency of the wavenumber contributions of wave driving D_F is similar to that of $F(z)$ as suggested by Fig. 2.4. Because the wave 2 activity is still

the main contributor to the total $F(z)$ in the lower stratosphere (not shown), the out-of-phase relationship seen in Fig. 2.1 do not appear to be due to the selective transmission of planetary scale waves.

In the upper stratosphere, on the other hand, it was shown in PART 1 that most of the wave activity for the 1981/82 winter in the NH is accounted for by wavenumber 1 planetary waves. Careful tracing of each wave event shows that wavenumber 2 activity is sometimes deformed into wavenumber 1 activity with increasing altitude. This strongly suggests a wave-wave interaction process (Smith 1983a; Smith *et al.* 1984); however, we will not discuss this possibility here. Moreover, when we look at the time variation of each wavenumber in Fig. 2.5, the rhythm of total $F(z)$ with a period of 10-15 days is obscured. Because of these reasons, we show total wave activity, not each wavenumber activity.

2.3 Features around the Tropopause Level

In this section we present the latitudinal variation of eddy properties ($F(z)$ and $F(y)$) and zonal mean field ($\bar{u}$ and refractive index) around the tropopause level from time-latitude cross-sections. We shall pay particular attention to the dynamical difference between the pre- and post-warming periods.

Figs. 2.6 (a), (b) and (c) show time-latitude cross-sections of $F(z)$ for 500, 300 and 100 mb, respectively From these figures we reconfirm the correspondence of $F(z)$ between the troposphere and stratosphere in detail. Throughout the period the time variation of $F(z)$ with a time scale of 10-15 days is obvious for the three levels. At the 500 mb level (Fig. 2.6 (a)) there are two major wave events in December (around December 12 and 26) Then at the 300 mb level (Fig. 2.6 (b)), one of the two events (around December 12) diminishes, the other (around December 26) disappears and a new major wave event appears (around 20 December) Finally, at the 100 mb level (Fig. 2.6 (c)) two major wave events around 20 December and early January are apparent. Thus the time variation of wave activity in the troposphere (Fig. 2.6 (a)) and the lower stratosphere (Fig. 2.6 (c)) looks out-of-phase as seen in Fig. 2.1 On the other hand, in the post-warming period, most of the major wave events can be traced through 500->300->100 mb with a time-lag.

Another interesting feature is latitudinal variation of the maximum $F(z)$

At the 500 mb level (Fig. 2.6 (a)) the maximum $F(z)$ lies around 50°N and the magnitude of $F(z)$ seems somewhat larger in the post-warming period than in the pre-warming period. At the 300 mb level (Fig. 2.6 (b)), however, it shifts around 40-45°N in the pre-warming period, while it still lies around 50°N in the post-warming period. At the 100 mb level (Fig. 2.6 (c)) it shifts poleward, around 60°N.

Fig. 2.7 shows a time-latitude cross-section of the horizontal component of the E-P flux, $F(y)$, at the 300 mb level; the features of $F(y)$ are almost the same around the tropopause levels. For most of the period we see a positive region at high latitudes, a negative region at middle latitudes and again a positive region at low latitudes. These latitudinal variations of $F(y)$ should contribute to wave driving D_F from $\partial F(y)/\partial y$ Fig. 2.4 showed, however, the contribution of $(\rho_0(z)a\cos\theta)^{-1}\partial F(y)/\partial y$ is smaller than that of $(\rho_0(z)a\cos\theta)^{-1}\ \partial F(z)/\partial z$, and that $(\rho_0(z)a\cos\theta)^{-1}\ \partial F(y)/\partial y$ is generally positive at the 40-70°N latitude band as expected from Fig. 2.7 Compared with the figure of $F(z)$ at the same level (Fig. 2.6 (b)), times of maximum $F(z)$ and minimum (negative maximum) $F(y)$ occur almost simultaneously in the pre-warming period, while minima of $F(y)$ are delayed a few days in the post-warming period. In their model calculation of the life cycle of baroclinic waves, Edmon *et al.* (1980) reported a similar feature in the post-warming period. The magnitude of $F(y)$, particularly positive $F(y)$ at high latitudes, is larger in the pre-warming period than in the post-warming period.

We have noted many differences of eddy properties in the pre- and post-warming period. Now, we will show zonal mean field such as mean zonal geostrophic wind and refractive index. Following Kanzawa (1982) we define the refractive index Q_k for a stationary linear wave by

$$Q_k = \frac{\bar{q}_y}{\bar{u}} - \frac{k^2}{(a\cos\theta)^2} - \frac{f^2}{4N^2H^2} \tag{14}$$

where

$$\bar{q}_y = \frac{2\Omega\cos\theta}{a} - \frac{\partial}{a\partial\theta}\left(\frac{1}{\cos\theta}\frac{\partial}{a\partial\theta}\bar{u}\cos\theta\right) - \frac{\partial}{\rho_0\partial z}\left(\rho_0\left(\frac{f}{N}\right)^2\frac{\partial\bar{u}}{\partial z}\right) \tag{15}$$

Here k is the zonal wavenumber In the real atmosphere, planetary waves are generally neither stationary nor linear Therefore we use the refractive index defined by (14) just as a rough indication of the mean state and we treat N as a constant ($=2.0\times10^{-2}\ s^{-2}$) for simplicity Because the first term of right hand side of (14) is dominant for the earth's atmosphere, we will show Q_0 as the refractive index in this study.

Fig. 2.8 shows the mean zonal geostrophic wind at the 400 mb level. The tropospheric jet is located around 35°N in December, while around 30°N in February. In connection with this movement, the meridional gradient of the zonal wind at high latitudes is steeper in December than in February Fig. 2.9 of the refractive index clearly shows these differences; low value regions (hatched under 60) around 50°N in December move equatorward to around 30-40°N in early January, and remain there until the end of March. In middle March, the tropospheric jet shifts poleward and the latitudinal gradient of the zonal wind at high latitudes becomes steeper again for about 10 days. It is interesting to find in Fig. 2.1 that, around March 16, the tropospheric wave activity is vigorous while the stratospheric wave activity is quiet, which is the same relation as typically seen in the pre-warming period.

According to the ray theory (*cf* Karoly and Hoskins, 1982), wave activity is refracted towards larger values of the refractive index. If we apply this principle to understand the dynamical difference between the pre- and post-warming period, we can suppose that in the pre-warming period waves are refracted more equatorward because of the positive slope of the refractive index at middle latitudes and that in the post-warming period waves are guided more upward into the stratosphere because of the minimum Q_0 around 30-40°N. This explanation is consistent with Fig. 2.6 (b) which shows more equatorward position of maximum $F(z)$ at the 300 mb level in the pre-warming period than in the post-warming period. Thus the two types of correspondence of the wave activity in the troposphere and stratosphere are closely related to the zonal wind profile.

2.4 Comparison between the Pre- and Post-Warming Periods

The previous section has shown many dynamical differences between the pre- and post-warming periods for the 1981/1982 winter in the NH. To summarize these features we chose two typical periods, 30 days of the pre-warming period (beginning at 4 December) and those of the post-warming period (beginning at 1 February), and make period-mean latitude-height cross sections for the two period. Hereafter, we call the selected pre-warming period 'period 1' and the selected post-warming period 'period 2'

In the cross-sections of the mean zonal geostrophic wind (Figs. 2.10 (a) and (b)), we see following differences between periods 1 and 2: The position

of the tropospheric jet is more poleward in period 1 (35°N) than in period 2 (25-30°N) The latitudinal gradient of the zonal wind at high latitudes (around 60-80°N) in the troposphere and lower stratosphere is steeper in period 1 than in period 2. Referring to a climatological study of monthly mean cross-sections for four years by Geller *et al.* (1984), we see that the latitudinal gradient of the zonal wind at high latitudes of the troposphere and lower stratosphere tends to become more gradual from December to February for each of their four years. The stratospheric westerlies in period 2 are weaker in the mid latitude upper stratosphere and slightly stronger in the high latitude stratosphere.

Figs. 2.11 (a) and (b) show the latitude-height cross-sections of the refractive index Q_0 calculated from period-mean wind fields (Figs. 2.10 (a) and (b)) The difference in the troposphere is not as noticeable as can be seen in Fig. 2.9; however, these two pictures look different in the stratosphere. Low value region in the mid-latitude lower stratosphere is more prominent in period 2 than in period 1 Another low value region in the high latitude upper stratosphere is pushed out more downward and equatorward in period 1 than in period 2. From these features, we can expect that the vertical propagation of planetary waves in the stratosphere would be more effective in period 2 than in period 1

Figs. 2.12 (a) and (b) show the latitude-height cross-sections of the E-P vectors and wave driving D_F They were calculated from 30 days average of daily values, not from 30 days mean field. In plotting the E-P flux in the vertical cross-section we follow the graphical convention as described by Baldwin *et al.* (1985); we have multiplied F by the factor $\exp(z/H)$ In the troposphere and lower stratosphere the E-P vectors branch off equatorward and poleward around the tropopause level in period 1, while they regularly point upward with a slight equatorward drift in period 2. In the stratosphere the E-P vectors at high latitudes point more equatorward in period 1 than in period 2. These features of the wave refraction in the troposphere and stratosphere are in broad agreement with Figs. 2.9 and 2.11 The magnitude of $F(z)$ in the lower troposphere is larger in period 2 than in period 1 and that of $F(y)$ around the tropopause level, both positive and negative, is larger in period 1 than period 2. As for the wave driving D_F, there exists a strong convergence zone at high latitudes at the 400 mb level. In period 1 another convergence zone exists around 35°N and 250 mb level; this may tend to maintain the weaker tropospheric jet in period 1 (see Fig. 2.10) In period 1,

there is a strong divergence zone in the polar middle stratosphere; this suggest the source of wave activity in the stratosphere. We can summarize these feature of Figs. 2.10- 2.12 as showing that the atmosphere in the troposphere and lower stratosphere is more barotropic in period 1 and more baroclinic in period 2.

Recently, using a stratospheric general circulation model, Boville (1986) have made a comparison of the tropospheric and stratospheric circulations before and after a major warming. By showing figures of zonal wind, refractive index and E-P vectors, he suggested that the stronger stratospheric winds in the pre-warming period tend to inhibit the vertical propagation of wave activity into the polar stratosphere, while the weaker stratospheric winds in the post-warming period provide more effective vertical propagation of wave activity into the polar stratosphere. There are some differences between our results and Boville(1986)'s; for example, our zonal winds at high latitudes are slightly weaker in the pre-warming period than in the post-warming period. However, our results of Figs. 2.10- 2.12 are consistent with those of Boville (1986), as for the point that the vertical propagation of wave activity is more effective in the post-warming period than in the pre-warming period.

2.5 Concluding Remarks

This study has shown that there are typically two types of correspondence between wave activity in the troposphere and stratosphere for the 1981/82 winter in the NH: one is characterized by an out-of-phase relationship between wave activity in the troposphere and stratosphere, and the other by upward propagation from the troposphere to the stratosphere. These two types of correspondence go on with durations of more than one month before and after the sudden warming respectively. The dynamical aspect of the two periods is summarized in section 2.4; briefly, the atmosphere in the troposphere and lower stratosphere is more barotropic in the pre-warming period and more baroclinic in the post-warming period for the 1981/82 winter in the NH. Moreover, it has been shown that there exists a strong convergence zone of the E-P flux in the upper troposphere, and that the magnitude of it varies with a typical time scale of 10-15 days. This is closely related to the time variation of wave activity in the troposphere and stratosphere.

Some of the readers may be curious whether these atmospheric features can

be seen for other winters or for the SH. Data set covering two years for both hemispheres is available to our laboratory (Kyoto) Therefore we will briefly describe another winter of the NH and the SH. In the 1982/83 winter in the NH, the two types of correspondence can sometimes be seen; however, most of the events are sporadic and not continuous. Also, there is no scenario of the pre- and post-warming period. For the 1981 winter of the SH, Cross-sections similar to Figs. 2.1 and 2.2 are shown in Figs. 2.13 and 2.14 respectively From late August to September the vertical propagation of planetary waves is clearly suggested in the troposphere and lower stratosphere. In late July and October wave activity between the troposphere and stratosphere looks out-of-phase. As for wave driving D_F, it is clear that there exists a strong convergence zone in the upper troposphere, and that the magnitude of it varies with a time scale of 15-20 days. Thus the features seen in Figs. 2.1 and 2.2 for the NH are present in the SH as well.

However, there is an interesting difference in the wavenumber contribution to $F(z)$ between the NH and the SH. Fig. 2.15 shows 120 day mean $F(z)$ of each wavenumber (from 1 to 6) averaged over the 250-500mb and 40-70°N. The difference of contribution from wavenumber 1 to 3 is apparent between the NH and the SH. In the NH most of the contribution comes from wavenumber 2 (and 3), while in the SH from wavenumber 3 to 5 (or 6) In the NH, because of the prominent land-sea contrast, the planetary scale waves generated in the troposphere by orographic forcing and diabatic heating are the main contributors to the total wave activity of $F(z)$ On the other hand, in the SH, where the land-sea contrast is not as prominent, baroclinic disturbances with synoptic scale can account for the total wave activity of $F(z)$ Although the main contribution to $F(z)$ comes from different horizontal scale eddies between the NH and the SH, it is interesting to see in Figs. 2.1, 2.2 and 2.13, 2.14 that the time variation of total wave activity in the troposphere of both hemispheres have similar periodicity about two weeks.

Regarding the physical mechanism of the vertically propagating type, interference of stationary and traveling waves is a possible idea. Recently, Madden (1983), Smith (1985) and Hirooka (1986) have shown the evidence of interference between traveling and stationary planetary waves in the stratosphere. This mechanism is helpful for understanding the vertical propagation type; for example, the mechanistic model study of Hirota (1971) simply showed that both the time-dependent upward propagation of planetary waves and the interference of stationary and traveling waves have originally the same

dynamical aspect (See Figs. 6 and 8 of Hirota 1971.) However, as Hirota (1971) *a priori* postulated a periodic forcing in the lower atmosphere, the generation of traveling waves in the atmosphere should be a last problem to be solved.

The physical interpretation of the out-of-phase relationship of wave activity in the troposphere and stratosphere is not yet apparent. As suggested by the present study and Boville (1986), the zonal wind structure in the pre-warming period tends to suppress the vertical propagation of wave activity into the stratosphere. However, there still remains question of why the stratospheric wave activity becomes vigorous when the tropospheric wave activity is quiet. It would be an interesting problem to reproduce this feature by using a numerical model.

The result of Boville (1986) is also suggestive concerning a question of what determines the choice of these two types of correspondence. In a general circulation model using external forcing *fixed*, he found two different mean states for the winter stratosphere before and after a sudden warming similar to this study. This means that the two states come from the internal process of wave-mean flow interactions. Recently. Yoden *et al.* (1986) have found two typical circulation patterns in the 1983 winter of the SH; one is a single jet regime and the other has a double jet. They observed the transition from one to the other regime several times and proposed that this low-frequency variation can be understood as almost intransitive with multiple weather regimes. The annual variation is larger in the NH than in the SH; however, the result presented here suggests that there exist multiple states of the general circulation.

The main thrust of this part is to show the importance of treating the troposphere and stratosphere as a whole, in order to understand real atmospheric behavior

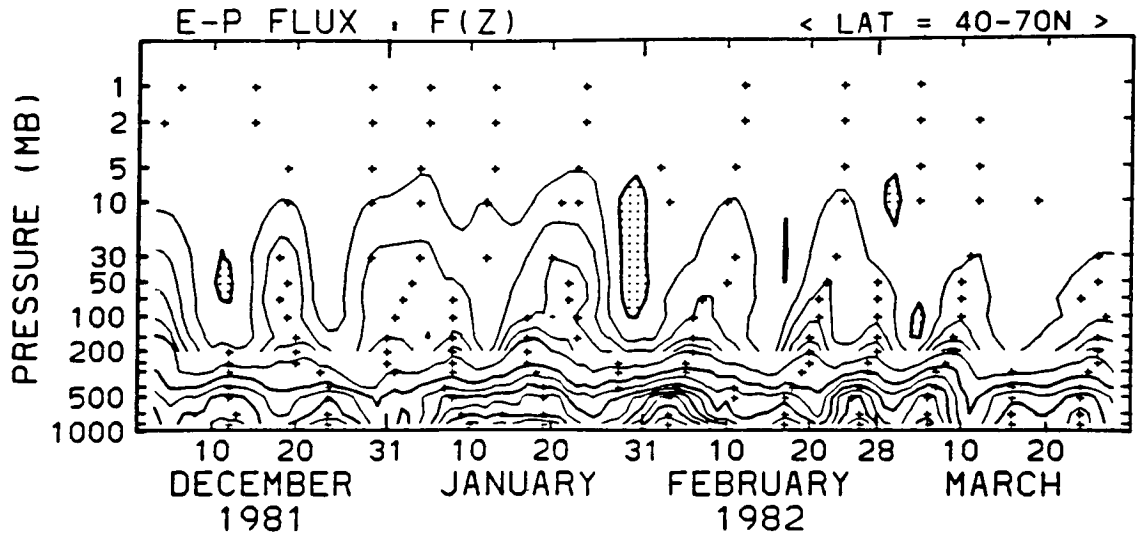

Fig. 2.1 Time-height section of vertical component of the E-P flux, $F(z)$, averaged over 40°N to 70°N. Contour interval is 2.5×10^{5} kg s^{-2}; above 200 mb it is magnified five times; negative values are shaded. Major maximum points are marked by '+' (see text).

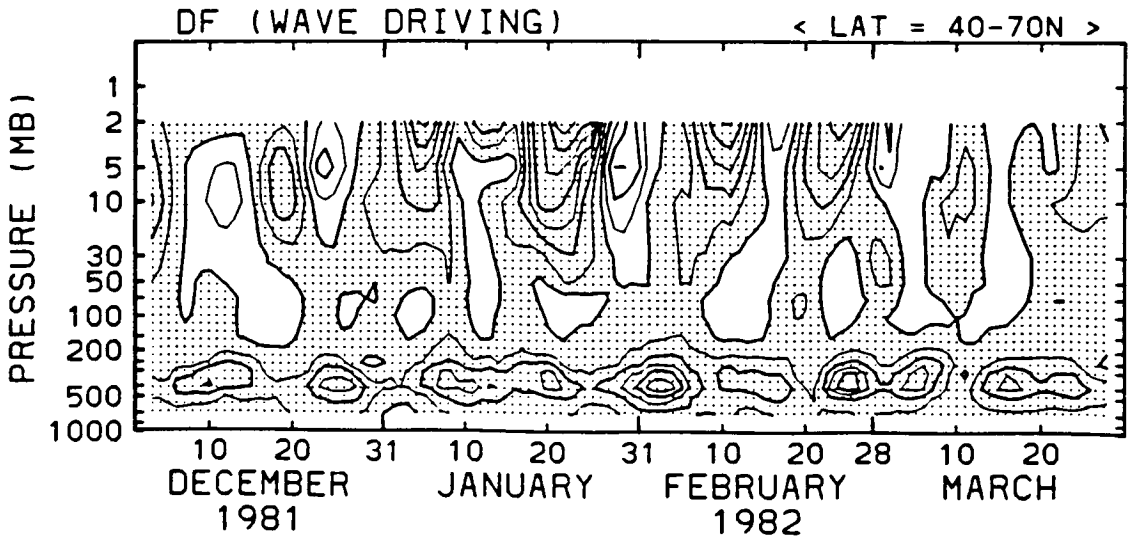

Fig. 2.2 Time-height section of wave driving D_F. averaged over 40°N to 70°N. Contour interval is 4.0×10^{-5} m s^{-2} ; negative values are shaded.

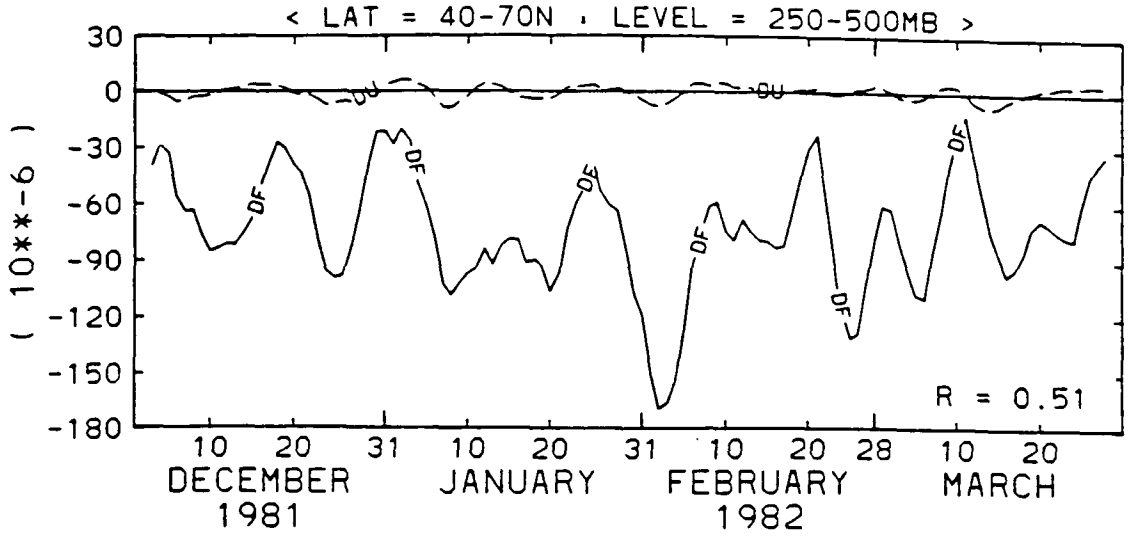

Fig. 2.3 Time series of $\partial\bar{u}/\partial t$ and wave driving D_F, averaged over 40°N to 70°N, 250-500 mb. Lines of $\partial\bar{u}/\partial t$ and D_F are labeled 'DU' and 'DF', respectively. Units are 10^{-6} m s^{-2}

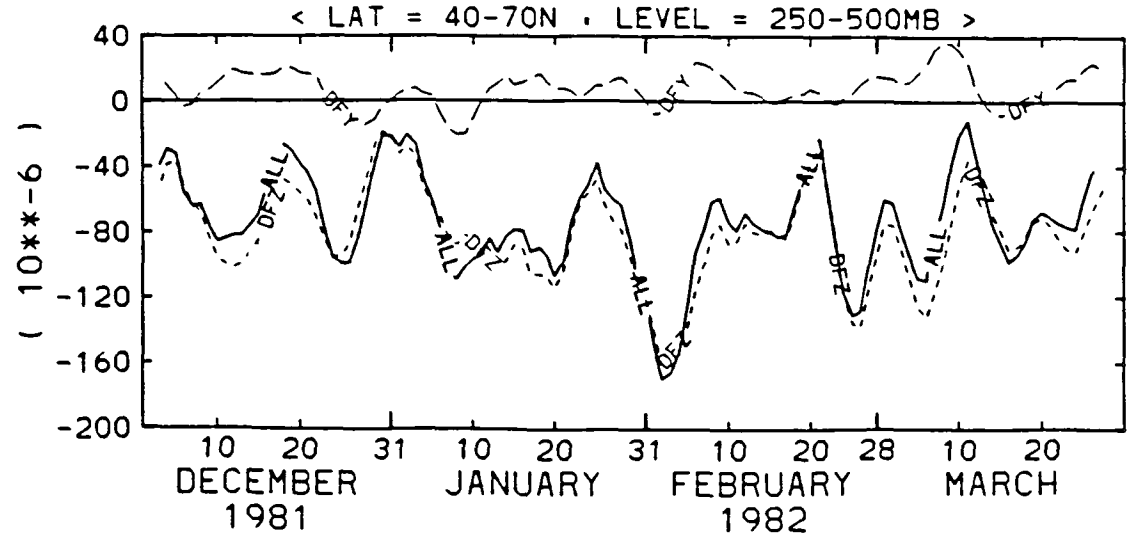

Fig. 2.4 Time series of D_F. $(\rho_0(z)a\cos\theta)^{-1}\ \partial F(y)/\partial y$ and $(\rho_0(z)a\cos\theta)^{-1}\ \partial F(z)/\partial z$ averaged over 40°N to 70°N, 250-500 mb. Lines of D_F. $(\rho_0(z)a\cos\theta)^{-1}\ \partial F(y)/\partial y$ and $(\rho_0(z)a\cos\theta)^{-1}\ \partial F(z)/\partial z$ are labeled 'ALL', 'DFY' and 'DFZ', respectively. Units are 10^{-6} m s^{-2}

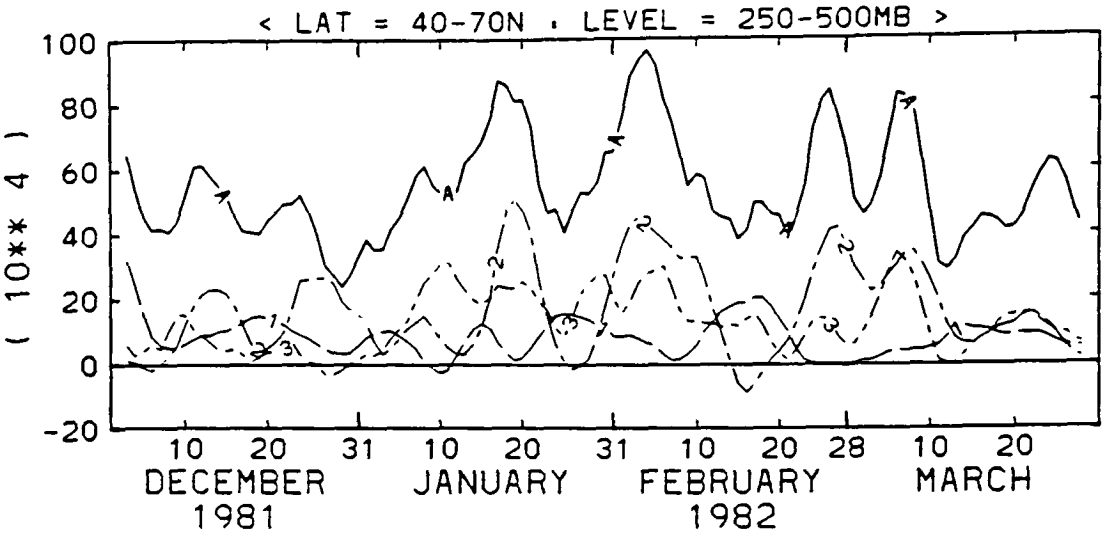

Fig. 2.5 Time series of $F(z)$ and the contribution from wavenumber 1 to 3, averaged over 40°N to 70°N, 250-500 mb. The thick solid line labeled 'A' represents total (wavenumber 1 to 6) $F(z)$. The thin chain line labeled 'i' represents the contribution from wavenumber i (i = 1 to 3)

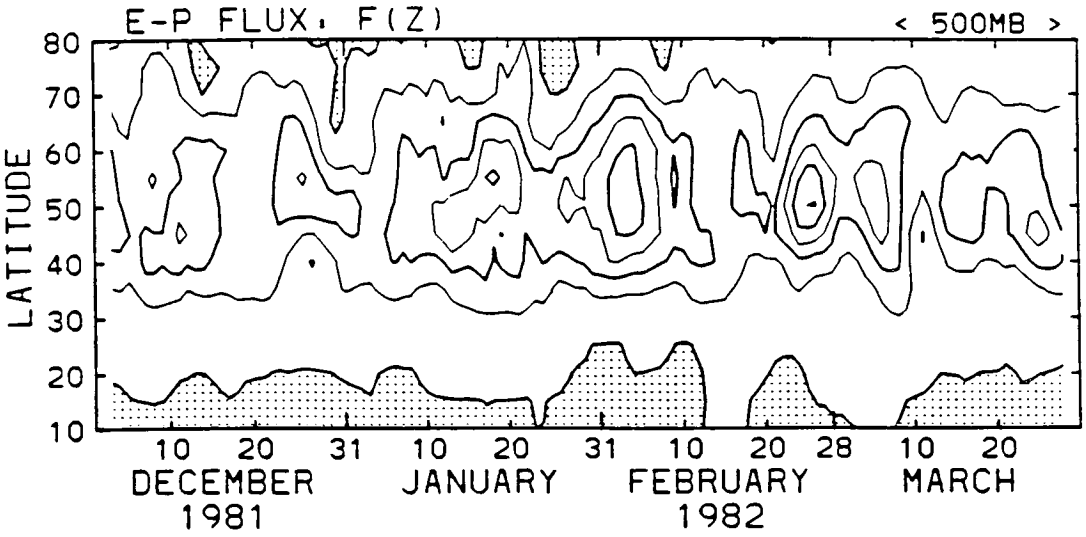
E-P FLUX: F(Z)
< 500MB >
LATITUDE
80
70
60
50
40
30
20
10
10 20 31 10 20 31 10 20 28 10 20
DECEMBER
1981
JANUARY
FEBRUARY
1982
MARCH

(a)

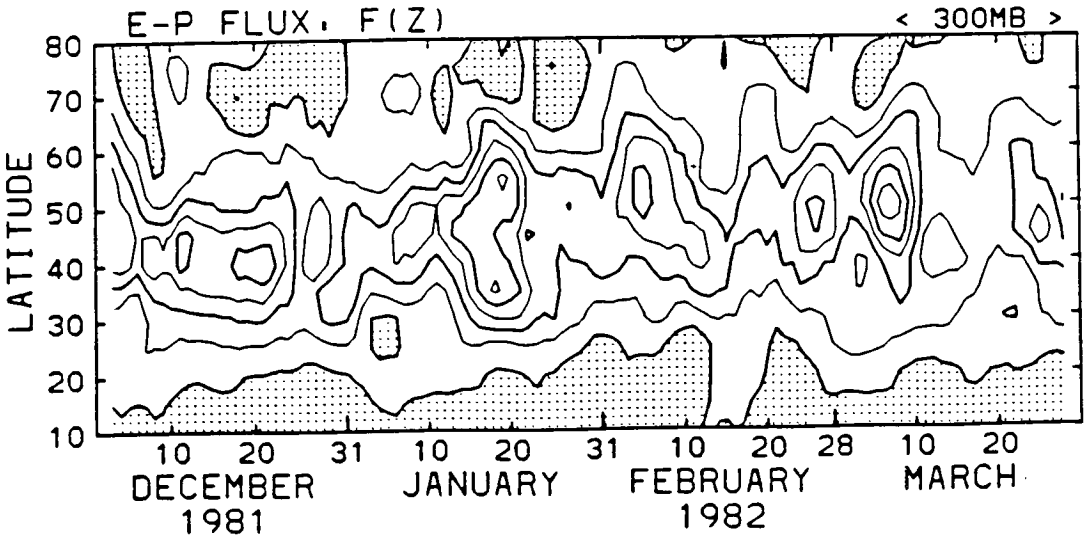
E-P FLUX: F(Z)
< 300MB >
LATITUDE
80
70
60
50
40
30
20
10
10 20 31 10 20 31 10 20 28 10 20
DECEMBER
1981
JANUARY
FEBRUARY
1982
MARCH

(b)

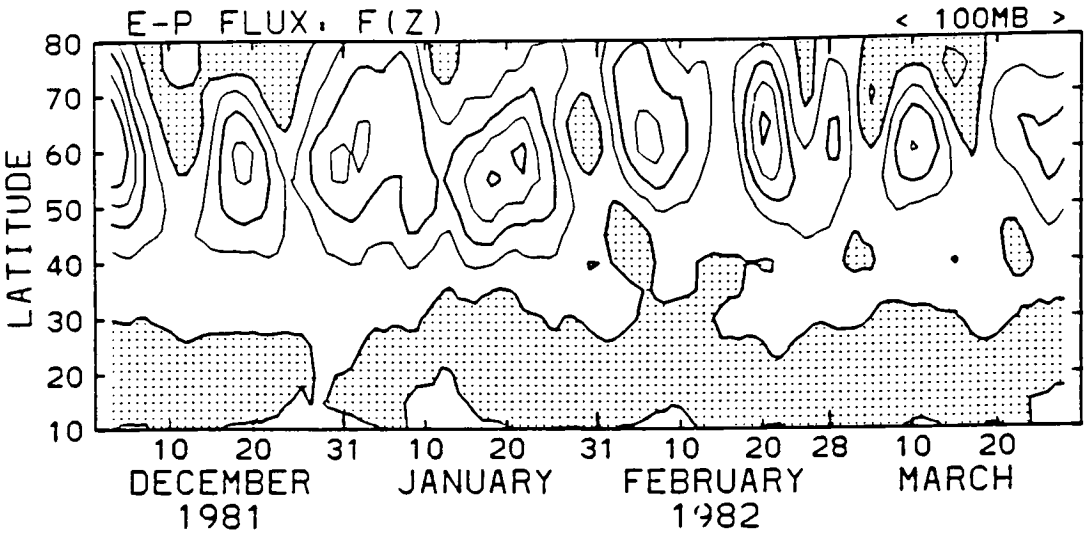

(c)

Fig. 2.6 Time-latitude sections of $F(z)$ at (a) 500 mb, (b) 300 mb and (c) 100 mb. Contour intervals are 5.0×10^{5} , 2.0×10^{5} and 6.0×10^{4} kg s^{-2}, respectively; negative values are shaded.

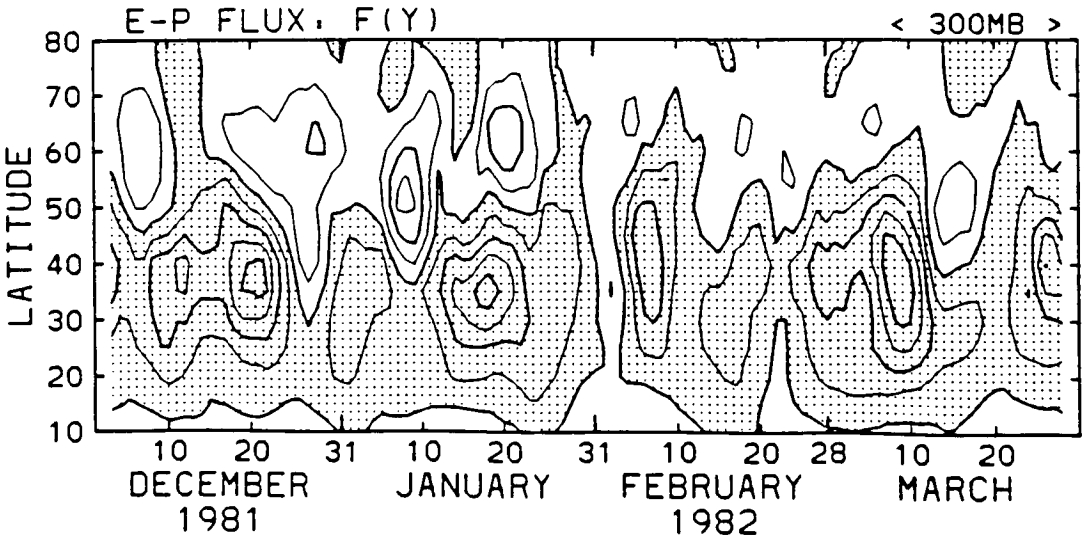

Fig. 2.7 Time-latitude section of $F(y)$ at 300 mb. Contour interval is 4.0×10^{7} kg s^{-2}; negative values are shaded.

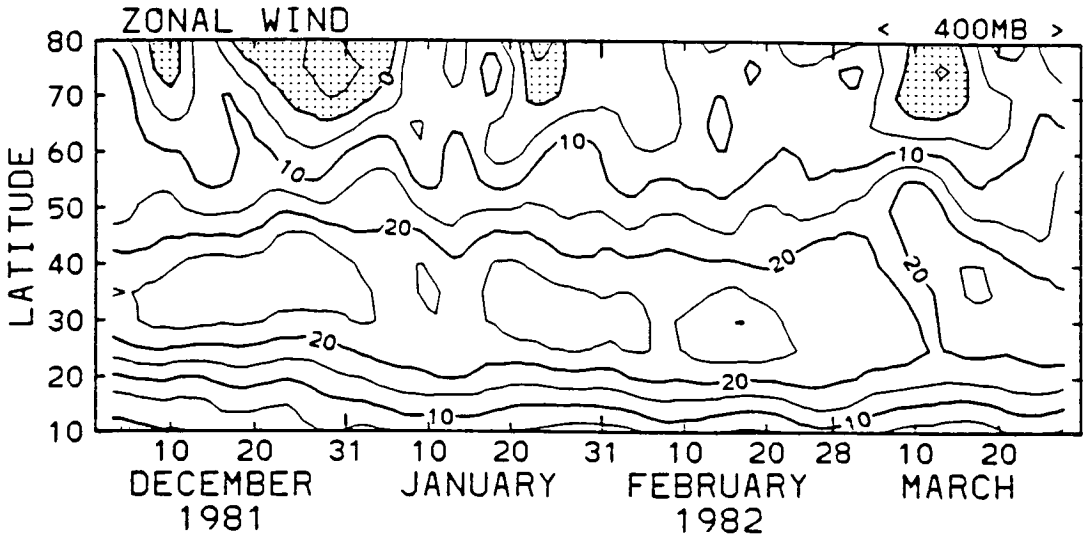

Fig. 2.8 Time-latitude section of mean zonal geostrophic wind at 400 mb. Contour interval is 5 m s^{-1} ; negative values are shaded.

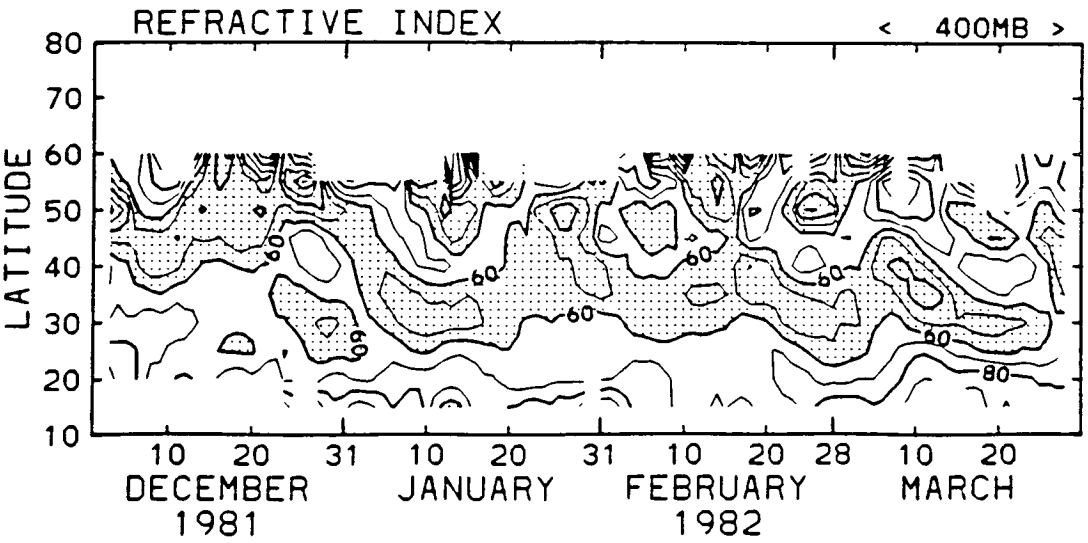

Fig. 2.9 Time-latitude section of the refractive index Q at 400 mb. Values are multiplied by a^2 (a: radius of the earth) Contour interval is 10; regions under 60 are shaded. Latitude band of 15°N to 60°N and value range of 0 to 100 are shown.

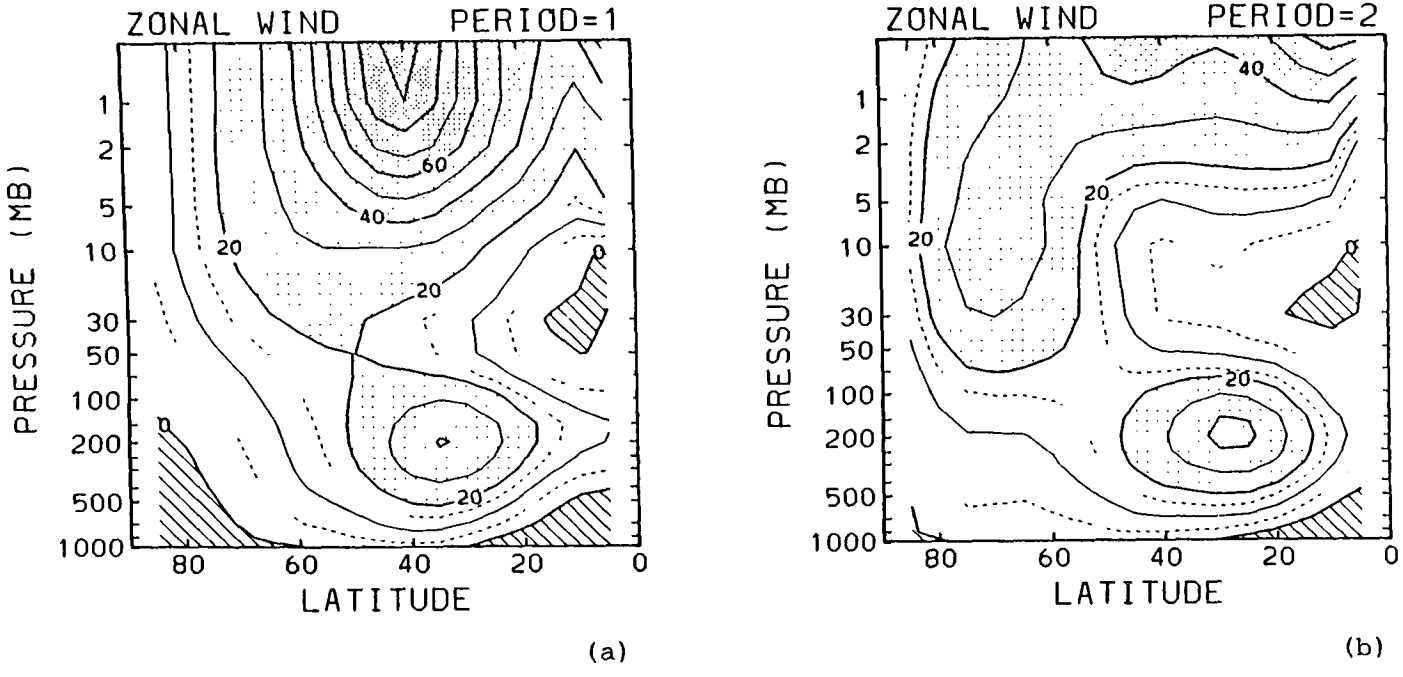

Fig. 2.10 Latitude-height sections of mean zonal geostrophic wind for (a) period 1 and (b) period 2 (see text for terminology). Solid contour interval is 10 m s^{-1} ; dashed lines are drawn for 5, 15 m s^{-1}

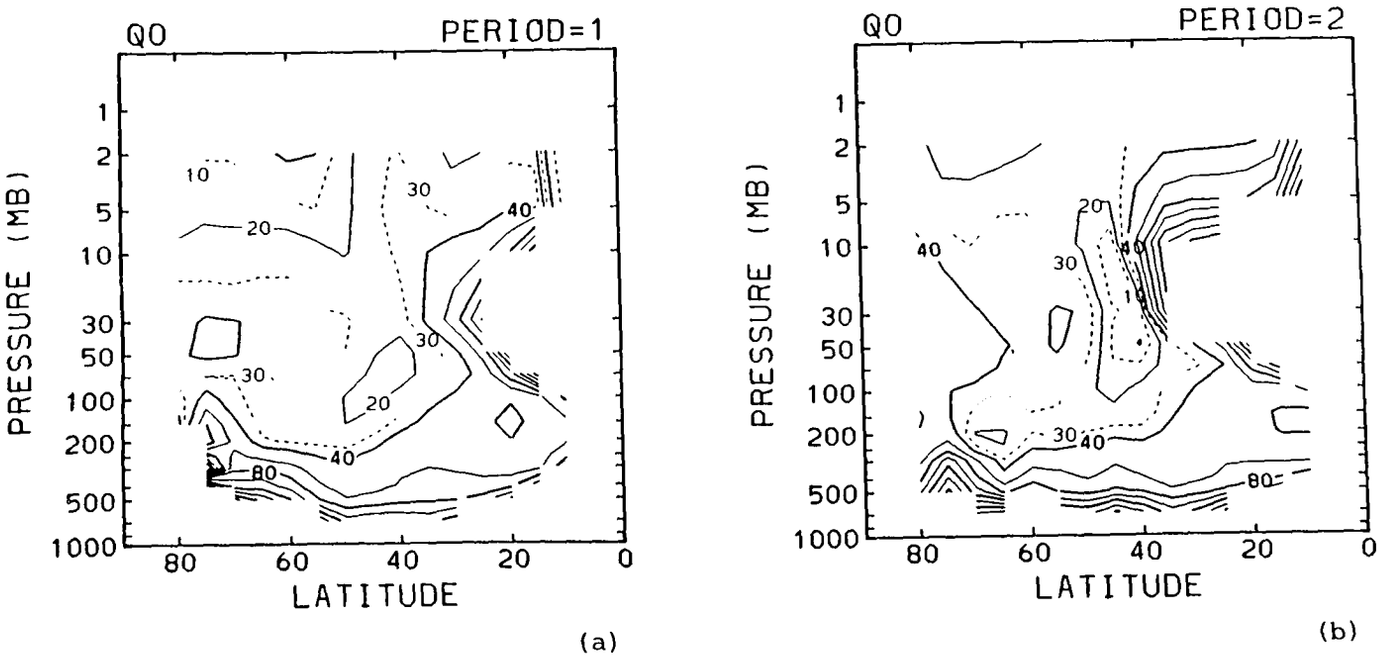

Fig. 2.11 As Fig. 2.10 but for the refractive index Q_0. Solid contour interval is 20; dashed lines are drawn for 10, 30. Value range of -200 to 200 are shown.

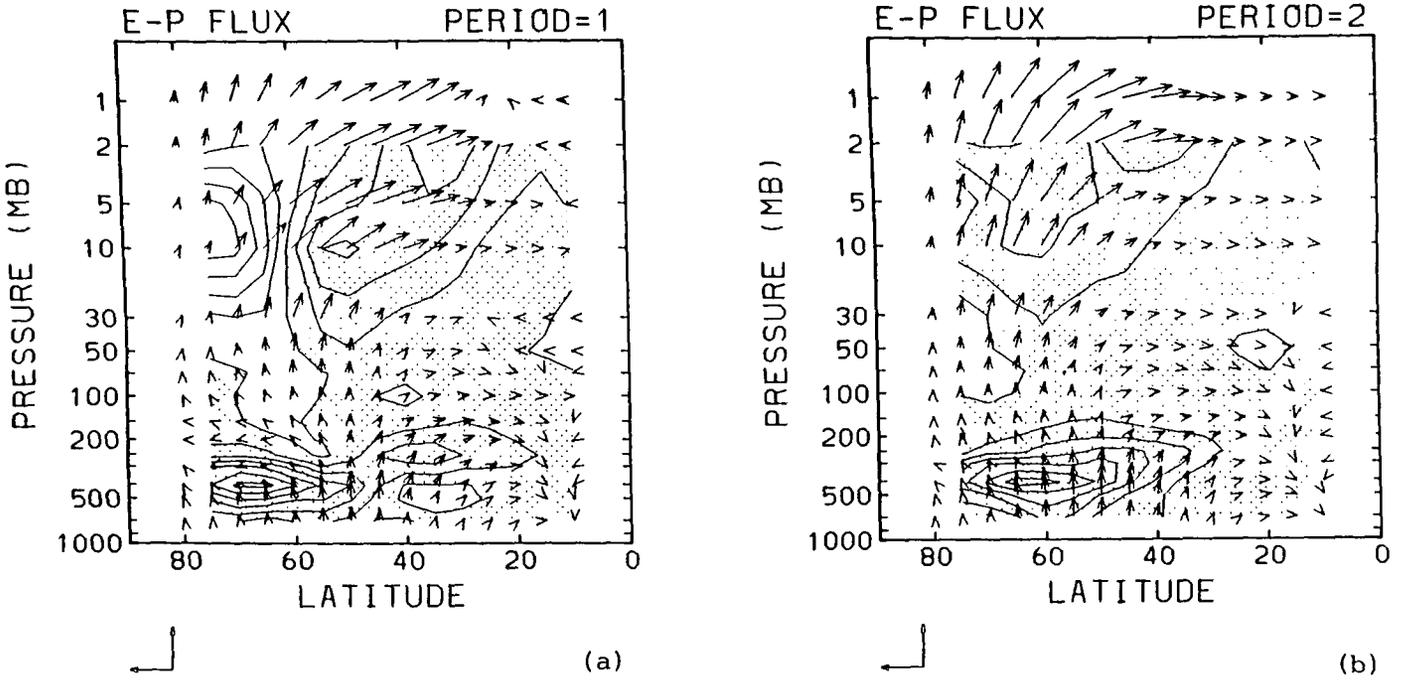

Fig. 2.12 As Fig. 2.10 but for the E-P flux and wave driving D_F Contour interval of D_F is 2.5×10^{-5} m s^{-2} ; negative values are shaded. Reference arrow shows 1.0×10^{9} kg s^{-2} for horizontal direction and $1.0\times10^{9}/c$ (c=182) kg s^{-2} for vertical direction. (see text for the scaling)

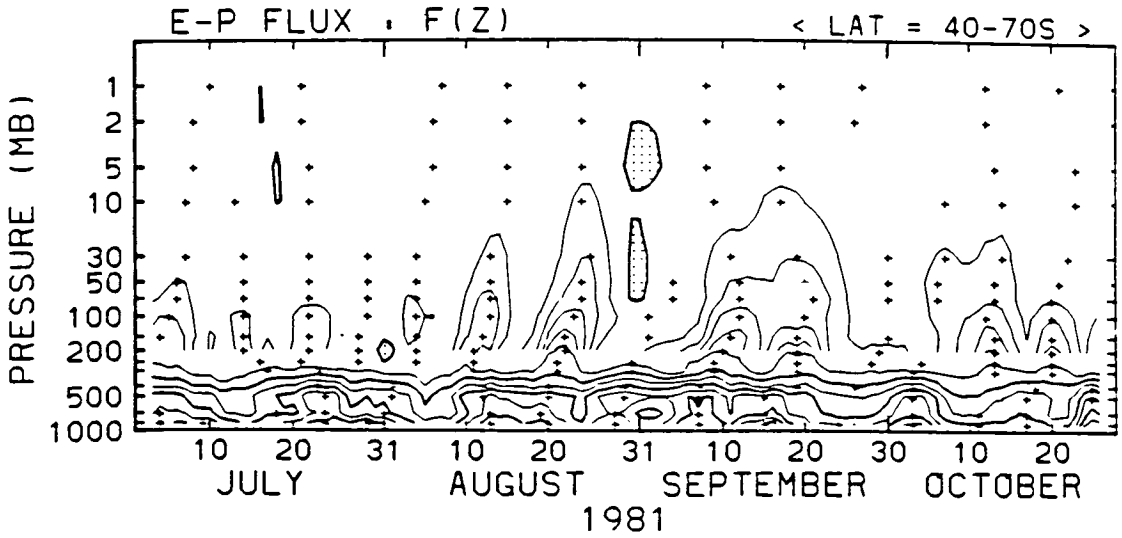

Fig. 2.13 As Fig. 2.1 but for the 1981 winter in the southern hemisphere. Contour interval is 3.0×10^{5} kg s^{-2}

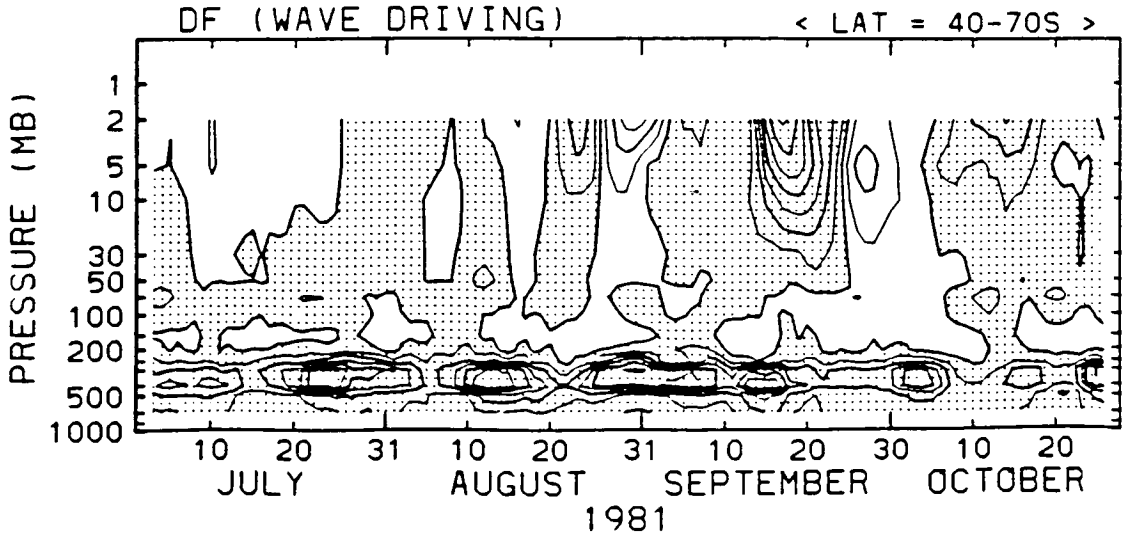

Fig. 2.14 As Fig. 2.2 but for the 1981 winter in the southern hemisphere. Contour interval is 2.0×10^{-5} m s^{-2}

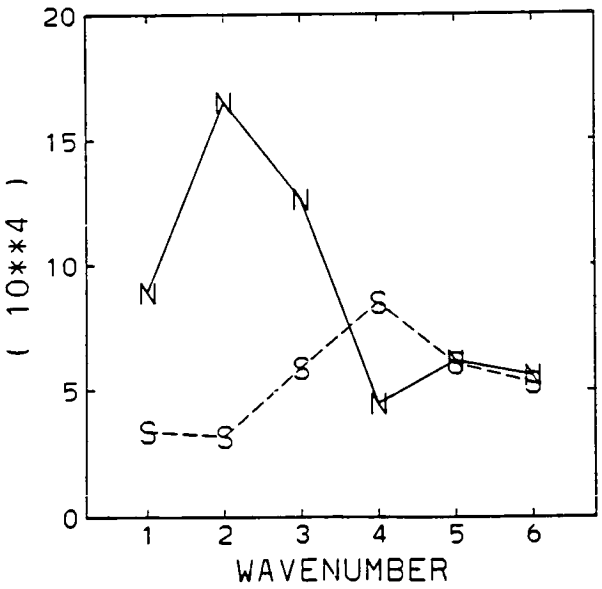

Fig. 2.15 120 day mean $F(z)$ of each wavenumber (from 1 to 6) averaged over the 250-500 mb and 70-40° for the northern and southern hemispheres. (See Figs. 1, 15 for the period of 120 days mean.) Marks of 'N' and 'S' mean northern hemisphere and southern hemisphere, respectively. Units are 10^4 kg s^{-2}

PART 3

Dynamical Factors Affecting Ozone Mixing Ratios in the Antarctic Lower Stratosphere

3.1 Introduction

Recently, a remarkable decrease of total ozone has been observed during springtime (September and October) at polar latitudes of the SH. Farman *et al.* (1985) first reported the decrease detected by ground-based observations at Halley Bay (76°S, 27°W), which have been made since 1957 Prior to this, Chubachi (1984) had pointed out that the total ozone observation at Syowa station (69°S, 40°E) recorded the lowest values in September and October 1982 since 1966. By using satellite-borne measurements from the solar backscatter ultraviolet (SBUV) instrument and the total ozone mapping spectrometer (TOMS) on board Nimbus 7, Stolarski *et al.* (1986) have confirmed the decrease of total ozone for seven years from the launch of Nimbus 7 (1978) to the most recent spring data available (1985), and have shown the phenomenon to be of continental size.

The springtime is also an interesting season because of the dynamical evolution of the stratospheric circulation in the SH. Unlike the NH, SH wave activity is vigorous during the spring (Hirota *et al.*, 1983; Shiotani and Hirota, 1985) Using satellite data, many authors have studied the stratospheric circulation in the SH (*e.g.* Harwood, 1975; Hartmann, 1976; Hartmann *et al.*, 1984; Mechoso *et al.*, 1985) Although each of their studies dealt with different years, they are in good agreement with each other, and show good repeatability of the circulation from year to year

However, it appears that no one has investigated the transition from winter to summer over Antarctica, and its relationship to the seasonal change of the ozone distribution. The aim of this study is to show how this change has taken place over the last few years, and thus to provide a background for a better understanding of the ozone decrease. It is not our purpose to propose a mechanism to explain the recently observed "ozone hole" Because balloon data from the Syowa Station (WMO, 1986; Solomon *et al.*, 1986) show that the largest changes occur near 50 mb, attention will be centered on the lower stratosphere.

3.2 Ozone Data and Estimation of the Wind Field

The ozone data were obtained from the SBUV instrument on board the Nimbus 7 spacecraft. These were obtained as profiles and total column amounts of ozone from the National Space Science Data Center The profiles give mixing ratios at 9 levels: 100, 70, 50, 30, 10, 5, 2, 1 and 0.4 mb. The profile data were then interpolated to 5° latitude circles for latitudes $\leqq 80°$ and mapped using a Kalman filter estimation procedure (Rodgers, 1977; Kohri, 1981) to yield a zonal mean and coefficients for 6 longitudinal waves.

The backscattered radiances provide little direct indication of the ozone mixing ratios below 10 mb, in part because of the complicating effects of multiple scattering. In the archival ozone profiles, information at these levels is obtained from the observed total ozone, the column amount above 10 mb, and regression relationships based on ozone distribution observed by balloon-borne instrument. While this procedure provides plausible values under conditions which are similar to those for which the statistics were developed, they can result in highly improbable values in the Antarctic spring (R. Hudson, 1986; personal communication) For these reasons we have used the ozonesonde data from the Syowa station to develop regression equations to estimate the high latitude ($\geqq 60°S$) ozone mixing ratios at levels from 30 to 100 mb, using SBUV total ozone and 10 mb mixing ratios, and NMC temperatures as predictors.

Fig. 3.1 shows line plots of the estimated SBUV data interpolated to the same latitude-longitude location as Syowa station, compared to the ozone observations at Syowa (marked by 'S') at 30 and 50 mb from September to December 1982. The corrected SBUV data are in reasonable agreement with the Syowa observations. There is similar agreement at 70 and 100 mb. There is also good agreement on individual profiles. The SBUV 10 mb data agree well with the Syowa soundings. In November and December the Syowa observations show large variations, because it is a season of the circulation reversal, when the ozone field might be spatially very variable.

To estimate the wind field we used balanced winds instead of geostrophic winds. Robinson (1986) pointed out that the momentum flux and its divergence calculated from the geostrophic wind field is overestimated in his numerical model, especially at high latitudes, because the geostrophic wind neglects local curvature effects. He proposed the use of balanced winds, which can be calculated easily from the geopotential height field. Compared with calcula-

tions from geostrophic winds, the momentum flux and its divergence calculated from the balanced winds are reduced, and are in good agreement with those calculated for his system described by the primitive equations.

In the calculation of balanced winds (u', v') for each wavenumber, we found that the equations can have a singularity at low latitudes and that this singular point moves poleward as the zonal wavenumber increases. Because of this singularity and the dominance of planetary waves in the stratosphere, we used balanced winds only for wavenumbers 1 and 2 at high and middle latitudes (poleward of 30°S)); for wavenumbers 1 and 2 at low latitudes and for wavenumbers 3 to 6 at all latitudes, we used the geostrophic wind approximation. As a zonal mean of the wind field we used the mean zonal gradient wind.

3.3 Zonal Mean Climatology

The seasonal evolution of the stratospheric circulation is much more repeatable in the SH than in the NH. Fig. 3.2 shows the annual march of the zonal mean temperature at 80° and 50 mb for the NH and the SH over nearly 7 years. From summer to winter the seasonal marches of the two hemispheres are repeatable. From winter to summer, however, these are different between the two hemispheres. In the NH, temporal variations of the zonal mean temperature are highly variable because major warmings occur there. On the other hand, in the SH the seasonal marches are repeatable, although there are small variations associated with minor warmings. Consequently, temperatures during the winter and spring time in the SH are much colder than in the NH. Because the interannual variability is rather limited, annual averages over the 5 year period 1979-1983 for which SBUV data are now available should be representative of the long term average.

First we describe the climatological monthly mean of the zonal mean temperature, the mean zonal gradient wind, the Eliassen-Palm (E-P) flux and its divergence for the three months of September, October and November, averaged over the 1979-1983 period. Our results for September are comparable to those of Mechoso *et al.* (1985) which showed the climatology in the SH from June to September averaged over four years from 1979 to 1982.

Fig. 3.3 (a) shows latitude-height sections of the zonal mean temperature for the three months. In September there exist cold temperatures (< 190 K) at high latitudes in the lower stratosphere; this region is colder in the earlier

months (Mechoso *et al.*, 1985). Referring to the climatology in the NH by Geller *et al.* (1983) or Fig. 3.2, even in mid-winter the minimum temperature at high latitudes is 198 K, emphasizing the different roles of planetary waves in the two hemispheres. As Mechoso *et al.* (1985) mentioned, there are two baroclinic zones in the upper and lower stratosphere. In particular, a reversal of the latitudinal gradient in the zonal mean temperature is a prominent feature in the upper stratosphere during the spring time (*e.g.*, Labitzke and Barnett, 1973; Barnett, 1974; Hirota *et al.*, 1983); these features in the zonal mean temperature are related to the mean zonal wind through the thermal wind relationship. In October the cold core at high latitudes warms and moves downward. In November the cold core still exists and moves downward to 200 mb (from 50 mb in September) The temperature gradients in the upper and lower stratosphere become smaller as the month progresses. The downward movement of the cold core continues until December at 300 mb. We will show this feature in more detail later

Fig. 3.3 (b) shows cross-sections of the mean zonal gradient wind. The mean zonal gradient wind is weaker than the mean zonal geostrophic wind because the mean zonal gradient wind takes into account the centrifugal force. In September the speed of maximum westerlies is about 75 m s^{-1} at 60°S and 5 mb. By October the stratospheric jet has weakened; at the same time, the tropospheric jet has also weakened. The stratospheric jet moves downward and slightly poleward. In November, when it is in the final warming stage, the stratospheric jet seems to be merged into the tropospheric jet. The transition of the mean zonal wind from September to November is gradual, but it is affected by minor warmings. We will see the interannual variability of the seasonal march of the mean zonal wind later

Fig. 3.3 (c) shows cross-sections of the E-P flux F and wave driving D_F In plotting the E-P flux in the vertical cross-section we applied the graphical convention as described by Baldwin *et al.* (1985); we have multiplied F by the factor exp(z/H) Fig. 3.3 (c) was calculated from the 5-year monthly average of daily values, not from the 5-year monthly mean field. In September the wave activity is the most vigorous of the three months. Since Mechoso *et al.* (1985) showed that the wave activity in September is most vigorous of the four months from June to September, September is the most active month of the year There are two large convergence regions of the wave driving D_F; at mid latitudes in the upper stratosphere, and at high and mid latitudes in the upper troposphere. Although the averaging period is different between our

study and Mechoso *et al.* (1985), values of the convergence zone in the upper stratosphere are similar However, the positive D_F in the high latitude middle stratosphere is much smaller than that calculated by Mechoso *et al.* (1985) This result is consistent with the results of Robinson (1986), who showed that the momentum flux and its divergence at high latitudes is overestimated by using the geostrophic wind field. In October the wave activity is weaker but still vigorous. The region of the large negative D_F in the stratosphere moves downward and poleward. Although in November the wave activity is low, a slight convergence zone in the stratosphere moves further downward and poleward.

We show the downward movement of the minimum temperatures and the maximum westerlies more clearly in the 5-year mean time-height sections (Figs. 3.4 and 3.5). A 5-day running mean was applied to most figures of time-height and time-latitude sections in this study, with the exception that a 15-day running mean was used for Figs. 3.4 (b) and 5 (b) At 80°S the minimum temperatures move downward from 50 mb in early September to 300 mb in early December (Fig. 3.4 (a)) while becoming warmer The time change of the zonal mean temperatures (Fig. 3.4 (b)) shows that the maximum temperature change also moves downward from 5 mb in early September to 200 mb in early December According to the monthly mean climatology by Mechoso *et al.* (1985), the maximum temperature tendency moves from 1 mb in June to 5-10 mb in September Thus, in the SH the maximum temperature tendency comes from the upper stratosphere in June and moves downward to the lower stratosphere in early December

The maximum westerlies (near 60°S) also move downward from 5 mb in early September to 200 mb in November (Fig. 3.5 (a)) Harwood (1975) reported similar downward movement of the maximum westerlies. The acceleration of the mean zonal wind (Fig. 3.5 (b)) shows the maximum deceleration moves downward from the upper stratosphere in September to the lower stratosphere in early December Because the E-P flux and its divergence are sporadic, a similar cross section of their 5-year mean does not show such a regular evolution as Figs. 3.4 (a) and 3.5 (a)

The downward motion of wave driving D_F in Fig. 3.3 (c) suggests that the region of large wave damping moves downward as the region of weak westerlies (or a critical line) moves downward. The downward motion of the cooling region just above the heating band in Fig. 3.4 (b) also suggests a dynamical effect. As predicted by Matsuno (1971), the temperature change caused by planetary waves incident on a critical level is positive below the critical level and

negative above it at high latitudes. The positive feedback of the downward motion is reminiscent of the mechanistic model of the quasi biennial oscillation.

We turn next to the climatology of the zonal mean ozone mixing ratio and the ozone transport by horizontal eddies. Fig. 3.6 (a) shows latitude-height sections of the zonal mean ozone mixing ratio for the three months from September to November averaged over the five years of 1979-83. In September there are maxima in both the upper and lower stratosphere at mid latitudes. Particularly in the lower stratosphere there exists a steep drop of the ozone mixing ratio toward the pole, a so-called ozone hole. In October the ozone mixing ratio at high latitudes in the middle stratosphere increases. (See, for example, the 6 ppm contour line.) In the lower stratosphere there is also an increase of ozone at high latitudes, and the ozone hole is gradually filled. By November the hole at high latitudes in the lower stratosphere has almost disappeared.

Fig. 3.6 (b) shows the ozone transport by the horizontal eddies, $\overline{v'O_3'}$ Wu *et al.* (1985) reported that large contributions to the ozone transport are due to mean vertical advection and horizontal eddy processes during the NH winter, based on SBUV ozone data. For the three months, the basic configurations of the horizontal eddy transport are similar; negative maxima are located at high latitudes in the middle stratosphere. In September a negative maximum of about -4.0 ppm m s^{-1} is located at 55°S and 10 mb. Paired with the negative maximum is a positive maximum at 50°S in the upper stratosphere. The zero line tilts downward toward the equator These features are similar to the results by Wu *et al.* (1985), although the level of the negative maximum is located higher (5 mb) in their results than in ours (10 mb) In October the positive maximum in the upper stratosphere is reduced, but the negative maximum in the mid stratosphere is enhanced with a value of about -6 ppm m s^{-1} The position of the negative maximum moves poleward to 60-65°S. In November both positive and negative maxima are reduced and the position of the negative maximum moves farther poleward at 70°S. This poleward movement may be related to the reduction of the ozone hole as we will see below

3.4 Synoptic climatology

In the SH the monthly mean fields, *e.g.* the temperature or ozone fields,

are also repeatable; wave structure of these time mean fields is almost the same for each year (See, monthly mean total ozone charts for 7 years from 1979 to 1985 by Stolarski *et al.*, 1986.) We show the 5 year average monthly mean field of the geopotential height, temperature and ozone mixing ratio at 50 mb for the three months of September, October and November The 50 mb level is a representative one for considering dynamical effects on total ozone, since the largest contribution to the total ozone occurs in the lower stratosphere. Our climatological charts of the geopotential height and temperature fields agree well with those by Knittel (1976) for the 5-year mean from 1968 to 1972.

Fig. 3.7 (a) shows the geopotential height field projected on a polar stereographic grid. The height field for the three months appears to be circular compared with the climatology during the NH winter In September, as might be expected from Fig. 3.3 (b), a steep slope of the vortex is located near 60°S. In October the vortex is still stable and strong. In fact, there are appreciable wave amplitudes (see Fig. 3.10) which are masked by the steep slope. By November, the vortex is weak and shallow; however, at this level the circulation is still cyclonic.

The temperature field (Fig. 3.7 (b)) in September and October is decidedly non-circular A cold core is located over the polar region, with a warm band at mid latitudes having a horse shoe shape (wavenumber 1) In the SH planetary wave 2 is also prominent; however, in the time mean field it is not detectable because of its eastward traveling nature (Harwood, 1975; Hartmann, 1976). In September the coldest temperature is 188 K near the pole, and the warmest temperature is 223 K at mid latitudes, while the climatology by Knittel (1976) shows the coldest temperature 187.8 K and the warmest temperature 225.6 K. The longitude of maximum temperatures between the two climatologies is somewhat different; our result shows the maximum around 105°E while Knittel's (1976) is around 150°E. In October the core of cold temperatures is still strong with the coldest temperature of 202 K (Knittel, 203.1 K) The high temperature band with a maximum of 229 K moves poleward and rotates clockwise (eastward) The longitude of maximum temperatures is still different between our climatology and Knittel (1976); however, the rotational direction and movement are similar to each other In November low temperatures are replaced by high temperatures around the polar region.

The ozone field at 50 mb (Fig. 3.7 (c)) is closely related to the temperature field. In September there exists a deep ozone hole over the polar region

and a high ozone band at mid latitudes with a horse shoe shape. Although the high ozone band lies slightly inside the high temperature band, the phase of the two is almost the same. In October there still exists the deep ozone hole over the polar region. As we see in the temperature field (Fig. 3.7 (b)), the high ozone band also moves poleward and eastward. Stolarski *et al.* (1986) showed a similar phase of wavenumber 1 in the total ozone averaged over October for seven years from 1979 to 1985, based on the TOMS observations. Hence the horse shoe shape of the ozone and temperature fields in September and October is a repeatable and prominent feature in the SH. In November the hole almost disappears, but there is a weak pair of low and high ozone regions over Antarctica.

The good correspondence between the horse shoe shaped temperature and ozone fields suggests that at mid latitude there exists downward motion that brings down high ozone with the adiabatic heating there, and that at the polar region there exists upward motion that brings up low ozone with the adiabatic cooling there. Tung *et al.* (1986) suggested the existence of such a reversed circulation to understand the Antarctic ozone hole. To confirm this hypothesis more extensive work on the net radiative heating and the residual mean circulation is needed.

We briefly mention the vertical structure of the geopotential height field, the temperature field and the ozone field. Fig. 3.8 shows longitude-height sections of the deviations from a zonal mean for the three quantities in October averaged over the five years at 60°S. (60°S is chosen because it is near the latitude of maximum amplitude; results at higher latitudes are similar) Height waves (Fig. 3.8 (a)) have maximum amplitudes of wavenumber 1 at 5 mb and tilt westward. Temperature waves have a westward tilt and two amplitude maxima for wavenumber 1 in the lower and upper stratosphere; there is a nodal point around 5 mb. On the other hand, ozone waves tilt westward in the lower stratosphere and eastward in the upper stratosphere. In the upper stratosphere the ozone waves are out of phase with the temperature waves (Figs. 3.8 (b) and (c)), which is expected in a region where ozone is photochemically controlled (see also Gille *et al.*, 1980) In the lower stratosphere Hartmann and Garcia (1979) showed with a simple mechanistic model that the ozone waves are in phase with the height waves because the ozone distribution is dynamically controlled. However, our results show a strong correspondence with the temperature waves in the lower stratosphere, The calculation of Hartmann and Garcia (1979) did not include the effect of

vertical advection in their model.

3.5 Interannual Variability

Although the interannual variability of the stratospheric circulation is much smaller in the SH than in the NH (*e.g.* Fig. 3.2 and Geller *et al.*, 1984), it is variable during the spring time. Moreover, recent ozone observations have shown a remarkable decrease of the total ozone over the southern polar region in October In this section we will see the interannual variability of the dynamical quantities and ozone distributions during the spring time in the SH.

Fig. 3.9 shows time-height sections of the mean zonal gradient wind in the stratosphere (100-0.4 mb) at 60°S for six years from 1979 to 1984. For each of the six years the downward movement of the maximum westerlies is clear, as was seen in Fig. 3.5. However, the seasonal evolution of the mean zonal wind is variable in October and November In 1979 a minor warming occurred in mid October and the wind speed suddenly decreased. (This warming is reported by Yamazaki and Mechoso, 1985.) After this event the wind speed in the stratosphere was highly stable for about a month, until a final warming in late November brought the easterlies down to the lower stratosphere. In 1980 the wind speed decreased slightly around October 10 in conjunction with a minor warming; however, it was not as effectively reduced as in 1979. The downward motion of the zero line was gradual from late October (0.4 mb) to late November (30 mb) Thus the strong westerlies (for example, see the 40 m s^{-1} contour line) remain until the end of October The seasonal evolution of the mean zonal wind in 1981 is similar to that in 1980; there is no sudden decrease in the wind speed, and the movement of the zero line is gradual. In 1982, in contrast, the seasonal evolution was similar to that in 1979; in mid October there was a minor warming that rapidly decreased the wind speed, followed by a gradual reduction. Consequently the wind speed in the mid and lower stratosphere was weaker in 1982 than 1980 and 1981 In 1983 the seasonal evolution of the zonal wind was similar to that in 1980 and 1981. The seasonal evolution in 1984 was slightly different from other years; a minor warming in early October decelerated the wind speed sufficiently in the upper stratosphere, but there remained strong westerlies in the middle and lower stratosphere. The times of changing circulation from westerlies to easterlies for

the six years seem to be getting later in the lower stratosphere. Note that for these months the flow remains westerly, is generally so at 70 mb and usually so at 50 mb. However, in October, when the ozone decrease has been observed, there is no clear trend of the wind speed. Rather, the times of minor warmings affect the wind speed in October The character of the zonal wind transition at 80°S (not shown) is rather different, although 1979 is similar to 60°S with the final change about November 20. In the following 5 years easterlies descend suddenly to 70 mb; the approximate dates for these transitions are November 25, December 2, December 8, November 26 and December 12. There is an indication that this date has gotten later during this period.

Fig. 3.10 shows time-latitude sections of the total amplitude A_0 for the height wave at 50 mb for the six years. A_0 is defined as

$$A_0 = \{\sum_{i=1}^{6}(A_k^2+B_k^2)\}^{1/2}, \qquad (16)$$

where A_k and B_k are the cosine and sine coefficents for the wavenumber k. Although Fig. 3.7 (a) shows nearly circular height field, the height wave activity is fairly large, because height wave amplitudes are masked by the steep slope of the strong vortex. As we see in the climatology of the temperature field (Fig. 3.7 (b)). the maximum amplitudes of the height wave also slowly moves poleward from around 55°S at the beginning of September to around 65°S in November Contribution to the total wave amplitude A_0 is mainly from wavenumbers 1 and 2; generally wave 1 is larger than wave 2. The difference of seasonal evolution between the two years (1979 and 1982) and other years is clear In October of 1979 and 1982 there is a big wave event following the sudden decrease of the mean zonal wind (Fig. 3.9) The wave amplitudes in the other years seem to be smaller than in 1979 and 1982.

Fig. 3.11 shows time-latitude sections of the zonal mean ozone mixing ratio at 50 mb for the six years. In 1984 the data are presently available only in September and October For each of the six years the ozone maximum, which is around 50°S at the beginning of September, slowly moves poleward, reaching polar latitudes in late November or December In 1979 the maximum value is 3.6 ppm at 60°S in late October and the minimum value is 2.2 ppm at 80°S in early September In 1980 the maximum value is reduced to 3.2 ppm at 55°S in early October and 3.5 ppm at 80°S in early December The minimum value is also reduced to 2.1 ppm at 80°S in the middle of October The low ozone mixing ratio at high latitudes continues longer in 1980 than in 1979. In 1981 the maximum value again increases to 3.5 ppm at mid latitudes in late Septem-

ber, but the minimum value is almost the same (2.1 ppm) as that in 1980. In 1982 the maximum value is reduced again (the 3.2 ppm contour line disappears) and the minimum value is 2.2 ppm in late September In mid-October the ozone mixing ratio at high latitudes increases, associated with a minor warming. In 1983, the 3.2 ppm contour line appears again, and the minimum value decreases to 1.8 ppm at 80°S in mid-October In 1984, although our plot is limited to September and October, the maximum value is 3.5 ppm at 45°S in early September and the minimum value is 1.7 ppm in early October, for a 26 % decrease over this period.

The seasonal evolution of the zonal mean ozone mixing ratio at 50 mb is repeatable; however, there are some variations in maximum values at mid latitudes and minimum values at polar latitudes. The minimum values of the zonal mean ozone mixing ratio at 50 mb, inferred from the SBUV data, show a decreasing trend in September and October from 1979 to 1984, similar to the decrease of the total ozone at polar latitudes reported by Farman *et al.* (1985) and Stolarski *et al.* (1986) On the other hand, for the maximum values at mid latitudes, there is no clear decreasing or increasing trend.

A time-latitude presentation of the SBUV zonal mean total ozone (Fig. 3.12) shows many of the same features. At the beginning of September there are low values at 80°S and high values at 50°S. The maximum moves toward the pole, slowly until mid-November, then very rapidly There is usually a mid-latitude maximum in October, corresponding to a minimum at high latitude, suggesting some latitudinal redistribution of the total ozone. However, in several years, the deepest high latitude minimum occurs earlier than the mid-latitude maximum. The high latitude minimum was 270 DU (1 Dobson Unit is 1 matm-cm) in 1979, but below 210 in 1984, for a 22 % decrease. The mid-latitude maximum, over 405 DU in 1979, has also decreased irregularly to about 365 DU over this period for a 10 % decrease. In addition, the 360 DU contour no longer reaches high latitudes.

Fig. 3.13 shows time-latitude sections of the zonal mean temperature at 50 mb for the six years. The ridge of the maximum temperatures corresponds to that of the maximum ozone mixing ratio at the same level (Fig. 3.11), although the latitudes of the maximum ozone mixing ratio or total ozone are located a little poleward of the maximum temperature (see, Figs. 3.7 (b), (c)). Fig. 3.13 illustrates the relationship between the seasonal marches of cold temperatures at high latitudes and the zonal mean wind. As shown in Fig. 3.9, for the years 1979 and 1982 there are minor warmings that bring easterlies in

the upper stratosphere at 60°S. If we look at cold temperatures at high latitudes (for example, see the 210 K contour line) in 1979 and 1982, the 210 K contour line reaches 80°S around October 10, while in 1980, 1981 and 1983 it reaches 80°S around November 1, and in 1984 around October 20. Thus a simple trend of the cold temperatures at high latitudes is not clear, but the year to year variations of the cold temperatures are affected by wave events related to minor warmings.

Fig. 3.14 shows time-latitude sections of the horizontal ozone transport $\overline{v'O_3'}$ at 50 mb for the six years. As we see in the climatology of Fig. 3.6 (b), there are negative regions at high latitudes, positive regions at around 20-40°S, and again small negative regions at equatorial latitudes. The variation of negative values at high latitudes is related to wave events. The large ozone transport associated with wave events is sporadic, and the times of the active periods are different for each year Although wave 1 height and ozone are considerably larger than wave 2, the mean transports by the two wave components are comparable, although one or the other may dominate in a particular event. Big wave events in October 1979, 1982 and 1984 caused minor warmings that sufficiently changed wind speeds in the upper stratosphere, while in September and October 1980, 1981 and 1983 wave activity is small corresponding to the strong mean zonal wind. Thus, Fig. 3.14 does not show a simple trend of the horizontal ozone transport, $\overline{v'O_3'}$

Finally we will summarize the interannual variability of the dynamical quantities and ozone distributions by paying special attention to the month of October when the ozone decrease has been observed. Fig. 3.15 (a) shows year-to-year variations of the zonal mean ozone mixing ratio at 80°S. The SBUV observations indicate a decreasing trend of the ozone mixing ratio in the whole stratosphere. Caution must be exercised in drawing a strong conclusions about a decrease in the ozone mixing ratio profiles because a systematic drift in the SBUV instrument may be at least partially responsible for the trend. Rather, we should pay attention to the high ozone mixing ratio in 1979 and 1982, which was observed especially in the middle stratosphere (30 and 10 mb) As Figs. 3.9 to 3.14 show, the seasonal marches of the dynamical quantities and ozone distributions are closely related to each other The year-to-year variations of the zonal mean temperature (Fig. 3.15 (b)) are similar to those of Fig. 3.15 (a) with high temperatures in 1979 and 1982 in the lower and middle stratosphere. The mean zonal wind speed at 60°S (Fig. 3.15 (c)) shows a close relation to these two. As we might expect from the dynamical relation-

ships, colder temperatures at high latitudes are related to the strong westerlies. Moreover, as was seen in Figs. 3.9 and 3.13, these are related to the wave activity Fig. 3.15 (d) shows the year-to-year variation of the vertical component of the E-P flux, which is a measure of the vertical propagation of planetary waves. Because the effect of wave activity should be considered to be cumulative, we chose an averaging period from August to October It is evident that warmer temperatures, weaker westerlies and high ozone are associated with more vigorous wave activity The ozone decrease in these years is probably true. However, if the year 1979 was the most active of the six years, these data by themselves may not be sufficient to demonstrate that there is a long term trend.

3.6 Conclusions

We have investigated the climatology and interannual variability of dynamical factors and their effects on the ozone mixing ratio during the SH spring. We have paid special attention to the Antarctic lower stratosphere where the decrease of the total ozone has been observed recently. Because the stratospheric circulation in the SH is highly repeatable, it is reasonable to look at the seasonal evolution of a multi-year average as a first step.

Mechanistically, the data are consistent with the following picture. The wave driving D_F is (negatively) large in middle latitudes of the upper stratosphere in September, and moves poleward and downward as well as weakens as the season progresses. As the zonal westerlies are decelerated, the wind structure is altered such that the maximum values are displaced downward and poleward as well as being reduced. The downward motions associated with the deceleration produce an adiabatic warming in the lower stratosphere, first at mid-latitudes, but increasingly poleward as time goes by Additionally, these motions bring ozone-rich air down to the lower stratosphere, so that the warm regions have higher ozone mixing ratios, and the high ozone region moves toward the pole with time as the warm region does.

In the synoptic description of the climatological field, the geopotential height field is almost circumpolar On the other hand, in the temperature and ozone fields planetary wavenumber 1 (with a horse shoe shape) is prominent in the lower stratosphere; moreover, these two fields are in good positive correlation. The generation of the planetary wave 1 must be affected by the

Antarctic continent whose shape has a strong wavenumber 1 component. Orographic effects or surface temperature contrast are two possible mechanism, but there may also be an effect of the surface albedo distribution.

Concerning interannual variability, the zonal mean ozone mixing ratio, the zonal mean temperature, the mean zonal gradient wind and the wave activity are related to each other When there is vigorous winter/spring wave activity (1979 and 1982), the mean zonal wind is weaker, the zonal mean temperature is warmer and the zonal mean ozone is richer at high latitudes than those in a quiet winter/spring. Clearly the zonal mean ozone at high latitudes is affected by the wave activity

This part has presented data on the seasonal evolution of the circulation and the ozone fields in the SH lower stratosphere from late winter to late spring. It is suggested that the changes are due to the seasonal changes in the wave-mean flow interaction, indicated by the wave driving. The interannual variability of the ozone and temperature values and the EP flux support this general picture.

This mechanism of itself does not explain the presence or growth of the ozone minimum seen at the end of each winter This might be due to an upward motion at high latitude, as suggested by Tung *et al.* (1986) Our preliminary calculations of the residual circulation do not support this for 1979, but one would expect that stronger wave activity would drive stronger downward motions at high latitudes, tending to overcome an upward motion. Weaker wave motions, on the other hand, would not drive as strong downward motions, and high latitudes would be colder, with smaller radiative cooling, making it easier to drive a reverse cell.

The data show two long term trends. At the upper levels in Fig. 3.15 (a) there is a fairly steady downward trend. This is also seen at other latitudes; it may be due to instrument drift for the shorter wavelengths that provide the upper altitude information, or a real effect. We will not comment further on this. At the lower levels, the time mean effects appear to be driven by wave activity, consistent with the interannual variations that are seen. It does not appear impossible that a long term trend in wave activity could lead to long term ozone changes at high southern latitudes.

These results, then, indicate the dynamical effects play a large role in year to year variations of ozone at high latitudes. They do not preclude a role for chemical effects over a longer period.

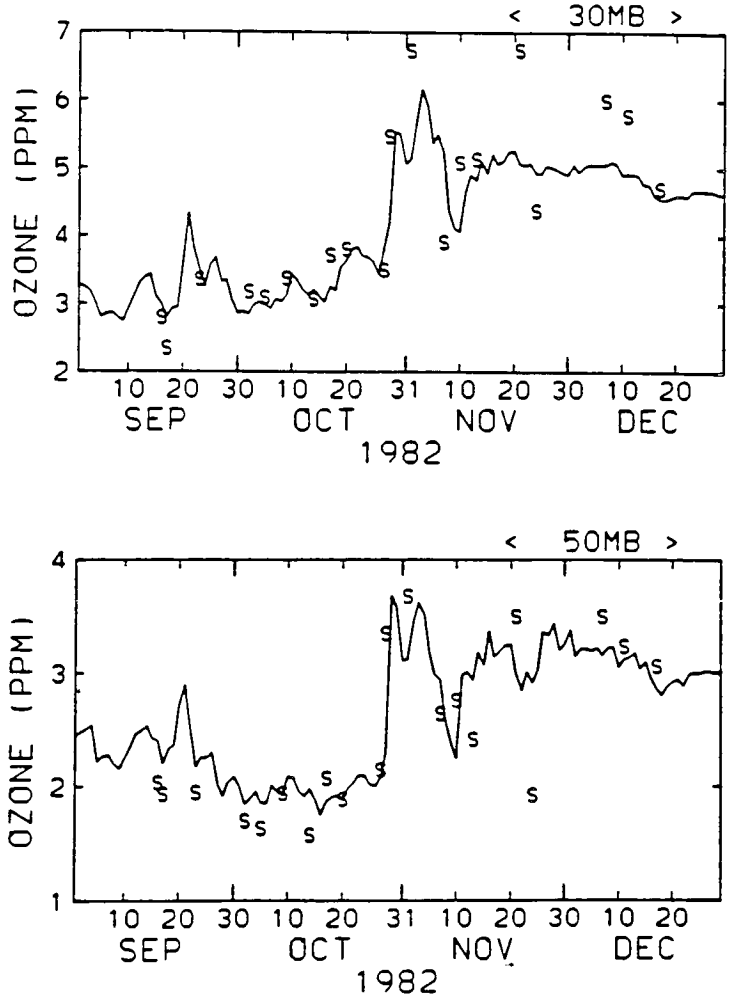

Fig. 3.1 Line plots of the corrected SBUV ozone data interpolated to the same latitude-longitude point as Syowa station, and ozone observations at Syowa (marked by 'S') from September to December 1982 for (a) 30 mb and (b) 50 mb.

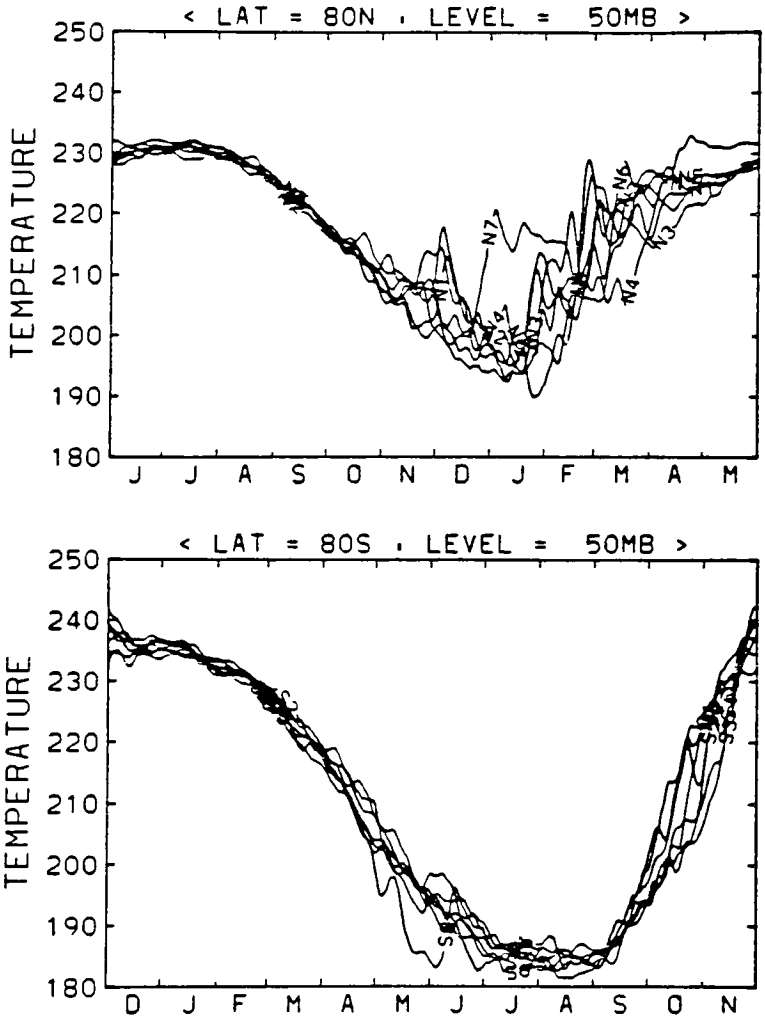

Fig. 3.2 Annual marches of the zonal mean temperature for about 6.7 years from October 1978 to July 1985 at 50 mb for (a) 80°N and (b) 80°S.

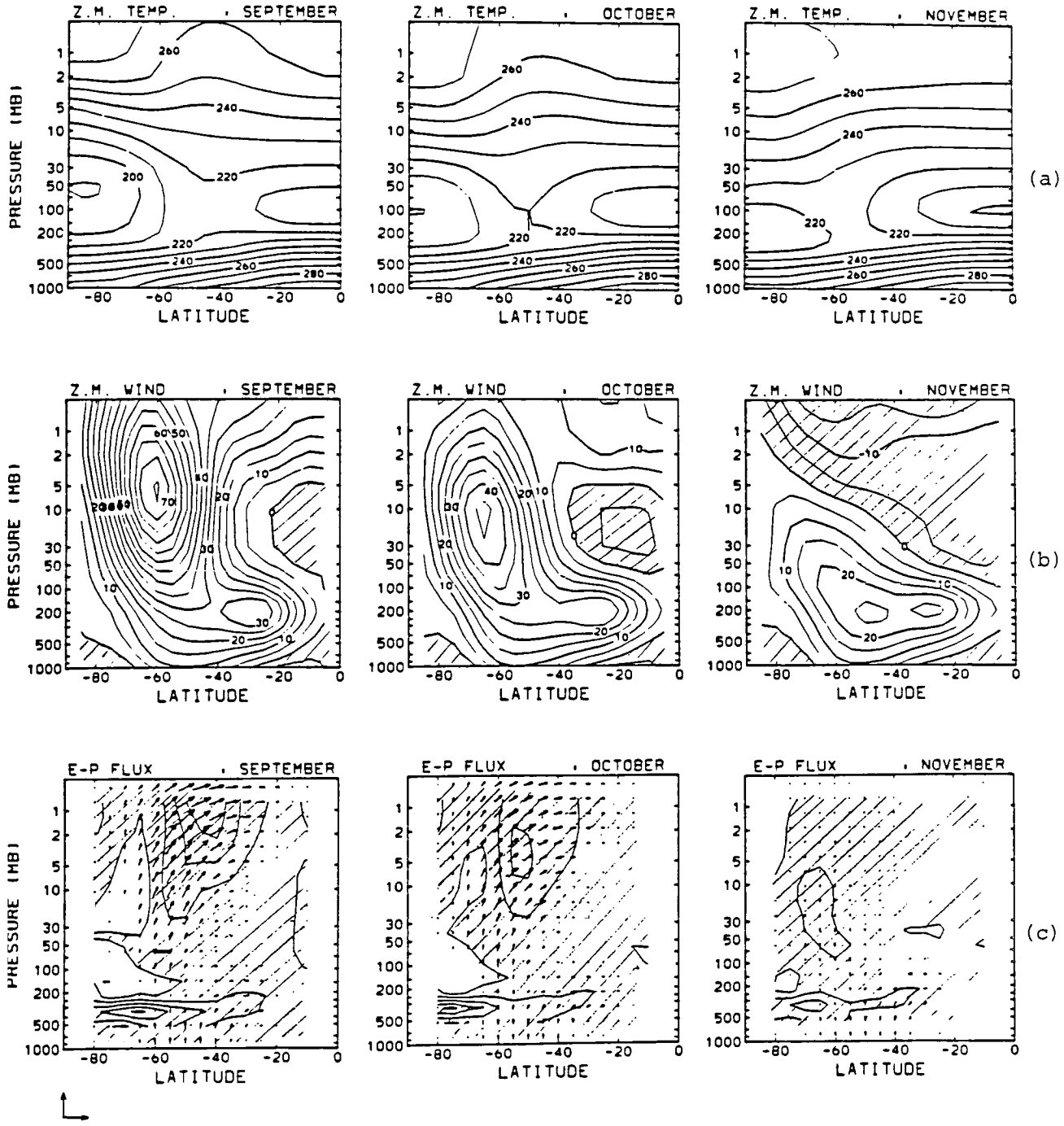

Fig. 3.3 Climatological latitude-height sections of (a) the zonal mean temperature (contour interval 10 K), (b) the mean zonal gradient wind (contour interval 5 m s^{-1}) and (c) the E-P flux and wave driving D_F (contour interval 2.5×10^5 m s^{-2}). Negative values are shaded. Reference arrow for the E-P flux shows 1.0×10^9 kg s^{-2} for horizontal direction and $1.0\times10^9/c$ (c=182) kg s^{-2} for vertical direction. (see text for the scaling.)

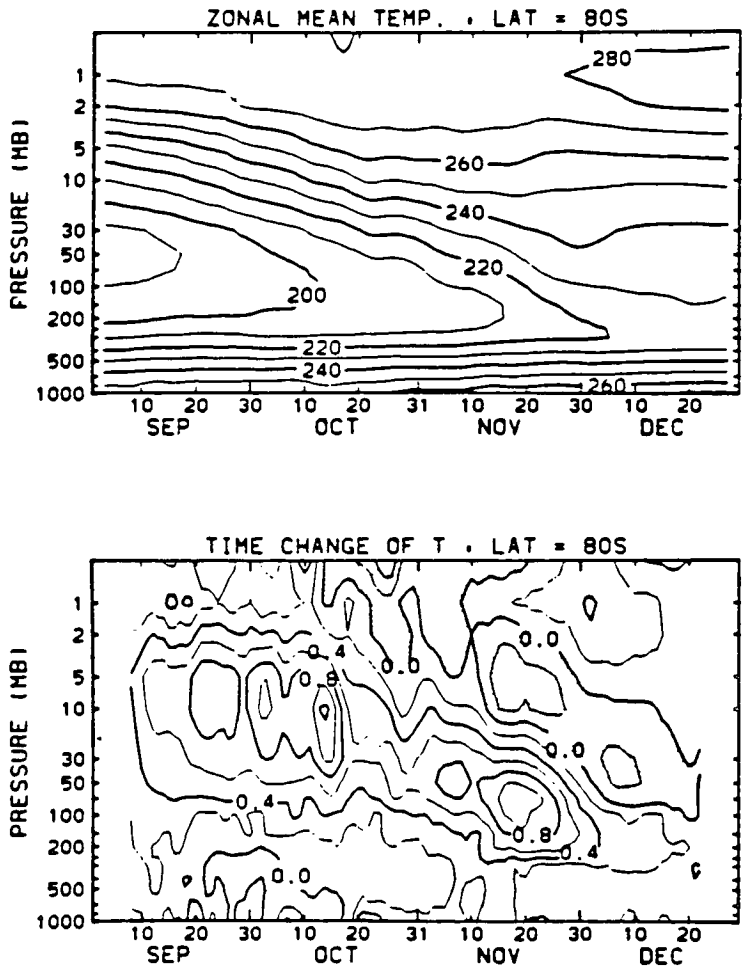

Fig. 3.4 Climatological time-height sections of (a) the zonal mean temperature (contour interval 10 K) and (b) rate of change of temperature (contour interval 0.2 K day^{-1}) at 80°S from September to December Negative values are shaded.

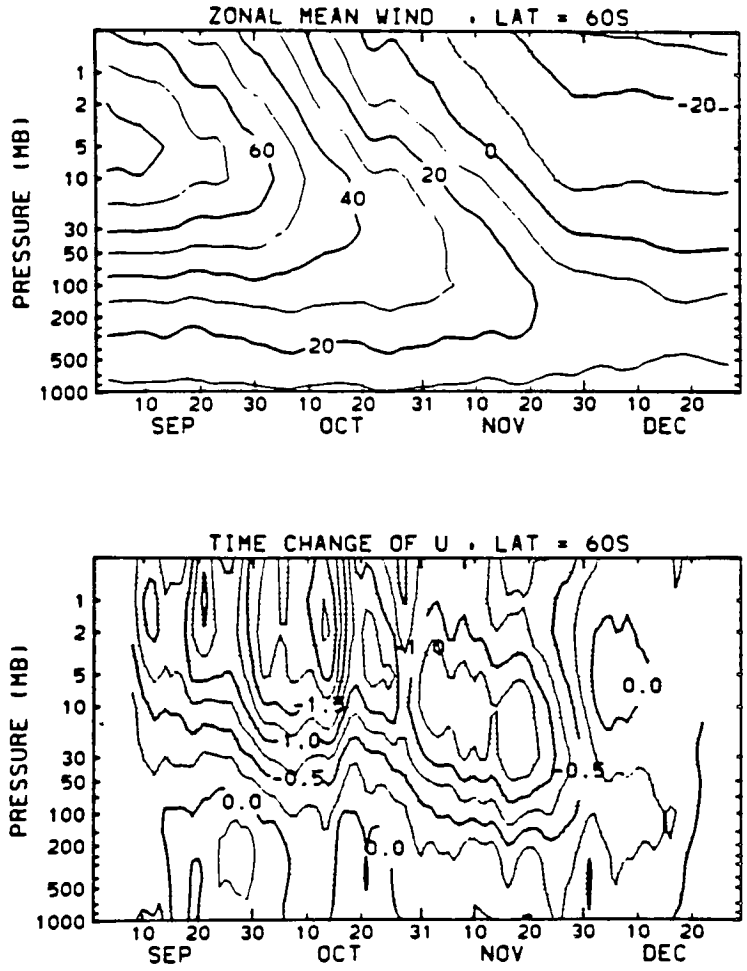

Fig. 3.5 As Fig. 3.4 but for (a) the mean zonal gradient wind (contour interval 10 m s^{-1}) and (b) wind acceleration (contour interval 0.25 m $s^{-1}day^{-1}$) at 60°S.

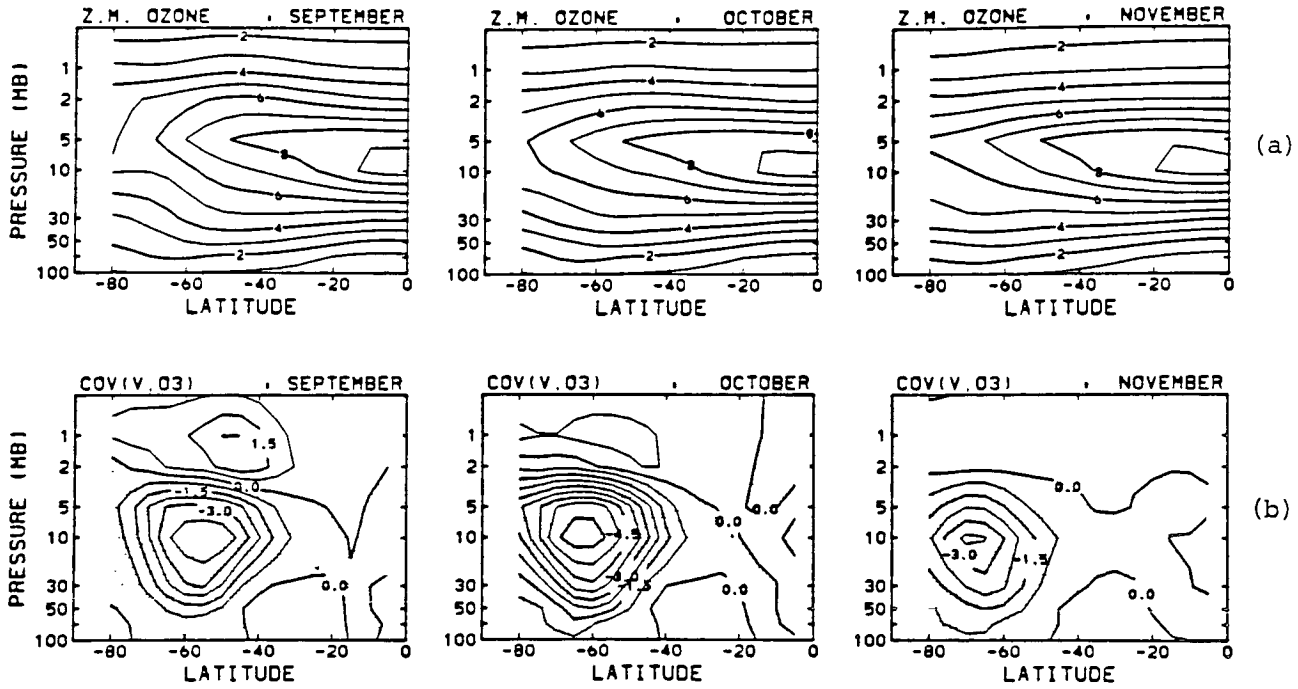

Fig. 3.6 As Fig. 3.3 but for (a) the zonal mean ozone mixing ratio (contour interval 1 ppm) and (b) the ozone transport of the horizontal eddy (contour interval 0.75 ppm m s^{-1})

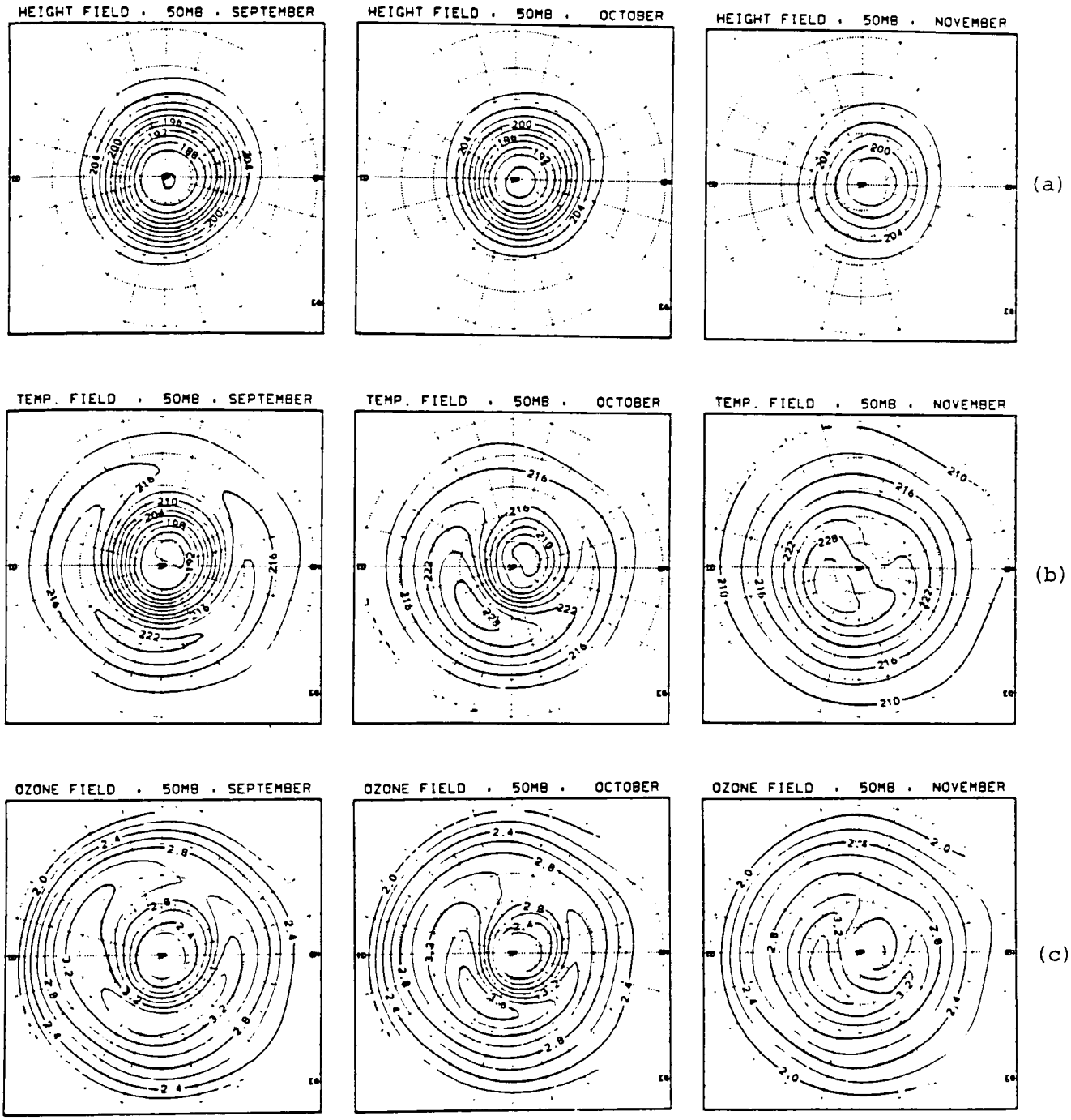

Fig. 3.7 Climatological synoptic charts projected on a stereographic grid (poleward from 15°S is shown) of (a) the geopotential height field (contour interval 2 hm), (b) the temperature field (contour interval 3 K) and (c) the ozone mixing ratio field (contour interval 0.2 ppm) at 50 mb in September, October and November

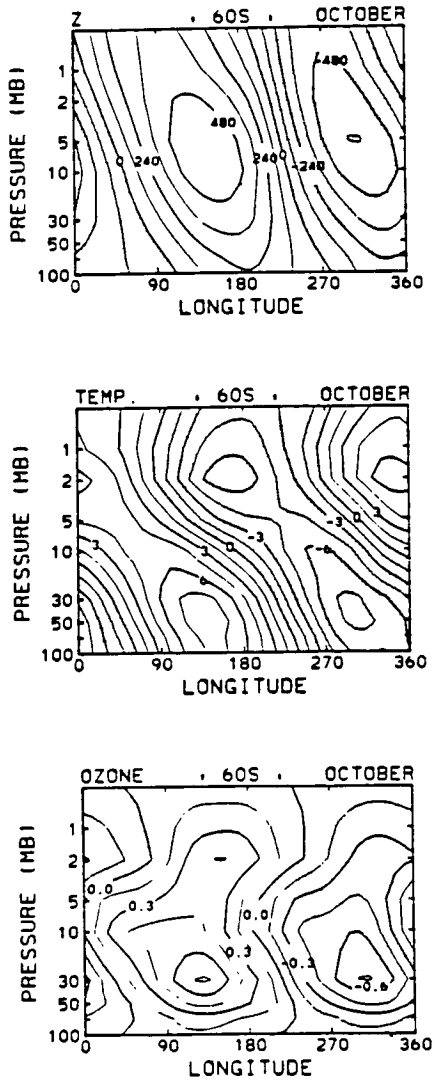

Fig. 3.8 Climatological longitude-height sections of deviation from a zonal mean for (a) the geopotential height wave (contour interval 120 m), (b) the temperature wave (contour interval 1.5 K) and (c) the ozone mixing ratio wave (contour interval 0.15 ppm) at 60°S in October Negative values are shaded.

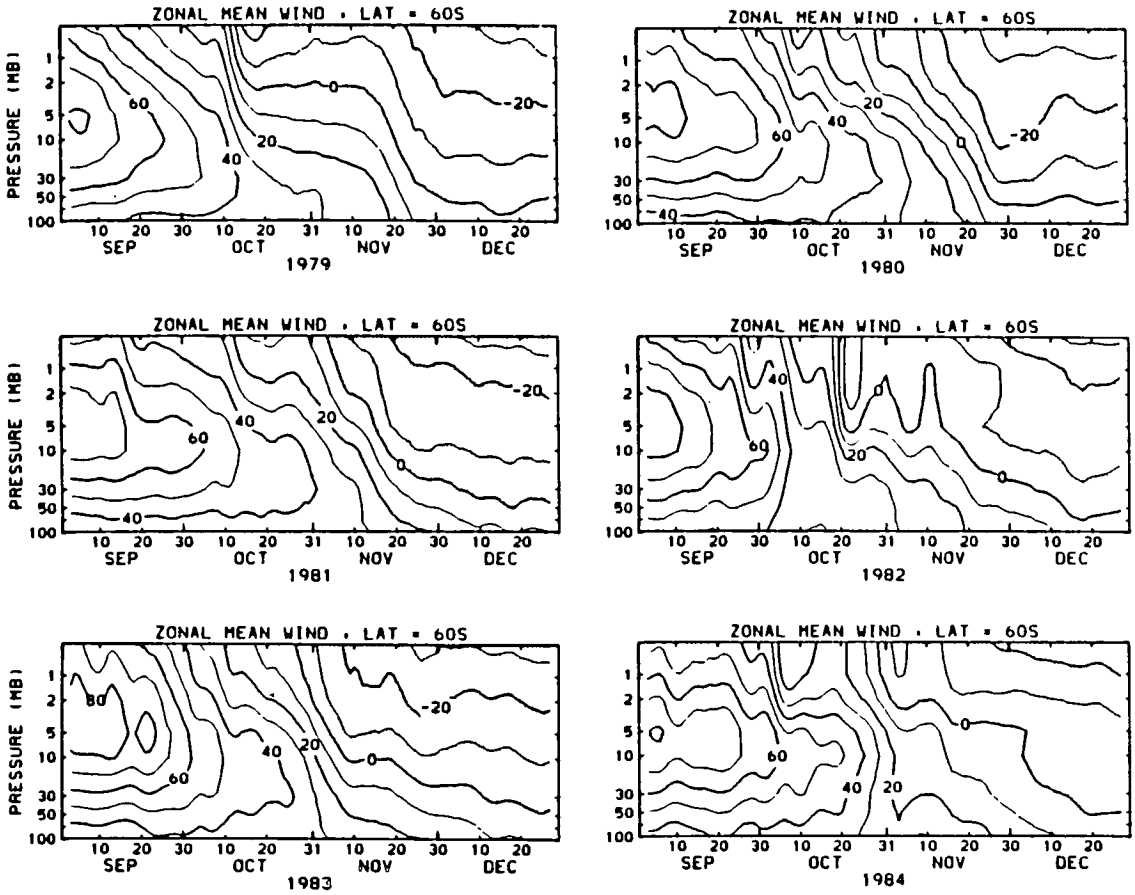

Fig. 3.9 Time-height sections of the mean zonal gradient wind (contour interval 10 m s^{-1}) at 60°S from September to December for the six years of 1979 to 1984. Negative values are shaded.

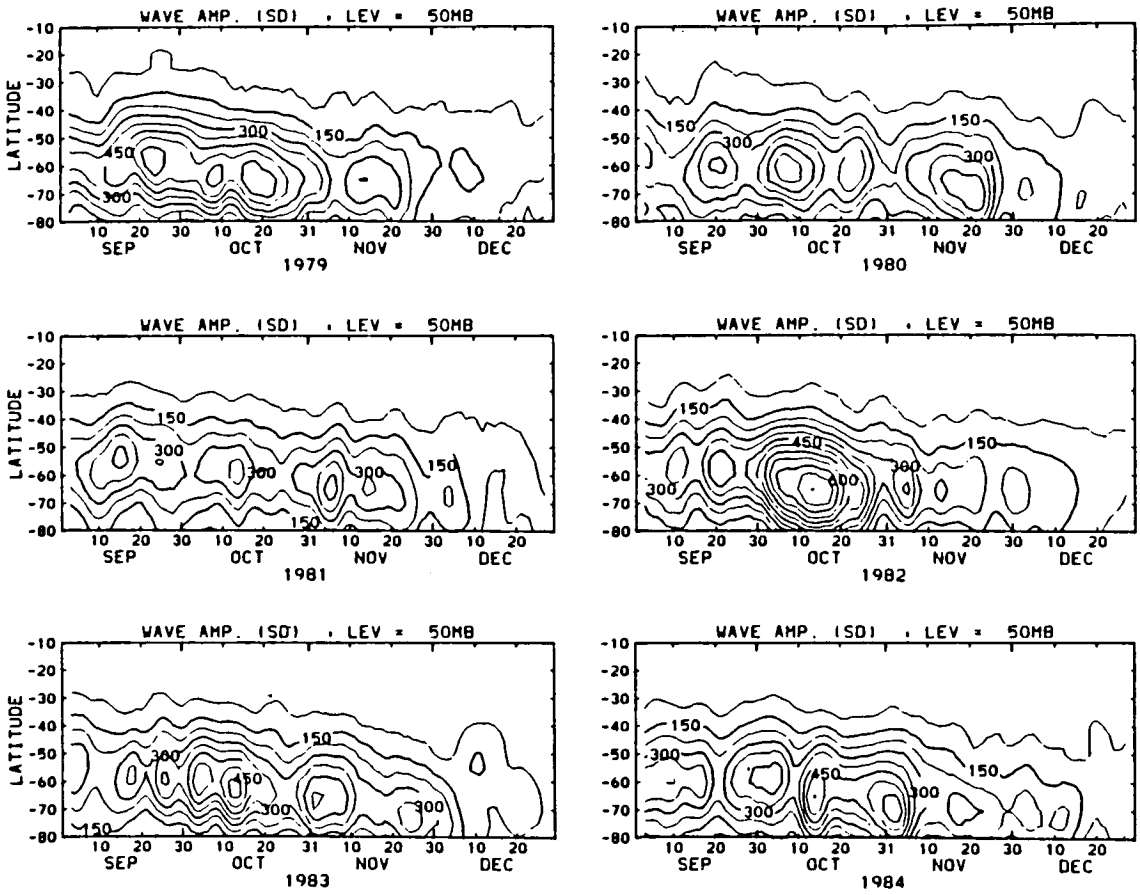

Fig. 3.10 Time-latitude sections of the total amplitude of the height wave (contour interval 75 m) at 50 mb from September to December for the six years of 1979 to 1984.

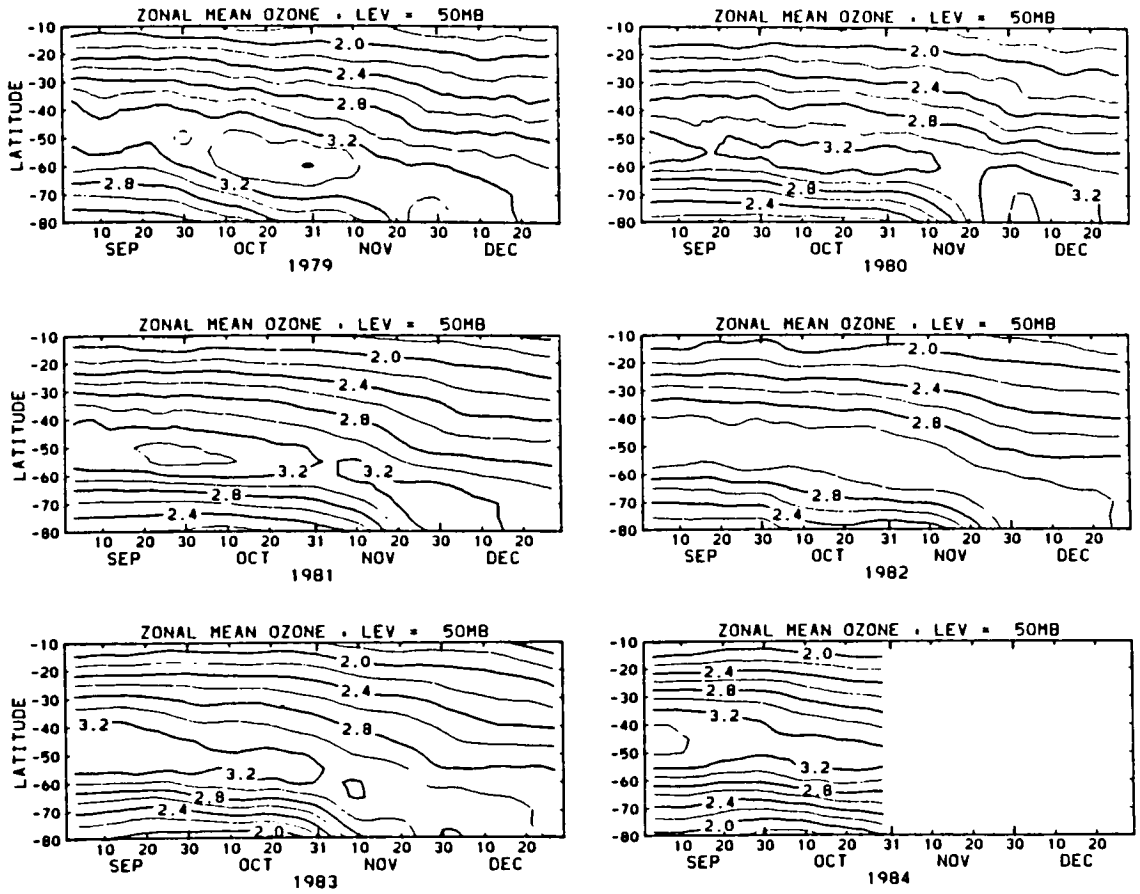

Fig. 3.11 As Fig. 3.10 but for the zonal mean ozone mixing ratio (contour interval 0.2 ppm). (In 1984 only September and October are shown.)

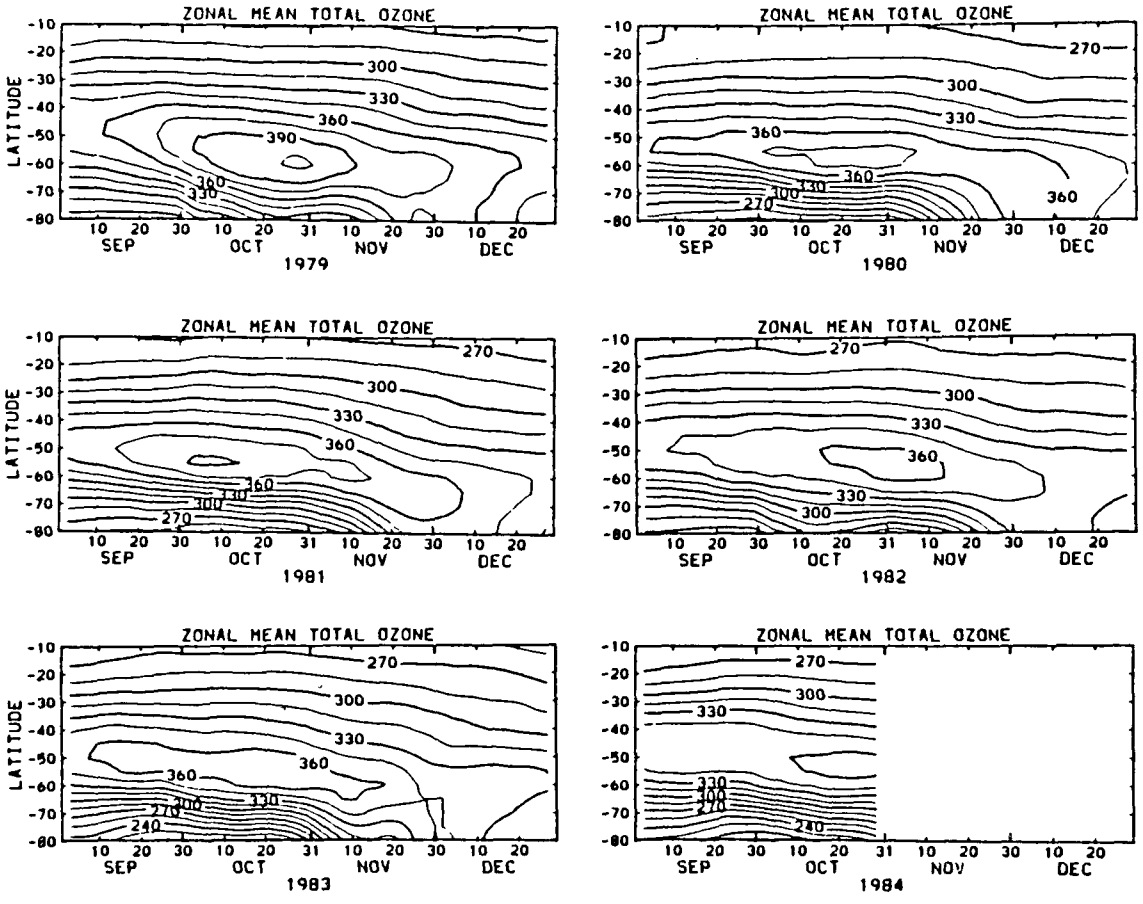

Fig. 3.12 As Fig. 3.10 but for the zonal mean total ozone (contour interval 15 DU) (In 1984 only September and October are shown.)

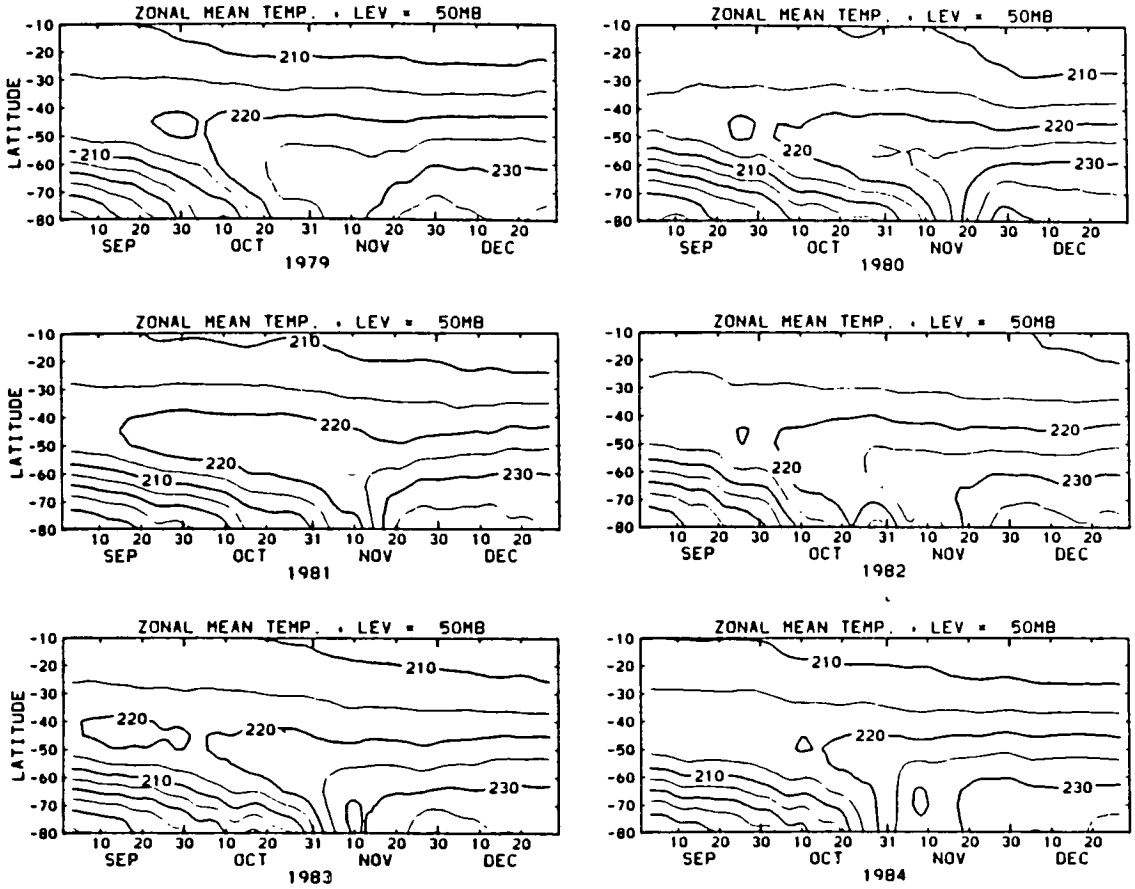

Fig. 3.13 As Fig. 3.10 but for the zonal mean temperature (contour interval 5 K).

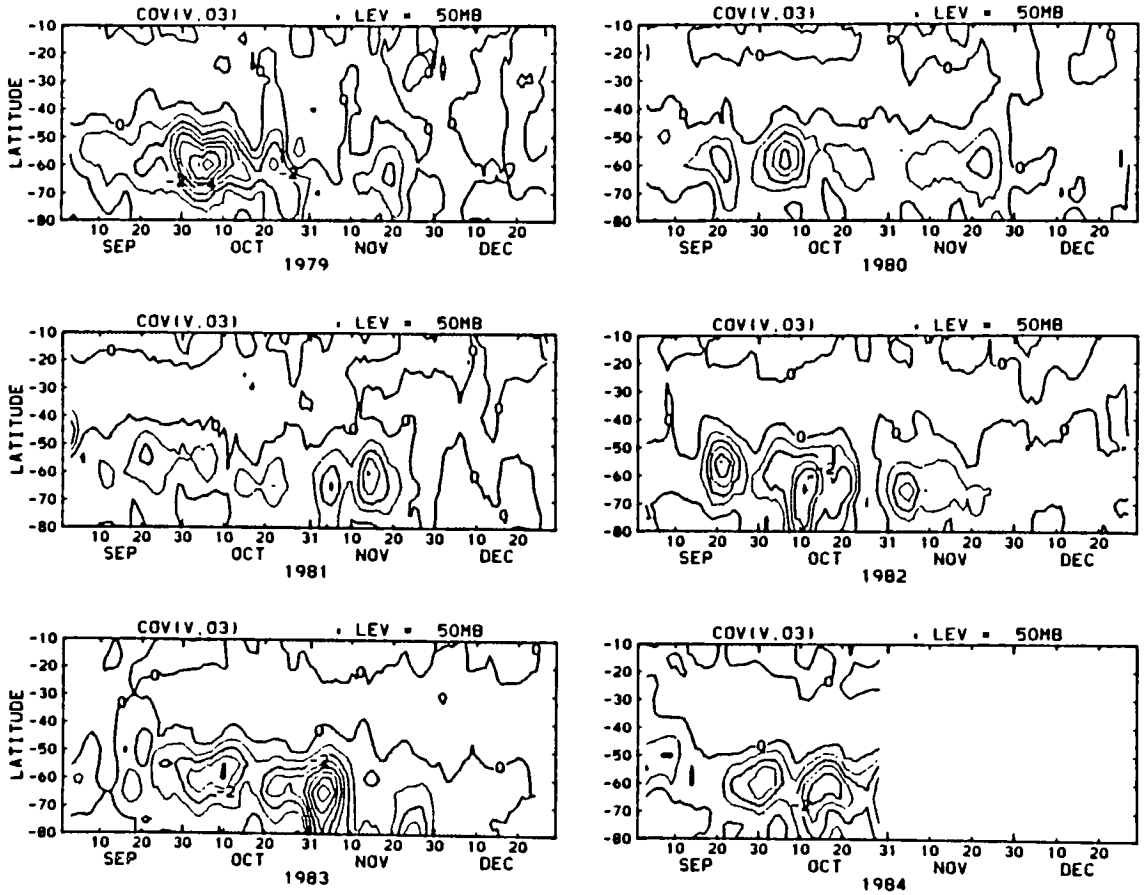

Fig. 3.14 As Fig. 3.10 but for the ozone transport of the horizontal eddy, $\overline{v'O_3'}$ (contour interval 1 ppm m s^{-1}). Negative values are shaded.

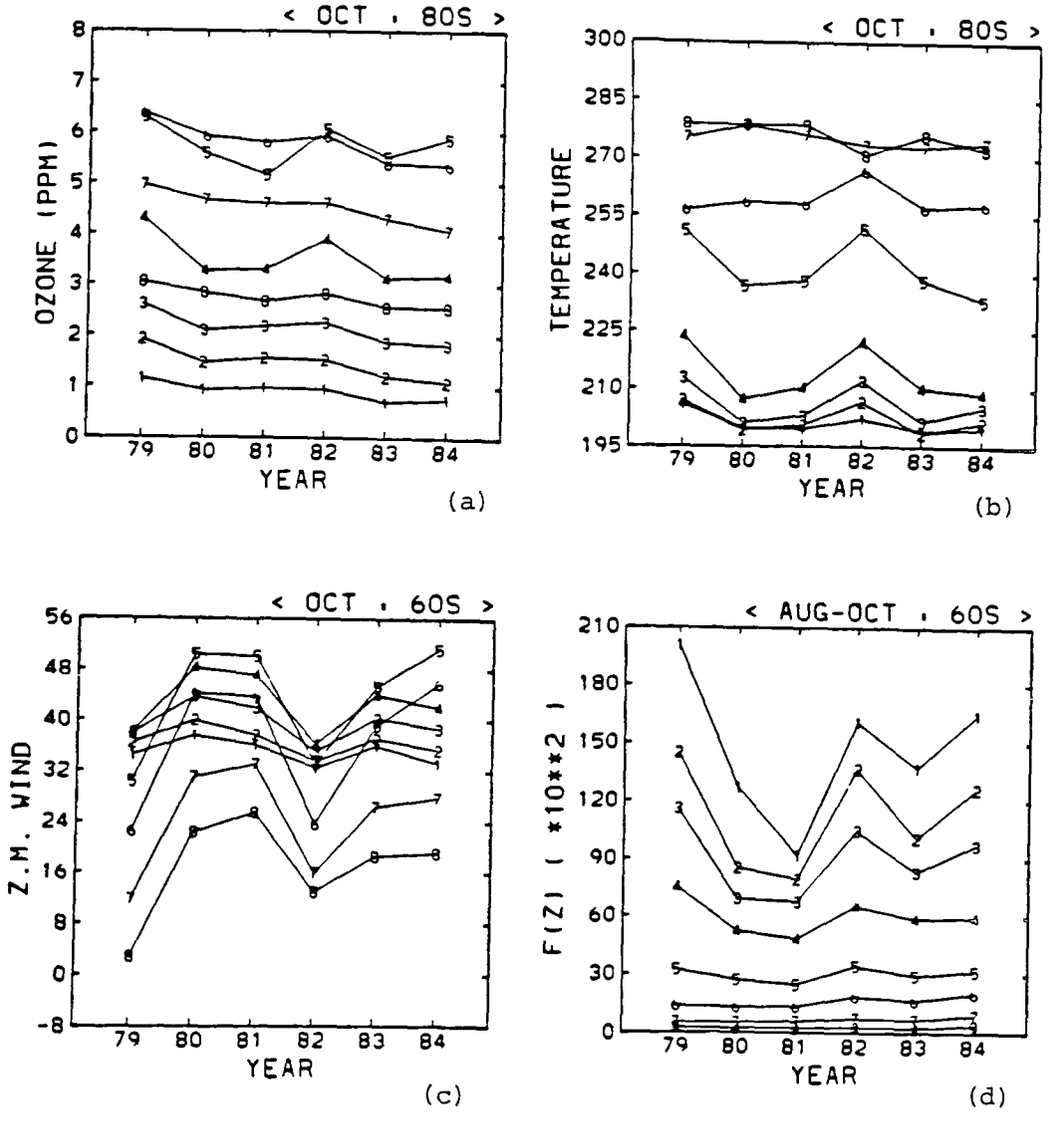

Fig. 3.15 Year to year variations of (a) the zonal mean ozone mixing ratio (unit ppm) at 80°S averaged over October, (b) the zonal mean temperature (unit K) at 80°S averaged over October, (c) the mean zonal gradient wind (unit m s^{-1}) at 60°S averaged over October and (d) the vertical component of the E-P flux (unit 10^2 kg s^{-2}) at 60°S averaged over August to October Marks of ' i ' (i = 1 to 8) correspond to the pressure levels in the following order: 100, 70, 50, 30, 10, 5, 2, 1 mb.

SUMMARY

A series of the three studies has shown observational evidence to obtain the better understanding of the general circulation in the troposphere and stratosphere, using global meteorological data set. Essence of the three studies is summarized as follows.

In PART 1 dynamical interaction between planetary waves and mean zonal winds in the stratosphere is investigated, by paying special attention to the difference between the NH and the SH. From winter to summer the seasonal march of the wave activity and the mean zonal wind is different between the two hemispheres. In the NH, the wave activity varies intermittently with a characteristic time scale of about 2 weeks. Once the core of the stratospheric westerly jet shifts poleward due to a minor warming, the subsequent wave activity breaks the westerlies dramatically to replace them by the easterlies in association with the sudden warming. While in the SH the wave activity in mid-winter is quiet corresponding to small time variations of the maximum westerly speed. In late winter the core of the stratospheric westerly jet suddenly shifts poleward and downward due to a wavenumber 2 minor warming. After the shifting of the westerly jet the wave activity of wavenumber 1 is enhanced, and continues until early summer

In PART 2 the propagation and temporal variation of planetary waves in the troposphere and stratosphere is investigated. It is found that there are two typical cases of correspondence during the NH winter from December 1981 to March 1982: In December and early January (period 1) the time variation of wave activity in the troposphere and stratosphere is out of phase; In February and March (period 2), after the stratospheric sudden warming, the tropospheric wave activity seems to propagate into the stratosphere. These two periods (period 1 and 2) are characterized by the following dynamical features: The mean zonal geostrophic wind at middle latitudes in the upper stratosphere is stronger in period 1 than in period 2. The meridional gradient of the mean zonal wind velocity at high latitudes in the troposphere and lower stratosphere is steeper in period 1 than in period 2. Consequently, significant changes in the refractive index are observed between the two period. The E-P flux vectors in the troposphere and lower stratosphere regularly point upward in period 2, while they branch off equatorward and poleward around the tropopause level in period 1 The feature of the E-P flux pattern is in broad agreement with the refractive index.

In PART 3 relation between ozone distribution and dynamical factors is investigated, by paying special attention to the Antarctic lower stratosphere where a remarkable decrease of total ozone has been observed during springtime. In the climatological sense, the maximum temperature tendency at high latitudes moves from the upper stratosphere to the lower stratosphere; this movement is related to the downward motion of the maximum westerlies. A steep decrease in zonal mean ozone mixing ratios is observed around 60°S toward the south pole in September With time, the ozone hole gets shallower in association with minor warmings and a final warming. Climatological synoptic charts in the lower stratosphere show the circumpolar circulation in the geopotential height field and a prominent planetary wave 1 in the temperature and ozone fields. The phases of the temperature and ozone waves in the lower stratosphere are very similar The year-to-year variation of the ozone mixing ratio at high latitudes is related to that of the wave activity during the winter and spring. When the wave activity is vigorous, we see weaker westerlies, higher temperatures and higher ozone mixing ratios at high latitudes. With the use of the SBUV data, the decrease of ozone mixing ratios is observed at high latitudes in the whole stratosphere. However, if we consider that the wave activity in 1979 was very vigorous, a simple comparison of atmospheric states between the 1979 and other recent years could lead to misleading conclusions on a chemical rate of ozone decrease over the Antarctic.

REFERENCES

Andrews, D.G. and McIntyre, M.E., 1976: Planetary waves in horizontal and vertical shear: the generalized Eliassen-Palm relation and the mean zonal acceleration. *J Atmos. Sci.*, **33**, 2031-2048.

Andrews, D.G. and McIntyre, M.E., 1978: Generalized Eliassen-Palm and Charney-Drazin theorems for waves on axisymmetric mean flows in compressible atmospheres. *J Atmos. Sci.*, **35**, 175-185.

Baldwin, M. P., Edmon, H. J and Holton, J. R., 1985: A diagnostic study of eddy-mean flow interaction during FGGE SOP-1. *J Atmos. Sci.*, **42**, 1838-1845.

Barnett, J. J, 1974: The mean meridional temperature behaviour of the stratosphere from November 1970 to November 1971 derived from measurements by The Selective Chopper Radiometer on Nimbus IV. *Quart. J. R. Met. Soc.*, **100**, 505-530.

Boville, B. A., 1984: The influence of the polar night jet on the tropospheric circulation in a GCM. *J Atmos. Sci.*, **41**, 1132-1142.

Boville, B. A., 1986: Wave-mean flow interactions in a general circulation model of the troposphere and stratosphere. *J Atmos. Sci.*, **43**, 1711-1725.

Charney. J.G. and Drazin, P.G., 1961: Propagation of planetary-scale disturbances from the lower into the upper atmosphere. *J Geophys. Res.*, **66**, 83-109.

Chubachi, S., 1984: Preliminary result of ozone observations at Syowa station from February 1982 to January 1983. *Memoirs of National Institute of Polar Research Special Issue*, **34**, 13-19.

Dickinson, R.E., 1969a: Vertical propagation of planetary Rossby waves through an atmosphere with Newtonian cooling. *J Geophys. Res.*, **74**, 929-938.

Dickinson, R.E., 1969b: Theory of planetary wave-zonal flow interaction. *J Atmos. Sci.*, **26**, 73-81

Dunkerton, T , Hsu, C.-P and McIntyre, M. E., 1981: Some Eulerian and Lagrangian Diagnostics for a model stratospheric warming. *J. Atmos. Sci.*, **38**, 819-843.

Edmon, H. J., Hoskins, B. J. and McIntyre, M. E., 1980: Eliassen-Palm cross sections for the troposphere. *J. Atmos. Sci.*, **37**, 2600-2616. (See also corrigendum, *J Atmos. Sci.*, **38**, 1115, especially second last item.)

Eliassen, A. and Palm, E., 1960: On the transfer of energy in stationary mountain waves. *Geofys. Publ.*, **22**, No.3, 1-23.

Farman, J. C., Gardiner, B. G. and Shanklin, J. D., 1985: Large losses of total ozone in Antarctica reveal seasonal ClO_x/NO_x interaction. *Nature*, **35**, 207-210.

Fritz, S. and Soules, S.D., 1970: Large-scale temperature changes in the stratosphere observed from Nimbus III. *J Atmos. Sci.*, **27**, 1091-1097

Geller, M. A., Wu, M.-F. and Gelman, M. E., 1983: Troposphere-stratosphere (surface-55km) monthly winter general circulation statistics for the northern hemisphere - four year averages. *J. Atmos. Sci.*, **40**, 1334-1352.

Geller, M. A., Wu, M.-F and Gelman, M. E., 1984: Troposphere-stratosphere (surface-55km) monthly winter general circulation statistics for the northern hemisphere - interannual variations. *J. Atmos. Sci.*, **41**, 1726-1744.

Gille, J. C., Bailey. P L. and Russell III, J. M., 1980: Temperature and composition measurements from the l.r.i.r and l.i.m.s. experiments on Nimbus 6 and 7 *Phil. Trans. R. Soc. Lond.*, **A 296**, 205-218.

Gille, J. C. and Lyjak, L. V , 1984: An overview of wave-mean flow interactions during the winter of 1978-79 derived from LIMS observations. *Dynamics of the Middle Atmosphere*. Holton, J. R. and Matsuno, T , Eds., Terra Scientific Publishing Company, 543pp.

Hartmann, D. L., 1976: The structure of the stratosphere in the southern hemisphere during late winter 1973 as observed by satellite. *J. Atmos. Sci.*, **33**, 1141-1154.

Hartmann, D. L. and Garcia, R. R., 1979: A mechanistic model of ozone transport by planetary waves in the stratosphere. *J Atmos. Sci.*, **36**, 350-364.

Hartmann, D. L., Mechoso, C. R. and Yamazaki, K., 1984: Observations of wave-mean flow interaction in the southern hemisphere. *J. Atmos. Sci.*, **41**, 351-362.

Harwood, R.S., 1975: The temperature structure of the southern hemisphere stratosphere August-October 1971. *Quart. J R. Met. Soc.*, **101**, 75-91.

Hirooka, T., 1986: Influence of normal mode Rossby waves on the mean field: interference with quasi-stationary waves. *J. Atmos. Sci.*, **43**, 2088-2097

Hirota, I., 1971: Excitation of planetary Rossby waves in the winter stratosphere by periodic forcing. *J Met. Soc. Japan*, **49**, 439-449.

Hirota, I., 1976: Seasonal variation of planetary waves in the stratosphere observed by the Nimbus 5 SCR. *Quart. J R. Met. Soc.*, **102**, 757-770.

Hirota, I. and Sato, Y , 1969: Periodic variation of the winter stratospheric circulation and intermittent vertical propagation of planetary waves. *J*

Met. Soc. Japan, 47, 390-402.

Hirota, I. and Barnett, J.J., 1977: Planetary waves in the winter mesosphere - preliminary analysis of Nimbus 6 PMR results. *Quart. J. R. Met. Soc.*, 103, 487-498.

Hirota, I., Hirooka, T. and Shiotani, M., 1983: Upper stratospheric circulations in the two hemispheres observed by satellites. *Quart. J R. Met. Soc.*, 109, 443-454.

Holton, J. R., 1975: *The Dynamic Meteorology of the Stratosphere and Mesosphere. Meteor Monogr* , No. 37, Amer Meteor Soc., 218 pp.

Holton, J.R. and Mass, C., 1976: Stratospheric vacillation cycles. *J. Atmos. Sci.*, 33, 2218-2225.

Holton, J.R. and Dunkerton, T., 1978: On the role of wave transience and dissipation in stratospheric mean flow vacillations. *J Atmos. Sci.*, 35, 740-744.

Holton, J.R. and Wehrbein, W.M., 1980: The role of forced planetary waves in the annual cycle of the zonal mean circulation of the middle atmosphere. *J. Atmos. Sci.*, 37, 1968-1983.

Holton, J.R. and Tan, H.C., 1982: The quasi-biennial oscillation in the northern hemisphere lower stratosphere. *J. Met. Soc. Japan*, 60, 140-148.

Kanzawa, H., 1980: The behavior of the mean zonal wind and planetary-scale disturbances in the troposphere and stratosphere during the 1973 sudden warming. *J Met. Soc. Japan*, 58, 329-356.

Kanzawa, H., 1982: Eliassen-Palm flux diagnostics and the effect of the mean wind on planetary wave propagation for an observed sudden stratospheric warming. *J Met. Soc. Japan*, 60, 1063-1073.

Karoly, D. J. and Hoskins, B. J., 1982: Three dimensional propagation of planetary waves. *J Met. Soc. Japan*, 60, 109-123.

Knittel, J., 1976: Ein Beitrag zur Klimatologie der stratosphäre der südhaldkugel. Meteorological reports, Institute for Meteorology and Institute for Geophysical Sciences, Free University Berlin.

Koermer, J. P and Kao, S. K., 1980: Major and minor stratospheric warmings and their interaction on the troposphere. *Pure Applied Geophys.*, 118, 428-451.

Kohri, W. J., 1981: LRIR observations of the structure and propagation of the stationary planetary waves in the northern hemisphere during December 1975. Cooperative Ph. D. Thesis 63, Drexel Univ. and Nat. Center for Atmos. Res., Boulder, Colorado.

Labitzke, K., 1982: On the interannual variability of the middle stratosphere during the northern winters. *J Met. Soc. Japan*, 60, 124-139.

Labitzke, K. and Barnett, J. J., 1973: Global time and space changes of satellite radiances received from the stratosphere and lower mesosphere. *J Geophys. Res.*, 78, 483-496.

Leovy, C.B. and Webster, P.J., 1976: Stratospheric long waves: comparison of thermal structure in the northern and southern hemispheres. *J. Atmos. Sci.*, 33, 1624-1638.

Madden, R.A., 1975: Oscillations in the winter stratosphere: Part 2. the role of horizontal eddy heat transport and interaction of transient and stationary planetary-scale waves. *Mon. Wea. Rev.*, 103, 717-729.

Madden, R. A., 1983: The effect of the interference of traveling and stationary waves on time variations of the large-scale circulation. *J Atmos. Sci.*, 40, 1110-1125.

Matsuno, T., 1971: A dynamical model of the stratospheric sudden warming. *J Atmos. Sci.*, 28, 1479-1494.

Matsuno, T., 1984: Dynamics of minor stratospheric warmings and preconditioning *Dynamics of the Middle Atmosphere*, Ed. J.R. Holton and T. Matsuno. 333-351.

Matsuno, T and Nakamura, K., 1979: The Eulerian- and Lagrangian-mean meridional circulations in the stratosphere at the time of a sudden warming. *J. Atmos. Sci.*, 36, 640-654.

McIntyre, M.E., 1982: How well do we understand the dynamics of stratospheric warmings? *J. Met. Soc. Japan*, 60, 37-65.

McIntyre, M.E. and Palmer, T.N., 1983: Breaking planetary waves in the stratosphere. *Nature*, 305, 593-600.

McIntyre, M.E. and Palmer, T.N., 1984: The 'surf zone' in the stratosphere. *J. Atmos. Terr Phys.*, in press.

Mechoso, C. R., Hartmann, D. L. and Farrara, J. D., 1985: Climatology and interannual variability of wave, mean-flow interaction in the southern hemisphere. *J. Atmos. Sci.*, 42, 2189-2206.

Muench, H. S., 1965: On the dynamics of wintertime stratospheric circulation. *J. Atmos. Sci.*, 22, 349-360.

O'Neill, A. and Youngblut, C. E., 1982: Stratospheric warmings diagnosed using the transformed Eulerian-mean equations and the effect of the mean state on wave propagation. *J Atmos. Sci.*, 39, 1370-1386.

Palmer, T.N., 1981a: Diagnostic study of a wavenumber-2 stratospheric sudden

warming in a transformed Eulerian-mean formalism. *J Atmos. Sci.*, 38, 844-855.

Palmer, T.N., 1981b: Aspects of stratospheric sudden warmings studied from a transformed Eulerian-mean viewpoint. *J. Geophys. Res.*, 86, 9679-9687

Palmer, T.N., 1982: Properties of the Eliassen-Palm flux for planetary scale motions. *J. Atmos. Sci.*, 39, 992-997

Palmer, T.N. and Hsu, C.-P.F., 1983: Stratospheric sudden coolings and the role of nonlinear wave interactions in preconditioning the circumpolar flow. *J Atmos. Sci.*, 40, 909-928.

Quiroz, R.S., Miller, A.J. and Nagatani, R.M., 1975: A comparison of observed and simulated properties of sudden stratospheric warmings. *J. Atmos. Sci.*, 32, 1723-1736.

Robinson, W. A., 1986: The application of the quasi-geostrophic Eliassen-Palm flux to the analysis of stratospheric data. *J Atmos. Sci.*, 43, 1017-1023.

Rodgers, C. D., 1977: Statistical principles of inversion theory. *Inversion Methods in Atmospheric Remote Sounding*, A. Deepak, Ed., Academic Press, New York, 1977, pp. 117-138.

Schoeberl, M.R., 1983: A study of stratospheric vacillations and sudden warmings on a β-plane. Part I: single wave-mean flow interaction. *J Atmos. Sci.*, 40, 769-787

Shiotani, M. and Hirota, I., 1985: Planetary wave-mean flow interaction in the stratosphere: a comparison between northern and southern hemispheres. *Quart. J R. Met. Soc.*, 111, 309-334.

Shiotani, M., 1986: Planetary wave activity in the troposphere and stratosphere during the northern hemisphere winter *J Atmos. Sci.*, in press.

Shiotani, M. and Gille, J C., 1987: Dynamical factors affecting ozone mixing ratios in the Antarctic lower stratosphere. submitted to *J Geophys. Res.*

Smith, A.K., 1983: Stationary waves in the winter stratosphere: seasonal and interannual variability. *J. Atmos. Sci.*, 40, 245-261

Smith, A. K., 1983: Observation of wave-wave interactions in the stratosphere. *J Atmos. Sci.*, 40, 2484-2496.

Smith, A. K., 1985: Wave transience and wave-mean flow interaction caused by the interference of stationary and traveling waves. *J Atmos. Sci.*, 42, 529-556.

Smith, A. K., Gille, J. C. and Lyjak, L. V., 1984: Wave-wave interactions in the stratosphere: observations during quiet and active wintertime period.

J. Atmos. Sci., 41, 363-373.

Solomon, S., Garcia, R. R., Rowland, F S. and Wuebbles, D. J., 1986: On the depletion of Antarctic ozone. *Nature*, 321, 755-758.

Stolarski, R. S, Krueger, A. J., Schoeberl, M. R., McPeters, R. D., Newman, P A. and Alpert, J. C., 1986: Nimbus 7 SBUV/TOMS measurements of the springtime Antarctic ozone hole. *Nature*, 322, 808-811.

Tung, K. K. and Lindzen, R. S., 1979: A theory of stationary long waves. Part II: resonant Rossby waves in the presence of realistic vertical shears. *Mon. Wea. Rev.*, 107, 735-750. Hoskins, B. J. and Pearce, R. P., Eds., Academic Press, 397pp.

Tung, K.-K., Ko, M. K. W., Rodriguez, J. M. and Sze, N. D., 1986: Are Antarctic ozone variations a manifestation of dynamics or chemistry? *Nature*, 322, 811-814.

Wallace J. M. and Blackmon M. L., 1983: Observations of low-frequency atmospheric variability. *Large-Scale Dynamical Processes in the Atmosphere.*

WMO, 1986: Atmospheric Ozone 1985. WMO-Report No. 16.

Wu, M.-F., Geller, M. A., Olson, J. G., Miller, A. J. and Nagatani, R. M., 1985: Computation of ozone transport using Nimbus 7 solar backscatter ultraviolet and NOAA/National Meteorological Center data. *J Geophys. Res.*, 90, 5745-5755.

Yamazaki, K. and Mechoso, C. R., 1985: Observations of the final warming in the stratosphere of the southern hemisphere during 1979. *J. Atmos. Sci.*, 42, 1198-1205.

Yoden, S., Shiotani, M. and Hirota, I., 1986: Multiple weather regimes in the southern hemisphere. submitted to *J Met. Soc. Japan.*